US 20120121455A1

(19) **United States**

(12) **Patent Application Publication**

**Murray et al.**

(10) **Pub. No.: US 2012/0121455 A1**

(43) **Pub. Date: May 17, 2012**

(54) **LOW LEAD INGOT**

(75) Inventors: **Michael Murray**, Chicago, IL (US); **Mahi Sahoo**, Ottawa (CA)

(73) Assignee: **Sloan Valve Company**

(21) Appl. No.: **13/317,785**

(22) Filed: **Oct. 28, 2011**

**Related U.S. Application Data**

(60) Provisional application No. 61/408,518, filed on Oct. 29, 2010, provisional application No. 61/410,752, filed on Nov. 5, 2010.

**Publication Classification**

(51) **Int. Cl.**

| | |
|---|---|
| ***C22C 9/04*** | (2006.01) |
| ***C22C 1/02*** | (2006.01) |

(52) **U.S. Cl.** ............ **420/471**; 420/473; 420/472; 75/646

(57) **ABSTRACT**

A composition for a low lead ingot comprising primarily copper and including tin, zinc, sulfur, phosphorus, nickel. The composition may contain manganese. The low lead ingot, when solidified, includes sulfur or sulfur containing compounds such as sulfides distributed through the ingot. The presence and a substantially uniform distribution of these sulfur compounds imparts improved machinability and better mechanical properties.

Table 1 – Commercially Available Copper Alloys

| Alloy Type | Cu | S | Sn | Pb | Zn | Fe | Sb | Ni | P | Al | Si | Mn | Bi | Se |
|---|---|---|---|---|---|---|---|---|---|---|---|---|---|---|
| Biwalite™ - C83470 | 90.0-96.0 | 0.20-0.60 | 3.0-5.0 | 0.09 | 1.0-3.0 | 0.50 | 0.20 | 0.1-1.0 | 0.05 | 0.01 | 0.01 | -- | -- | -- |
| **Bismuth Brass** | | | | | | | | | | | | | | |
| Sebiloy™ - C89520 | 85-87 | 0.08 | 5.0-6.0 | 0.25 | 4.0-6.0 | 0.20 | 0.25 | 1.0 | -- | 0.005 | -- | -- | 1.6-2.2 | 0.8-1.1 |
| C89836 | 87.0-91.0 | 0.08 | 4.0-7.0 | 0.25 | 2.0-4.0 | 0.35 | 0.25 | 0.90 | 0.06 | 0.005 | 0.005 | - | 1.5-3.5 | |
| **Silicon Brass** | | | | | | | | | | | | | | |
| C87500 | >79.0 | -- | -- | 0.09 | 12.0-16.0 | -- | -- | -- | -- | 0.50 | 3.0-5.0 | -- | -- | -- |
| Ecobrass™ - C87850 | 74.0-78.0 | -- | 0.30 | 0.09 | Rem. | 0.10 | -- | 0.20 | -- | -- | 2.7-3.4 | 0.1 | -- | -- |
| **Leaded Semi-Red Brass** | | | | | | | | | | | | | | |
| C84400 | 78.0-82.0 | 0.08 | 2.3-3.5 | 6.0-8.0 | 7.0-10.0 | 0.40 | 0.25 | 1.0 | 0.02 | 0.005 | 0.005 | -- | -- | -- |
| C90300 | 86-89 | 0.05 | 7.5-9 | 0.3 | 3-5 | 0.2 | 0.2 | 1.0 | 0.05 | 0.005 | 0.005 | -- | -- | -- |

FIG. 1

Table 2 Alloy Groups target ranges

| Alloy | Cu | S | Sn | Pb | Zn | Fe | Sb | Ni | P | Al | Si | Mn | Zr | B | C | Ti |
|---|---|---|---|---|---|---|---|---|---|---|---|---|---|---|---|---|
| **Low-Lead Semi-Red Brass - Sand Cast** | | | | | | | | | | | | | | | | |
| **I-A** | 83.0-89.0 | 0.1-0.8 | 2.0-4.0 | <0.09 | 4.0-14.0 | <0.1 | <0.02 | 1.0-2.0 | 0-0.05 | 0.005 | <0.005 | 0.02 | 0-0.2 | 0-0.2 | -- | -- |
| **I-B** | 83.0-91.0 | 0.1-0.8 | 2.0-4.0 | <0.09 | 4.0-14.0 | <0.1 | <0.02 | 1.0-2.0 | 0-0.05 | 0.005 | <0.005 | 0.01-0.7 | 0-0.2 | 0-0.2 | -- | -- |
| **I-C** | 83.0-88.0 | 0.1-0.8 | 2.0-4.0 | <0.09 | 4.0-14.0 | <0.1 | <0.02 | 1.0-2.0 | 0-0.05 | 0.005 | <0.005 | 0.01-0.7 | 0-0.2 | 0-0.2 | 0--0.5 | 0-0.5 |
| **Lead-Free Tin Bronze - Sand Cast** | | | | | | | | | | | | | | | | |
| **II-A** | 86.0-89.0 | 0.1-0.8 | 7.5-8.5 | <0.09 | 1.0-5.0 | <0.2 | <0.02 | 1 | 0-0.05 | 0.005 | <0.005 | 0.02 | 0-0.2 | 0-0.2 | -- | -- |
| **II-B** | 86.0-89.0 | 0.1-0.8 | 7.5-8.5 | <0.09 | 1.0-5.0 | <0.2 | <0.02 | 1 | 0-0.05 | 0.005 | <0.005 | 0.01-0.7 | 0-0.2 | 0-0.2 | -- | -- |
| **II-C** | 86.0-89.0 | 0.1-0.8 | 7.5-8.5 | <0.09 | 1.0-5.0 | <0.2 | <0.02 | 1 | 0-0.05 | 0.01 | <0.01 | 0.01-0.7 | 0-0.2 | 0-0.2 | 0--0.5 | 0-0.5 |
| **Lead-Free Yellow Brass - Permanent Mold Cast** | | | | | | | | | | | | | | | | |
| **III-A** | 58.0-62.0 | 0.1-0.8 | 1.5 | <0.09 | 31.0-41.0 | <0.5 | 0.2 | 1.5 | 0-0.01 | 0.1-0.6 | <0.25 | 0.02 | 0-0.2 | 0-0.2 | -- | -- |
| **III-B** | 58.0-62.0 | 0.1-0.8 | 1.5 | <0.09 | 31.0-41.0 | <0.5 | 0.2 | 1.5 | 0-0.01 | 0.1-0.6 | <0.25 | 0.01-0.7 | 0-0.2 | 0-0.2 | -- | -- |
| **III-C** | 58.0-62.0 | 0.1-0.8 | 1.5 | <0.09 | 31.0-41.0 | <0.5 | 0.2 | 1.5 | 0-0.01 | 0.1-0.6 | <0.25 | 0.01-0.7 | 0-0.2 | 0-0.2 | 0-0.5 | 0-0.5 |
| **Lead-Free Yellow Brass Wrought** | | | | | | | | | | | | | | | | |
| **IV-A** | 58.0-62.0 | 0.1-0.8 | -- | <0.09 | 31.0-41.0 | <0.35 | -- | -- | -- | -- | -- | 0.02 | 0-0.2 | 0-0.2 | -- | -- |
| **IV-B** | 58.0-62.0 | 0.1-0.8 | -- | <0.09 | 31.0-41.0 | <0.35 | -- | -- | -- | -- | -- | 0.01-0.7 | 0-0.2 | 0-0.2 | -- | -- |
| **IV-C** | 58.0-62.0 | 0.1-0.8 | -- | <0.09 | 31.0-41.0 | <0.35 | -- | -- | -- | -- | -- | 0.01-0.7 | 0-0.2 | 0-0.2 | 0-0.5 | 0-0.5 |

FIG. 2

Table 3 Alloy Group I-A alloy compositions for mechanical property tests

| Heat No. | Cu | S | Sn | Pb | Zn | Fe | Sb | Ni | P | Al | Si |
|---|---|---|---|---|---|---|---|---|---|---|---|
| Target Alloy Range | 83-89 | 0.01-0.75 | 2.5-3.5 | 0.09 | 7-11 | 0.01-0.4 | 0.01-0.2 | 0.75-1.4 | <0.025 | <0.005 | <0.005 |
| Alloy-1-A-3a | 87.19 | 0.077 | 3.22 | 0.017 | 8.43 | 0.075 | 0.001 | 0.955 | 0.018 | 0.001 | 0.004 |
| Alloy-1-A-3b | 88.63 | 0.151 | 3.12 | 0.016 | 6.85 | 0.14 | 0.003 | 0.912 | 0.016 | 0.002 | 0.002 |
| Alloy-1-A-3c | 88.31 | 0.06 | 3.0 | 0.018 | 7.59 | 0.09 | 0.002 | 0.906 | 0.009 | 0.002 | 0.002 |
| Alloy-1-A-3d | 89.37 | 0.169 | 3.19 | 0.018 | 6.23 | 0.074 | 0.001 | 0.921 | 0.011 | 0.002 | 0.003 |
| Alloy-1-A-3e | 89.42 | 0.161 | 3.14 | 0.021 | 6.20 | 0.121 | 0.002 | 0.914 | 0.006 | 0.001 | 0.003 |
| Alloy-1-A-3f | 88.82 | 0.105 | 2.99 | 0.017 | 6.98 | 0.146 | 0.001 | 0.916 | 0.009 | 0.001 | 0.004 |
| Alloy-1-A-3g | 87.05 | 0.126 | 2.84 | 0.016 | 8.92 | 0.132 | 0.005 | 0.886 | 0.010 | 0.002 | 0.002 |
| Alloy-1-A-3h | 87.79 | 0.157 | 2.73 | 0.060 | 8.24 | 0.124 | 0.008 | 0.867 | 0.008 | 0.001 | 0.004 |

FIG. 3A

Table 4 Alloy Group I-A average mechanical properties

| Heat No | UTS (ksi) | YS (ksi) | E% |  | BHN | MoE (Mpsi) |
|---|---|---|---|---|---|---|
| Alloy-1-A-3a | 40.9 | 16.66 | 48 | 61 | 13.3 |  |
| Alloy-1-A-3b | 40.1 | 17.56 | 44 | 65 | 13.7 |  |
| Alloy-1-A-3c | 40.3 | 16.40 | 51 | 66 | 13.2 |  |
| Alloy-1-A-3d | 40.65 | 17.94 | 41 | 62 | 13.7 |  |
| Alloy-1-A-3e | 39.5 | 17.78 | 50 | 61 | 13.8 |  |
| Alloy-1-A-3f | 40.4 | 17.19 | 48 | 63 | 13.5 |  |
| Alloy-1-A-3g | 40.3 | 16.37 | 49 | 62 | 13.3 |  |
| Alloy-1-A-3h | 39.85 | 16.86 | 45 | 61 | 13.3 |  |
| Average | **40.25** | **17.1** | **47** | **63** | **13.5** |  |

FIG. 3B

Table 5 Alloy Group I-B alloy compositions for mechanical property tests

| Heat No | Cu | S | Sn | Pb | Zn | Fe | Sb | Ni | P | Al | Si | Mn |
|---|---|---|---|---|---|---|---|---|---|---|---|---|
| Target Alloy Range | 83-91 | 0.3-0.8 | 2.5-4 | 0.09 | 4-14 | 0.01-0.1 | 0.01-0.02 | 1-1.5 | <0.5 | <0.01 | <0.01 | 0.01-0.8 |
| Alloy-1-B-5a | 87.88 | 0.265 | 2.91 | 0.016 | 7.66 | 0.138 | 0.007 | 1.10 | 0.009 | 0.002 | 0.001 | 0.006 |
| Alloy-1-B-5b | 87.34 | 0.357 | 2.94 | 0.015 | 8.03 | 0.149 | 0.008 | 1.13 | 0.008 | 0.001 | 0.002 | 0.009 |
| Alloy-1-B-5c | 86.64 | 0.236 | 3.57 | 0.011 | 8.17 | 0.112 | 0.005 | 1.12 | 0.010 | 0.002 | 0.003 | 0.011 |
| Alloy-1-B-5d | 84.97 | 0.169 | 4.22 | 0.013 | 10.65 | 0.121 | 0.003 | 1.1 | 0.013 | 0.001 | 0.001 | 0.01 |
| Alloy-1-B-5e | 86.75 | 0.255 | 4.19 | 0.013 | 8.88 | 0.125 | 0.003 | 1.07 | 0.01 | 0.002 | 0.002 | 0.009 |
| Alloy-1-B-5f | 86.74 | 0.253 | 4.21 | 0.014 | 8.93 | 0.121 | 0.004 | 1.05 | 0.01 | 0.001 | 0.002 | 0.009 |
| Alloy-1-B-5h | 83.02 | 0.219 | 3.14 | 0.019 | 12.26 | 0.21 | 0.004 | 1.09 | 0,02 | 0.001 | 0.004 | 0.010 |

FIG. 4A

Table 6 Alloy Group I-B average mechanical properties

| Heat No | UTS, ksi | YS, ksi | %Elong | BHN | Modulus of Elasticity, Mpsi |
|---|---|---|---|---|---|
| Alloy-1-B-5a | 37.85 | 18.00 | 34 | 64 | 13.85 |
| Alloy-1-B-5b | 37.45 | 17.74 | 33 | 64 | 13.65 |
| Alloy-1-B-5c | 39.5 | 17.84 | 31 | 63 | 13.9 |
| Alloy-1-B-5d | 38.9 | 16.88 | 38 | 63 | 13.75 |
| Alloy-1-B-5e | 37.85 | 17.38 | 29 | 63 | 13.7 |
| Alloy-1-B-5f | 38.25 | 18.23 | 30 | 64 | 14.0 |
| Alloy-1-B-5h | 36.6 | 16.25 | 31 | 70 | 13.4 |
| | | | | | |
| **Average** | **38.1** | **17.5** | **32** | **64** | **13.8** |

FIG. 4B

Table 7 Alloy Group II-A alloy compositions for mechanical property tests

| Heat No | Cu | Sn | Zn | Ni | S | P | Pb | Fe | Sb | Al | Si |
|---|---|---|---|---|---|---|---|---|---|---|---|
| Aim | 86-89 | 7.5-8.5 | 2.5-4 | 1.0 | 0.01-0.75 | 0.05 | 0.02 | 0.025-0.5 | 0.05-0.08 | 0.005 | 0.05 |
| Alloy II-A-7a | 87.93 | 8.01 | 2.75 | 0.866 | 0.236 | 0.011 | 0.011 | 0.161 | 0.005 | 0.001 | 0.002 |
| Alloy II-A-7b | 87.94 | 8.03 | 2.59 | 0.836 | 0.375 | 0.008 | 0.012 | 0.179 | 0.006 | 0.001 | 0.003 |
| Alloy II-A-7c | 88.35 | 8.0 | 2.29 | 0.812 | 0.346 | 0.009 | 0.065 | 0.101 | 0.006 | 0.005 | 0.003 |
| Alloy II-A-7d | 87.82 | 8.05 | 2.89 | 0.835 | 0.181 | 0.010 | 0.011 | 0.176 | 0.005 | 0.003 | 0.004 |
| Alloy II-A-7e | 88.03 | 8.01 | 2.47 | 0.978 | 0.321 | 0.012 | 0.007 | 0.151 | 0.003 | 0.001 | 0.003 |
| Alloy II-A-7f | 87.80 | 7.89 | 2.75 | 0.888 | 0.416 | 0.011 | 0.008 | 0.215 | 0.003 | 0.002 | 0.003 |
| Alloy II-A-7g | 88.06 | 7.81 | 2.63 | 0.874 | 0.343 | 0.012 | 0.007 | 0.239 | 0.005 | 0.002 | 0.003 |
| Alloy II-A-7h | 87.84 | 7.95 | 2.77 | 0.890 | 0.322 | 0.013 | 0.045 | 0.246 | 0.005 | 0.002 | 0.003 |

FIG. 5A

Table 8 Alloy Group II-A average mechanical properties

| Heat No | UTS, ksi | YS, ksi | %Elong | BHN | Modulus of Elasticity, Mpsi |
|---|---|---|---|---|---|
| Alloy II-A-7a | 44.3 | 22.9 | 28 | 78 | 14.65 |
| Alloy II-A-7b | 43.8 | 22.9 | 27 | 78 | 15.0 |
| Alloy II-A-7c | 44.2 | 22.8 | 28 | 80 | 14.9 |
| Alloy II-A-7d | 43.8 | 22.7 | 28 | 79 | 15.0 |
| Alloy II-A-7e | 46.0 | 23.2 | 31 | 81 | 15.0 |
| Alloy II-A-7f | 42.8 | 23.1 | 25 | 81 | 14.95 |
| Alloy II-A-7g | 43.6 | 23.3 | 24 | 81 | 14.95 |
| Alloy II-A-7h | 42.0 | 23.5 | 21 | 80 | 14.95 |
|  |  |  |  |  |  |
| **Average** | **43.8** | **23** | **27** | **80** | **15.0** |

FIG. 5B

Table 9: Typical and Minimum Mechanical Properties

| Alloy | UTS, ksi | | YS, ksi | | % Elongation | | Brinell Hardness | Modulus of Elasticity(ksi) | CVN Impact Toughness |
|---|---|---|---|---|---|---|---|---|---|
| | Minimum | Typical | Minimum | Typical | Minimum | Typical | | | |
| Leaded Semi-Red Brass | | | | | | | | | |
| C84400 | 29 | 34 | 13 | 15 | 18 | 26 | 55 | 13,000 | |
| Low-Lead Semi-Red Brasses | | | | | | | | | |
| Alloy I-A | 39.0 | 40.2 | 16.2 | 17.9 | 39 | 47 | 63 | | |
| Alloy I-B | 36.5 | 38.5 | 16.9 | 17.7 | 27 | 32 | 63 | | |
| Sebiloy™ - C89520 | 26.0 | 31.0 | 18.0 | 21.0 | 6 | 10 | 54 | | |
| C89836 | 33.0 | 37.0 | 15.0 | 19.0 | 20 | 30 | 65 | | |
| Biwalite™ -C83470 | 29.0 | 36.0 | | | 17 | 25 | | | |
| Silicon Brass | | | | | | | | | |
| C87500 | 60.0 | 67.0 | 24.0 | 30.0 | 16 | 21 | 115 | 15,400 | |
| Ecobrass™ - C87850 | | 63 | | 26 | | 25 | 78 | 15,400 | |
| Tin Bronze | | | | | | | | | |
| Alloy II-A | 41.1 | 43.8 | 22.8 | 23.0 | 20 | 26.5 | 80 | 14,900 | |
| C90300, Leaded | 40.0 | 45.0 | 18 | 21 | 20 | 30 | 70 | 14,000 | 14 |

FIG. 6

Table 10: Alloys for SEM/EDS Testing Examples

| Alloy Type | Cu | S | Sn | Pb | Zn | Fe | Sb | Ni | P | Al | Si | Mn | Ag | As | Bi |
|---|---|---|---|---|---|---|---|---|---|---|---|---|---|---|---|
| Alloy I-A-10a | 88.94 | 0.16 | 3.39 | 0.02 | 6.49 | 0.07 | >0.01 | 0.92 | 0.010 | <0.01 | <0.01 | <0.01 | <0.01 | <0.01 | <0.01 |
| Alloy I-A-10b | 88.26 | 0.11 | 3.23 | 0.02 | 7.32 | 0.16 | <0.01 | 0.88 | 0.012 | -- | -- | <0.01 | <0.01 | -- | -.01 |
| Alloy I-B-10a | 87.10 | 0.31 | 2.98 | 0.02 | 8.27 | 0.12 | <0.01 | 1.14 | 0.009 | 0.04 | <0.01 | 0.01 | <0.01 | <0.01 | <0.01 |
| Alloy I-B-10b | 90.46 | 0.13 | 3.63 | 0.02 | 4.45 | 0.05 | <0.01 | 1.13 | 0.006 | -- | -- | 0.01 | <0.01 | -- | 0.01 |
| Alloy II-A-10a | 87.83 | 0.30 | 7.92 | <0.01 | 2.76 | 0.17 | <0.01 | 0.92 | 0.011 | <0.01 | <0.01 | <0.01 | 0.03 | <0.01 | 0.06 |
| Alloy II-A-10b | 87.46 | 0.19 | 8.18 | 0.01 | 2.99 | 0.16 | <0.01 | 0.89 | 0.015 | -- | -- | 0.01 | 0.03 | -- | 0.07 |
| Biwalite™ - C83470 | 91.82 | 0.59 | 4.02 | 0.02 | 2.58 | 0.26 | <0.01 | 0.69 | 0.012 | -- | -- | <0.01 | <0.01 | -- | 0.01 |
| Alloy III-A | 63.12 | 0.011 | 1.04 | 0.01 | 34.10 | 0.24 | 0.17 | 1.14 | 0.052 | 0.03 | 0.01 | 0.07 | <0.01 | 0.01 | <0.01 |

FIG. 7

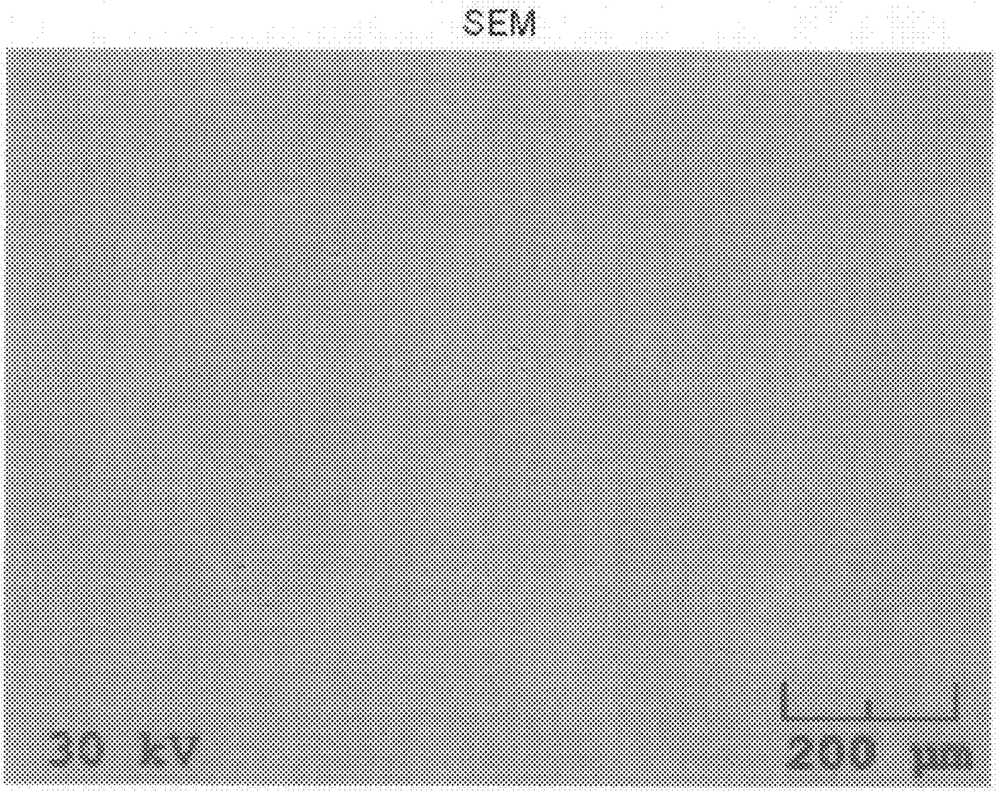

FIGURE 8A

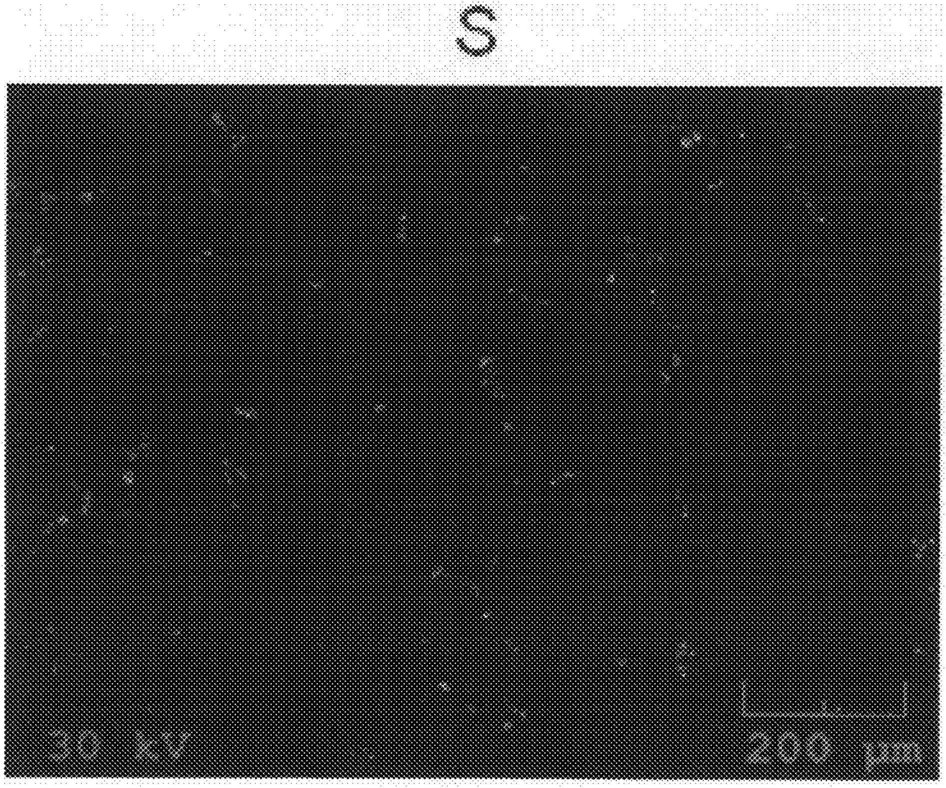

FIGURE 8B

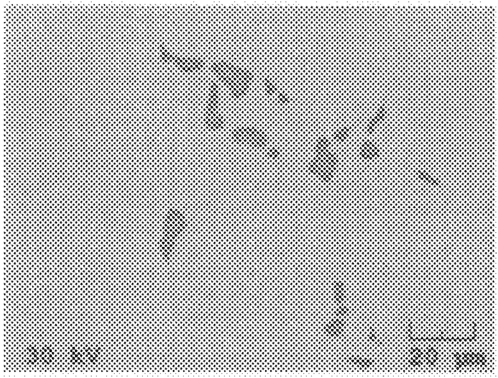

FIGURE 9A

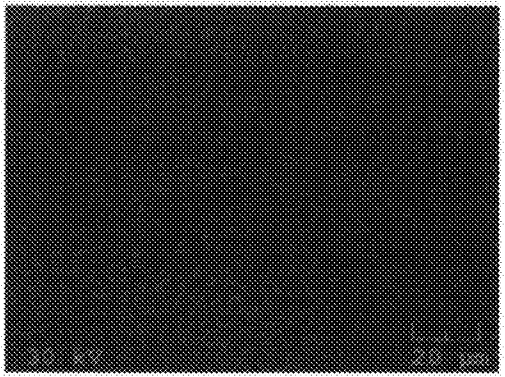

FIGURE 9B

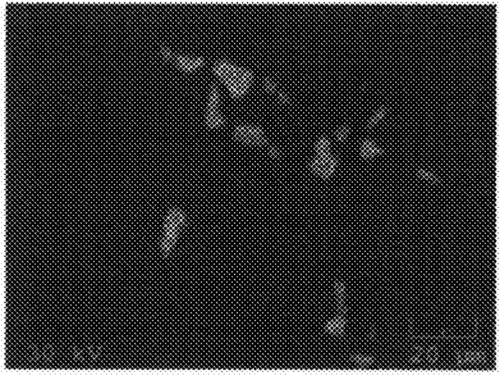

FIGURE 9C

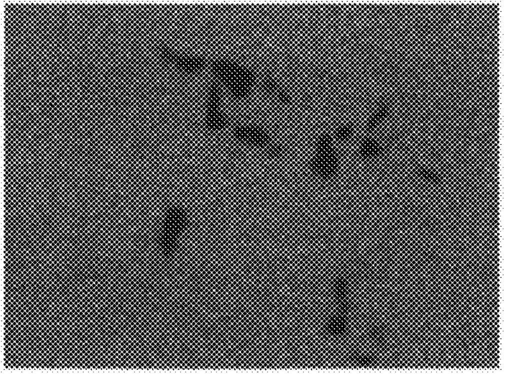

FIGURE 9D

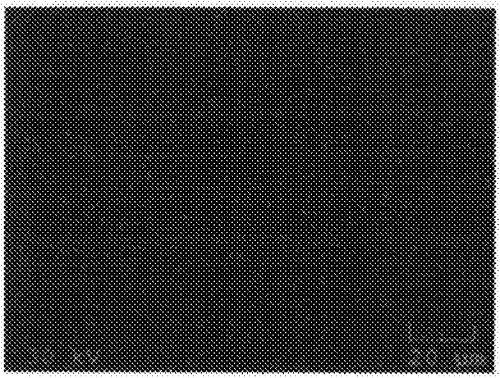

FIGURE 9E

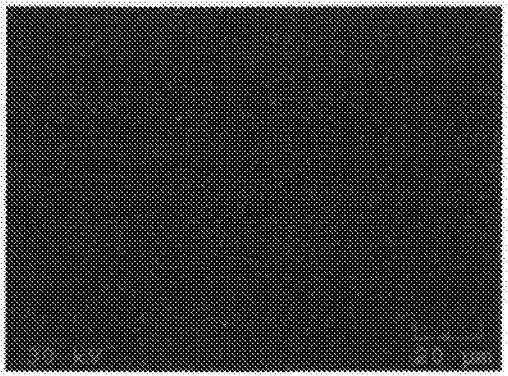

FIGURE 9F

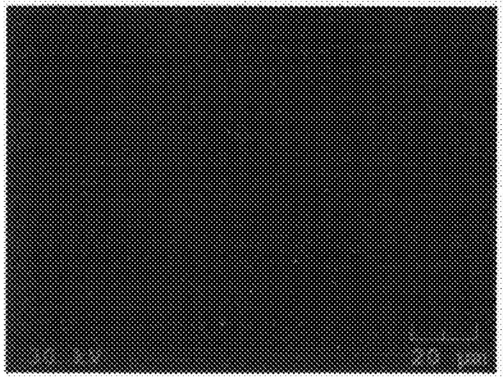

FIGURE 9G

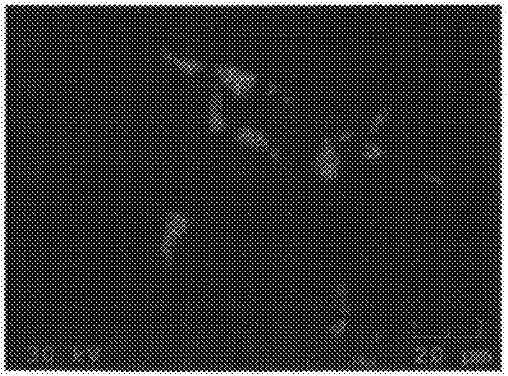

FIGURE 9H

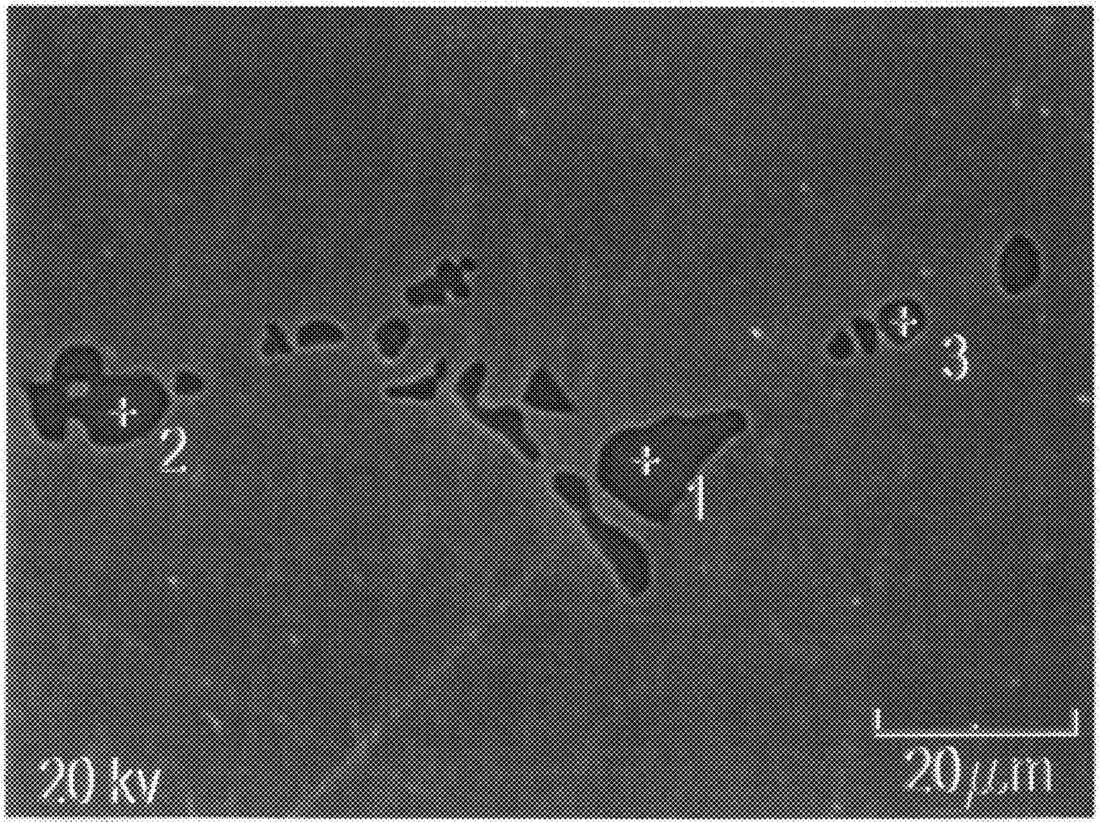

FIG. 10A

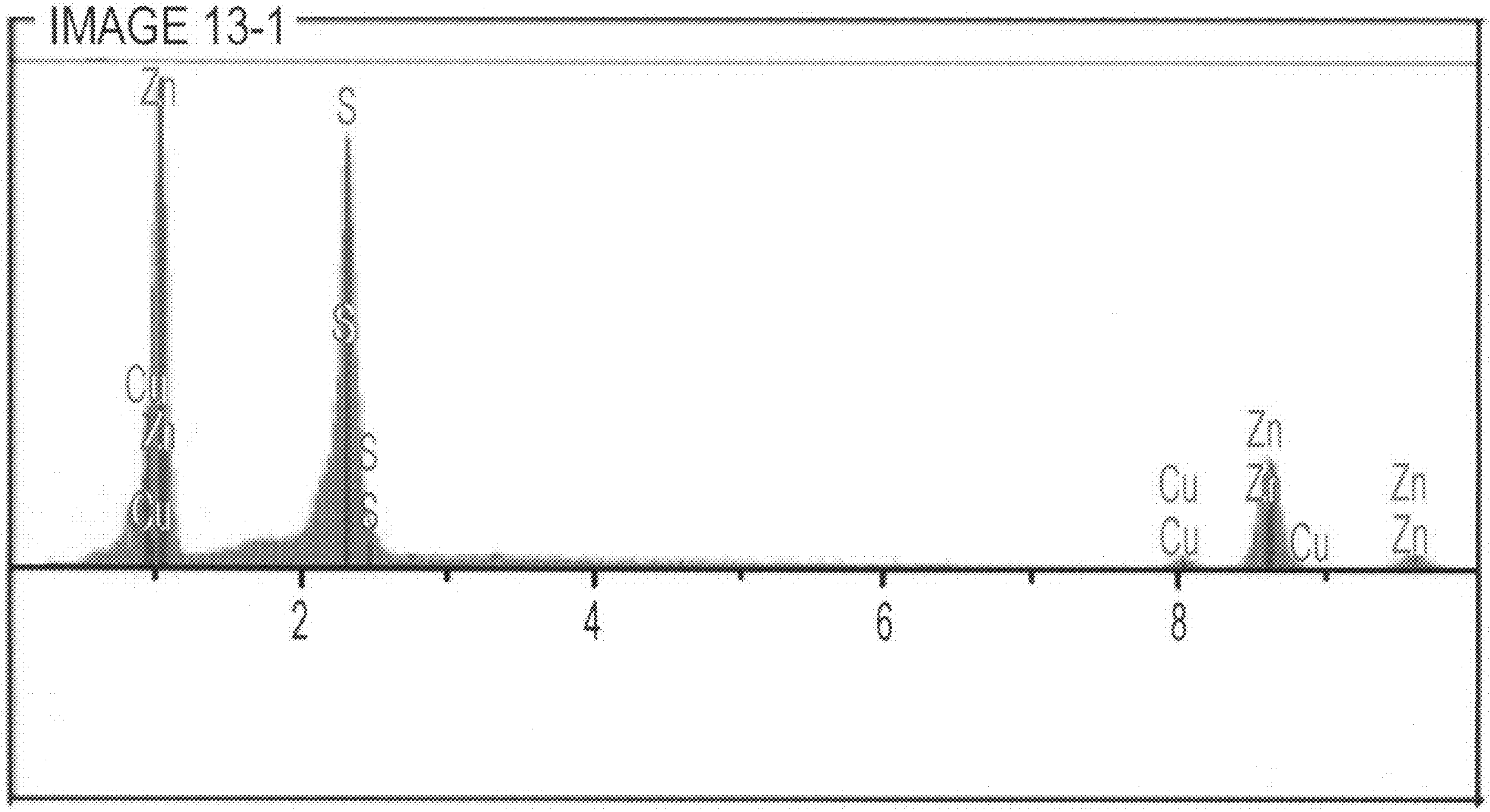

FIG. 10B

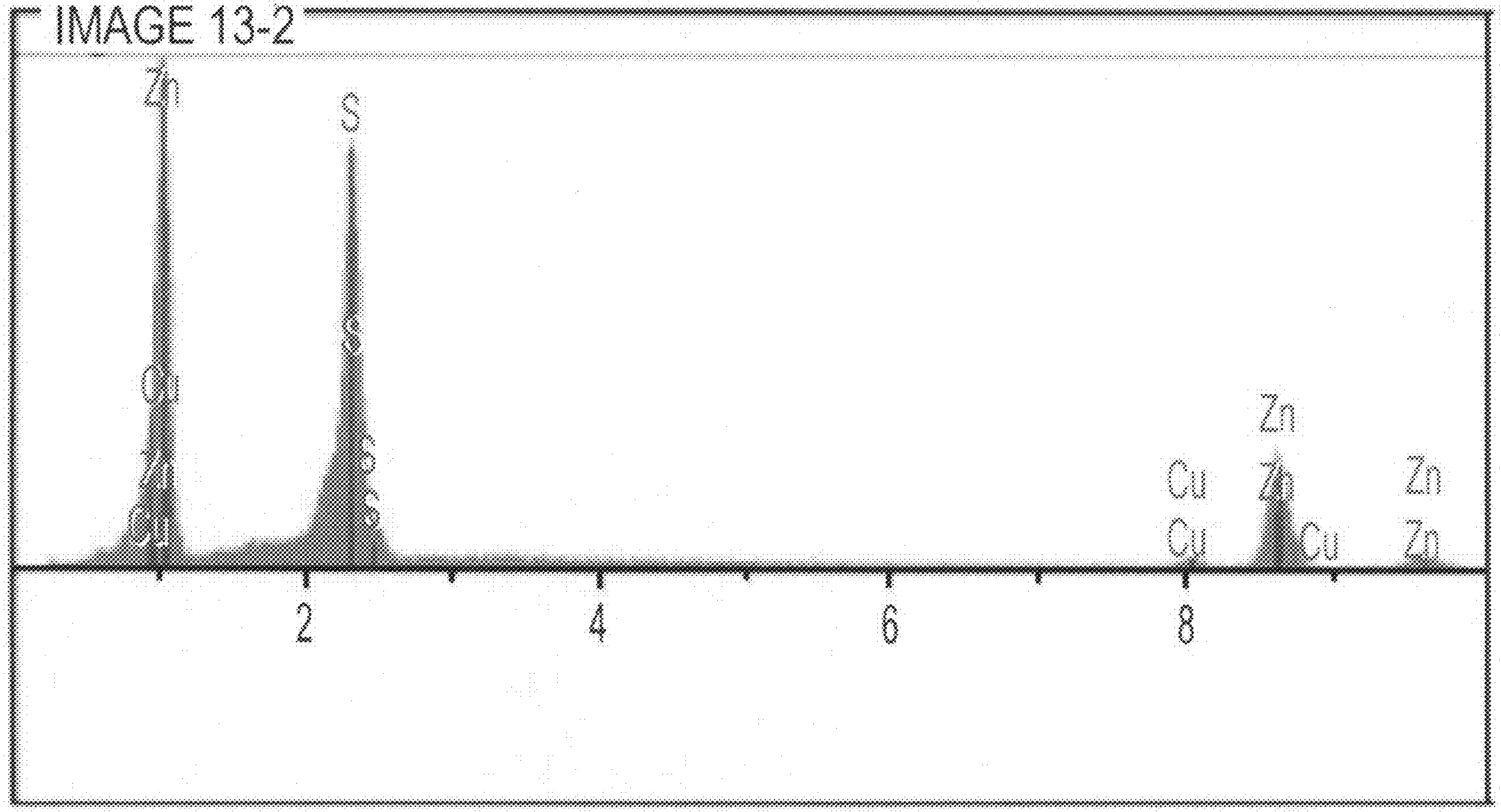

FIG. 10C

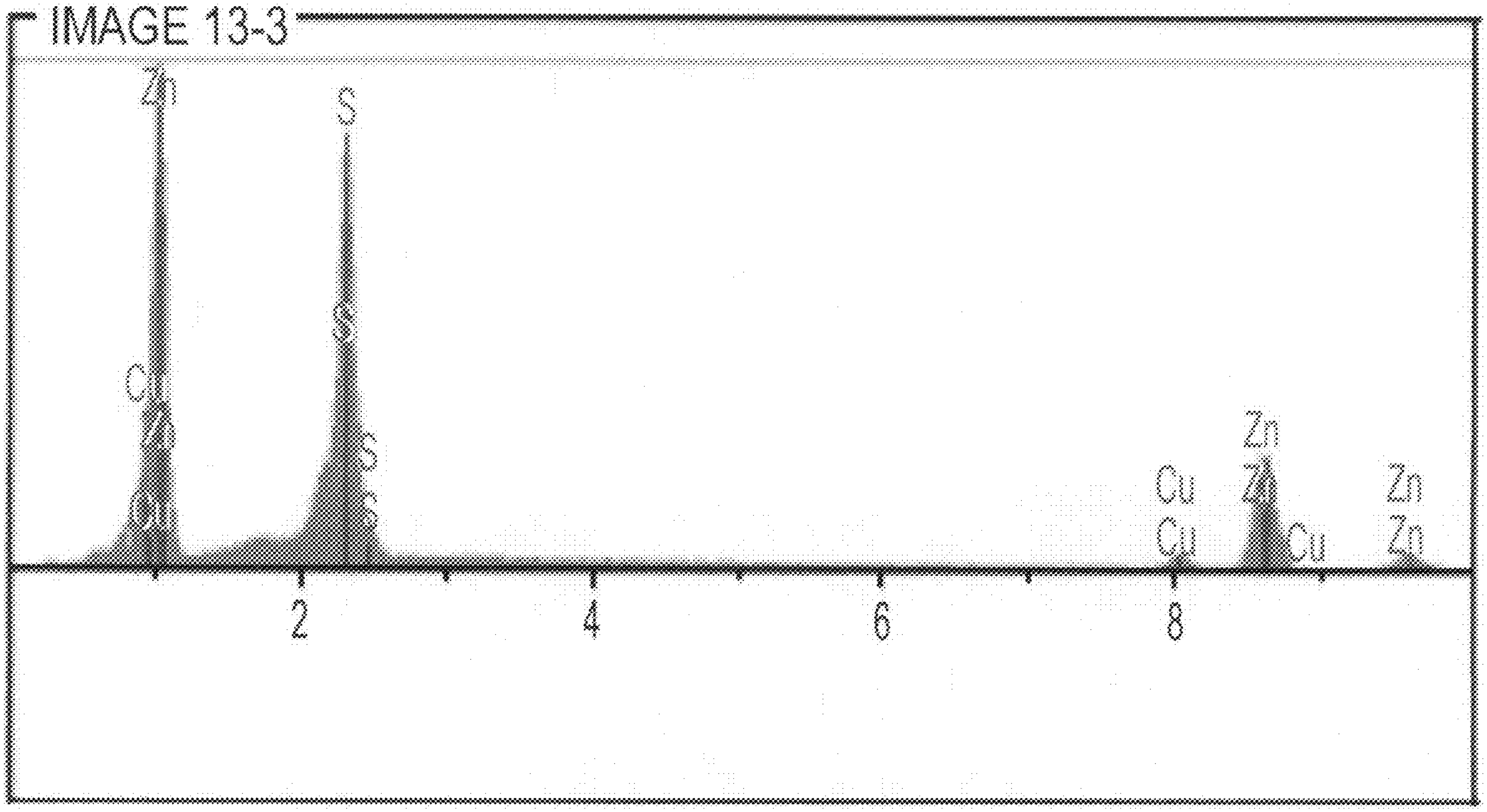

FIG. 10D

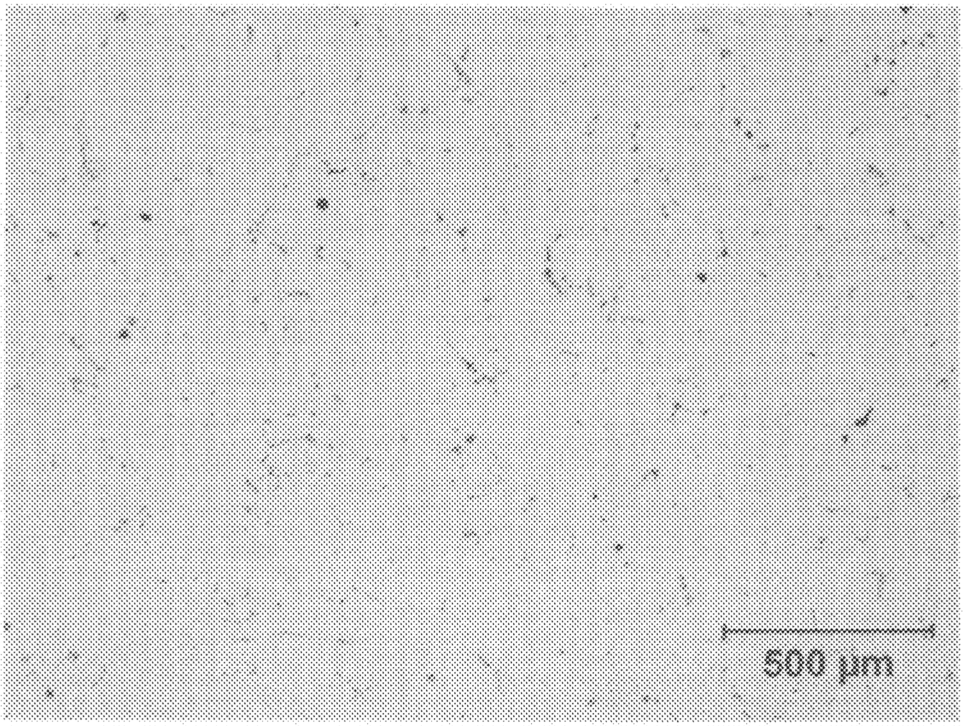

FIGURE 11A

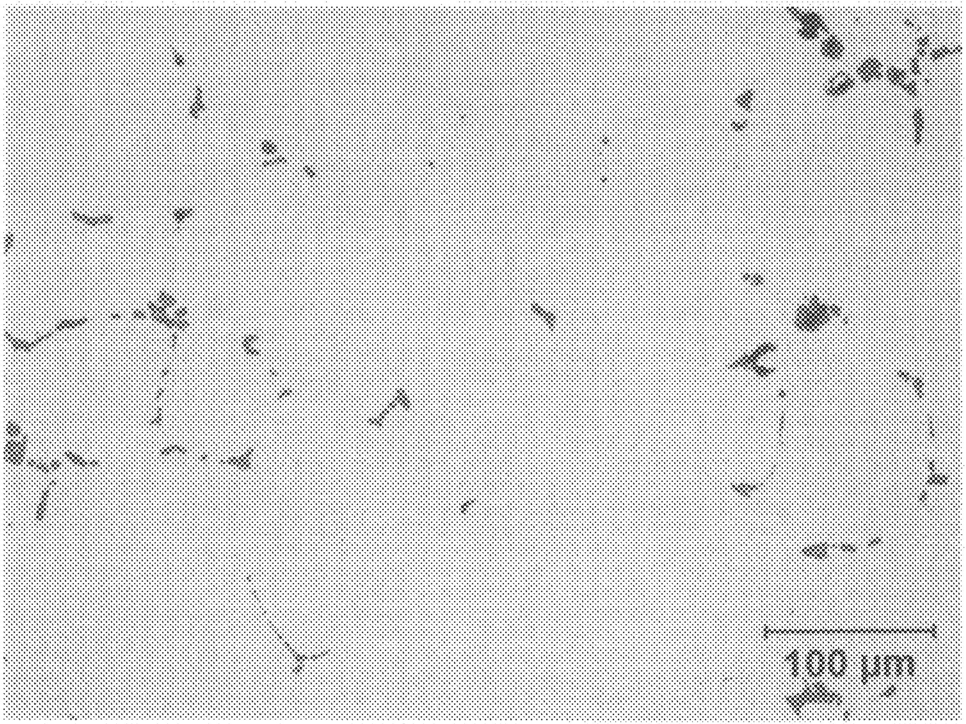

FIGURE 11B

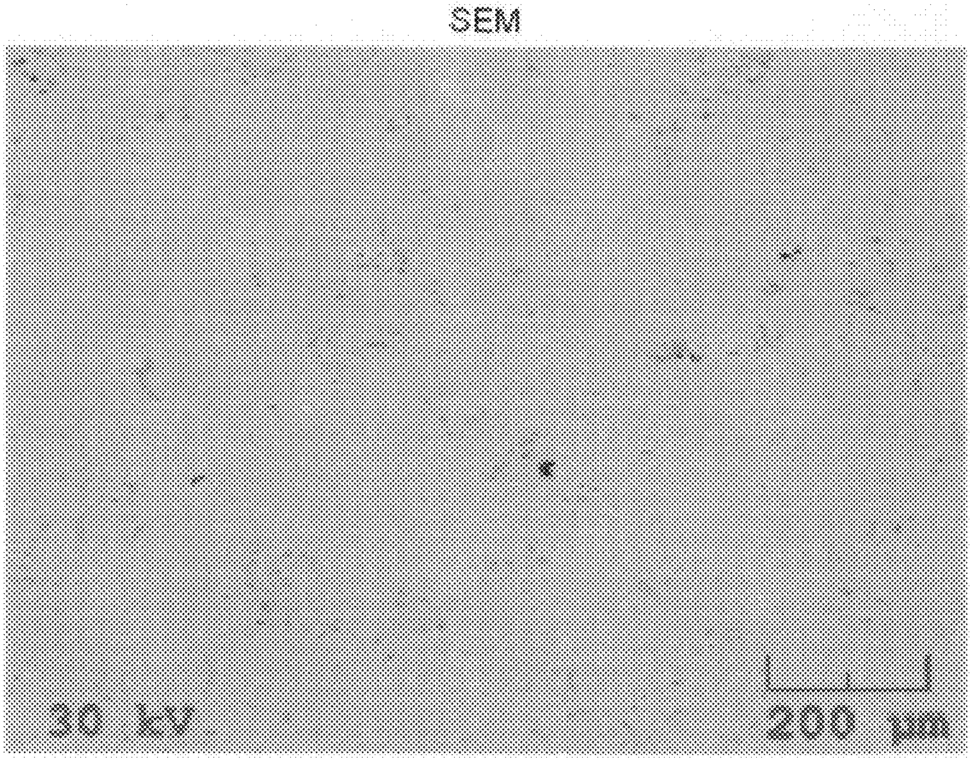

FIGURE 12A

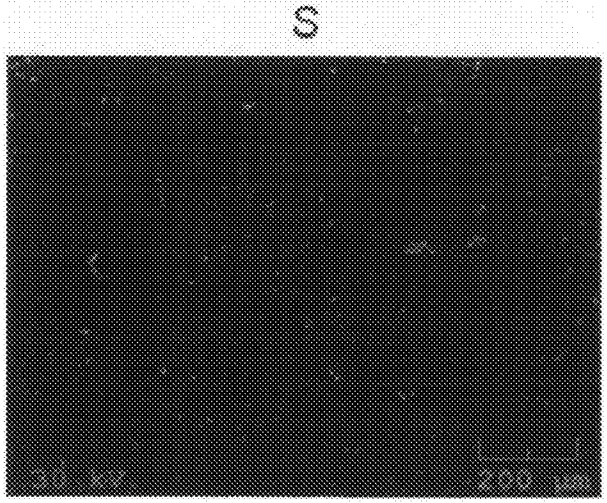

FIGURE 12B

SEM FIGURE 13A

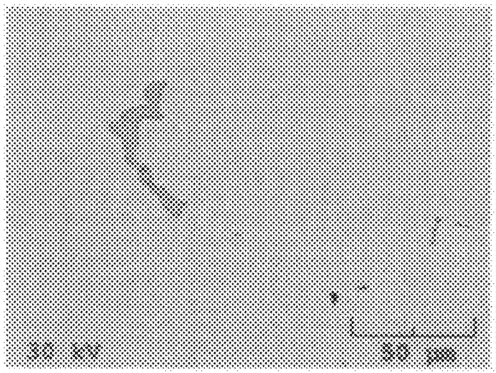

Sn FIGURE 13B

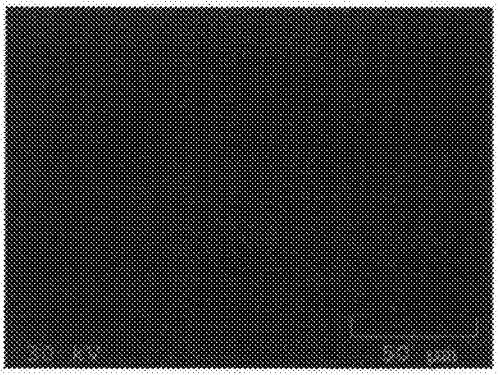

Zn FIGURE 13C

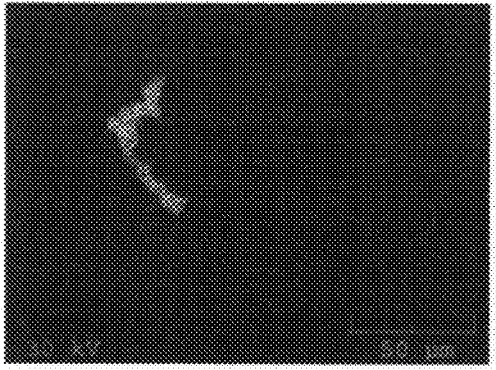

Cu FIGURE 13D

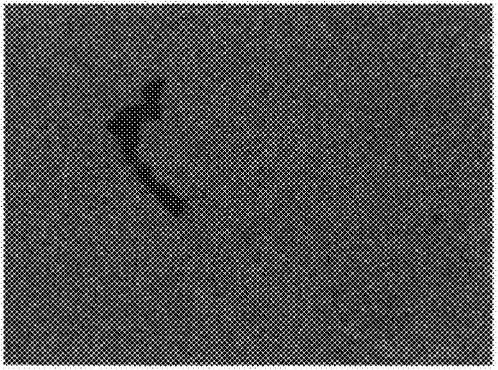

Fe FIGURE 13E

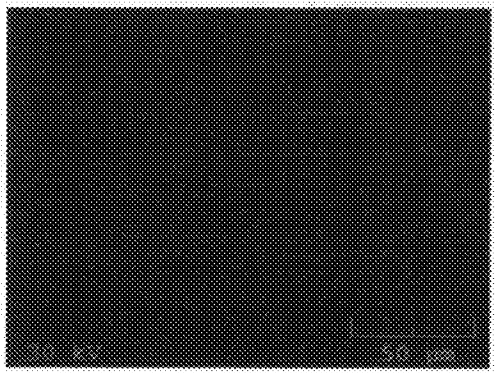

Ni FIGURE 13F

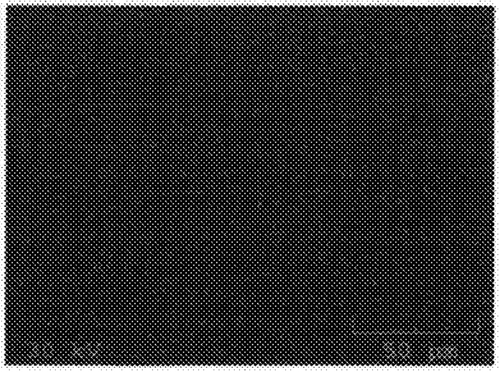

P FIGURE 13G

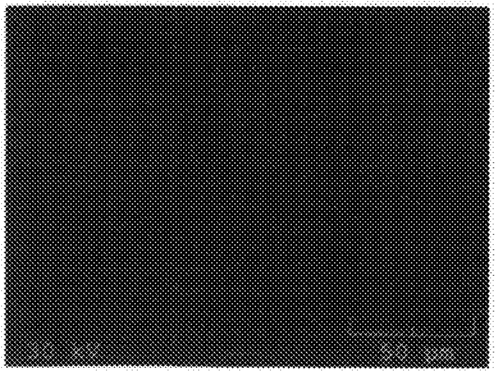

S FIGURE 13H

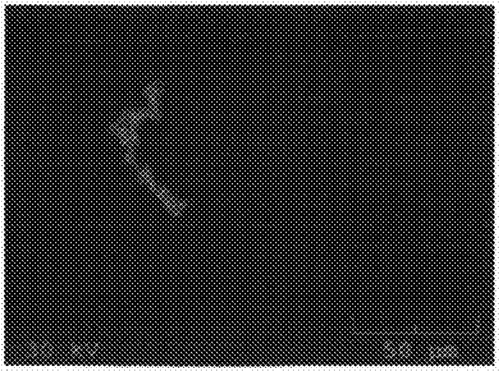

FIGURE 14A

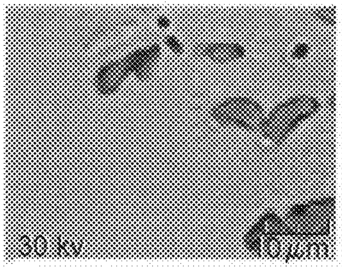

FIGURE 14B

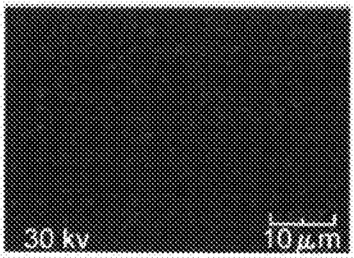

FIGURE 14C

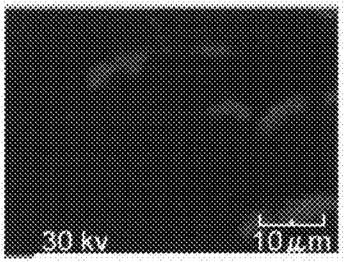

FIGURE 14D

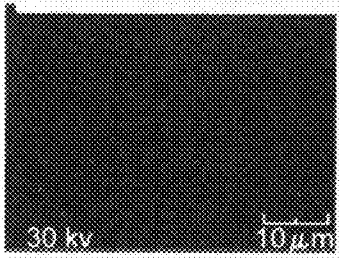

FIGURE 14E

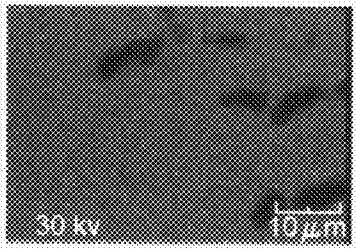

FIGURE 14F

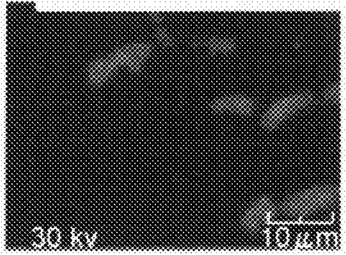

FIGURE 14G

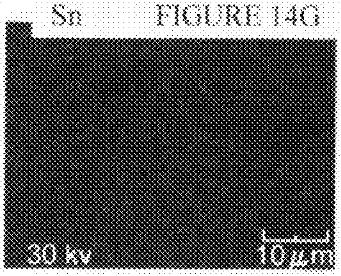

FIGURE 14H

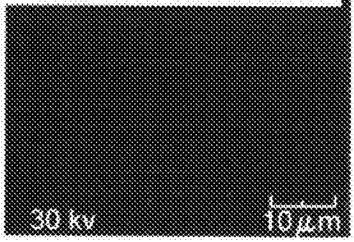

FIGURE 14I

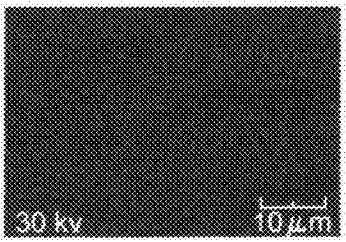

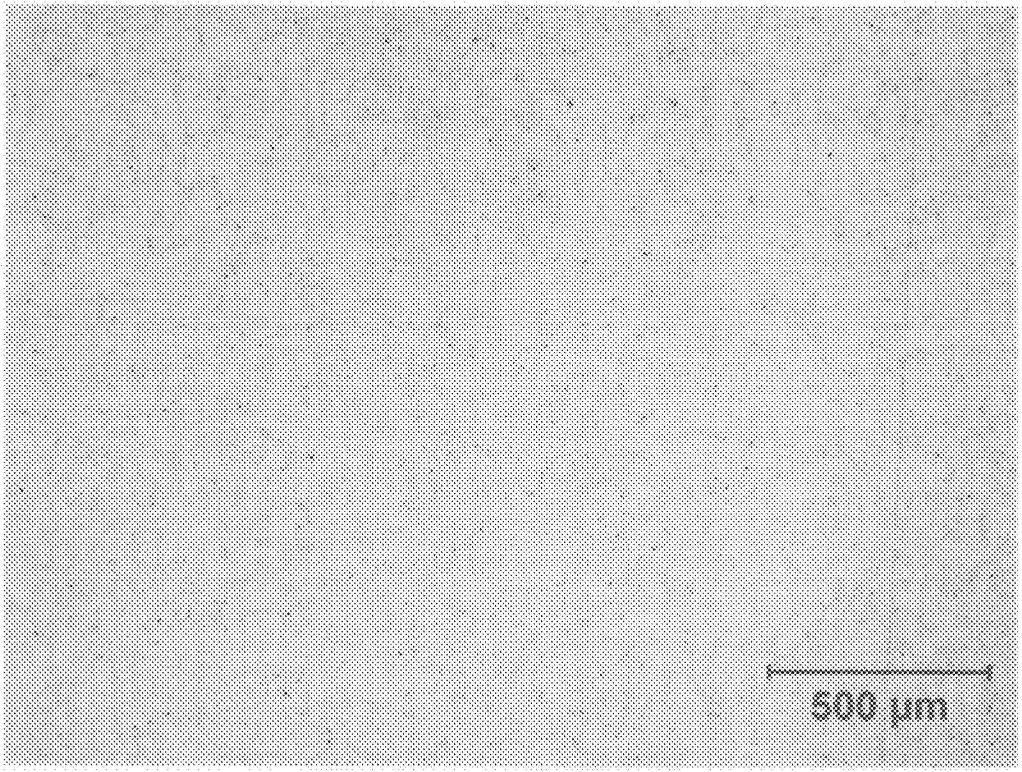

FIGURE 15A

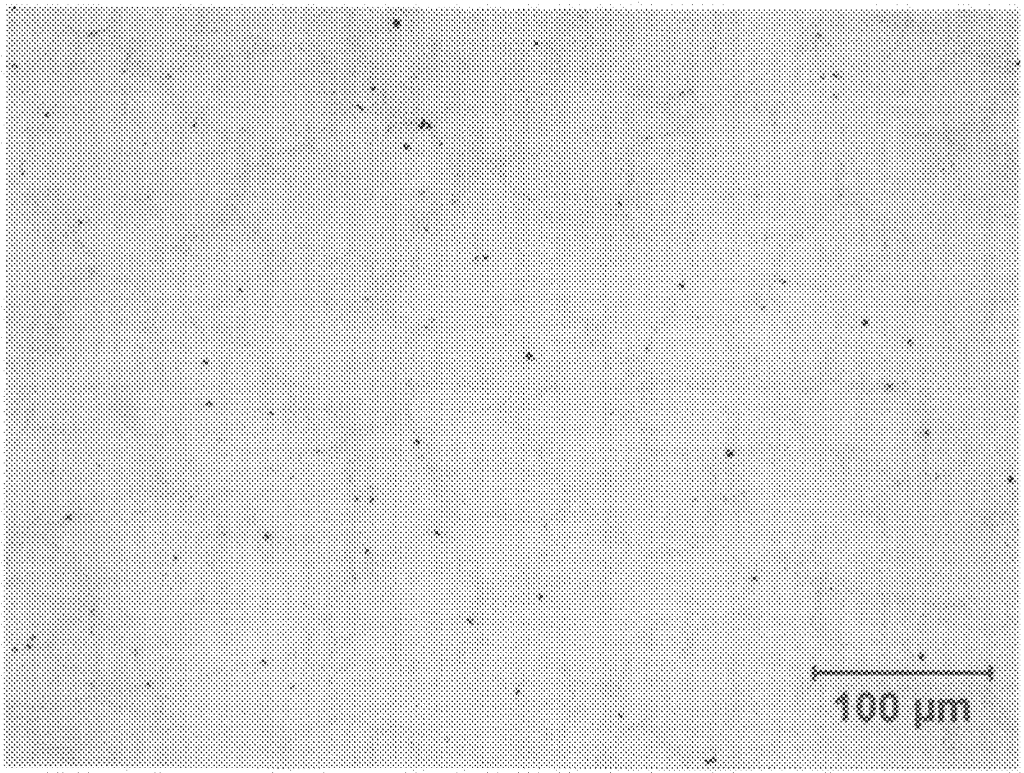

FIGURE 15B

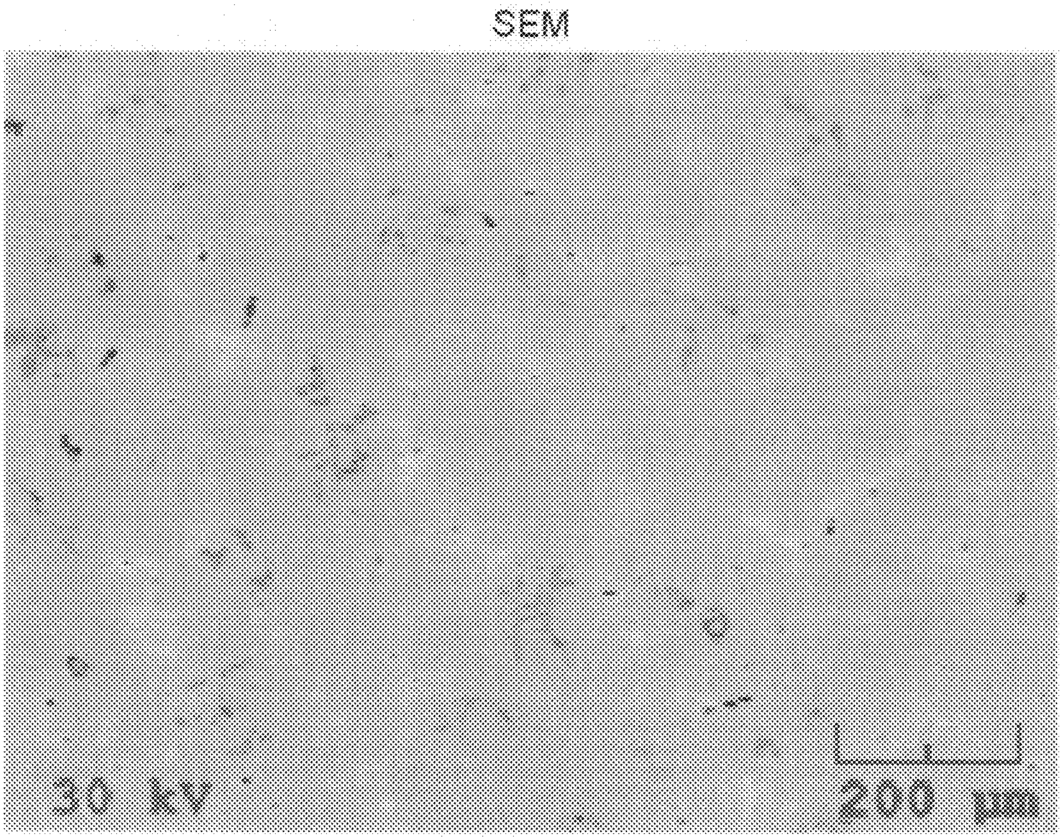

FIGURE 16A

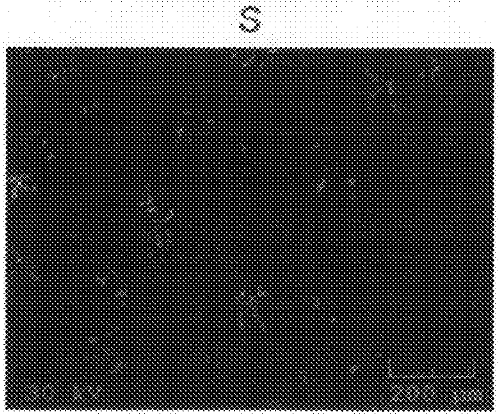

FIGURE 16B

SEM FIGURE 17A

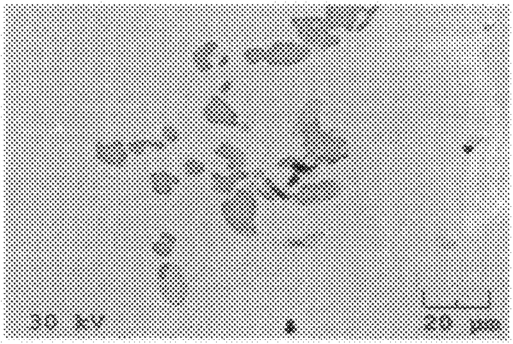

Sn FIGURE 17B

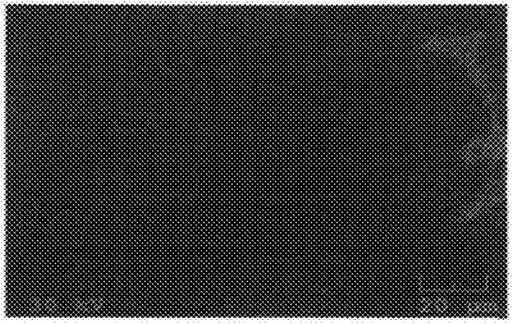

Zn FIGURE 17C

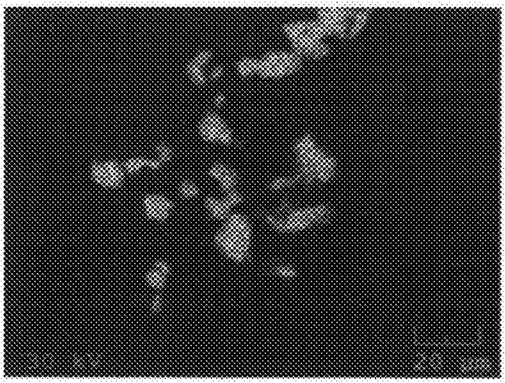

Cu FIGURE 17D

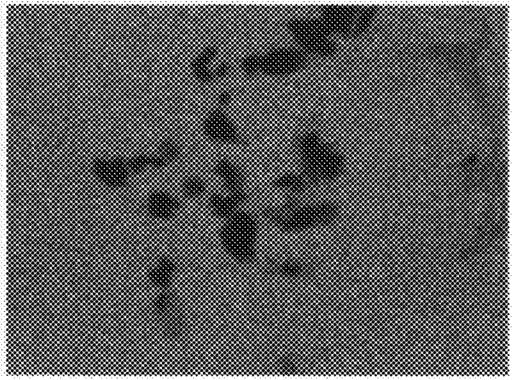

Fe FIGURE 17E

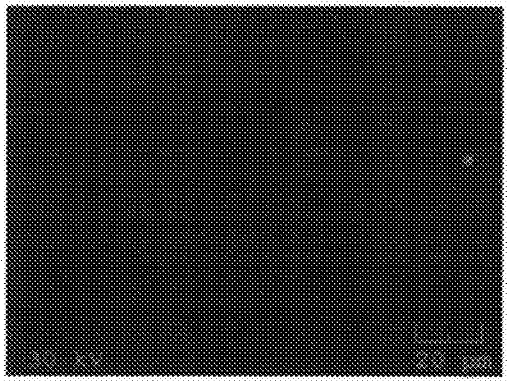

Ni FIGURE 17F

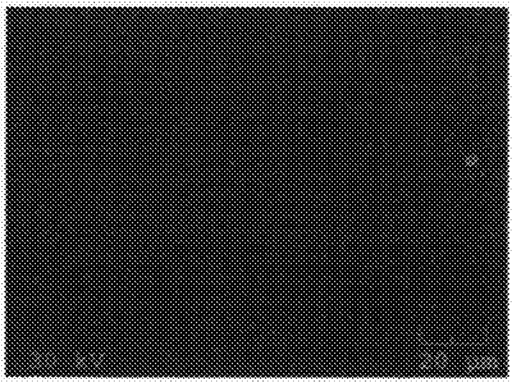

P FIGURE 17G

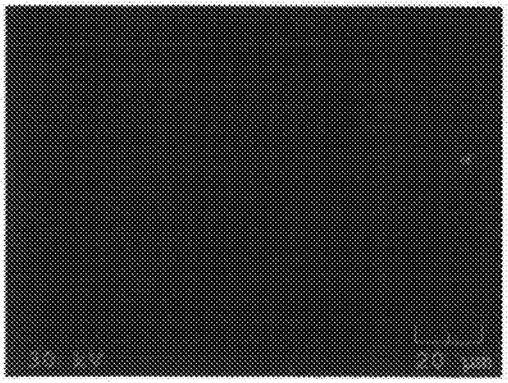

S FIGURE 17H

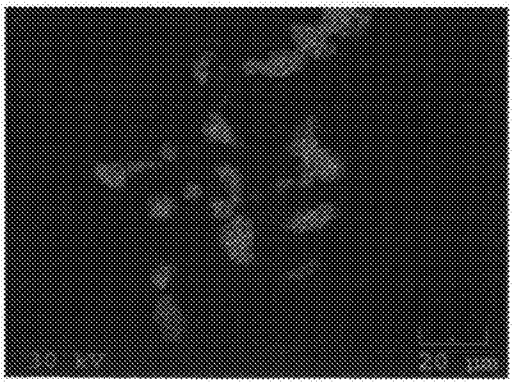

SEM FIGURE 18A

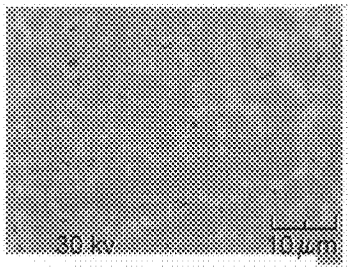

Si FIGURE 18B

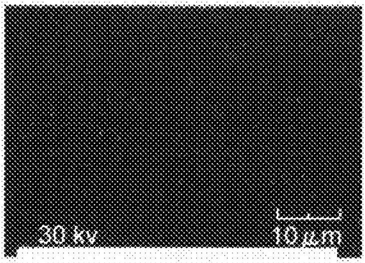

S FIGURE 18C

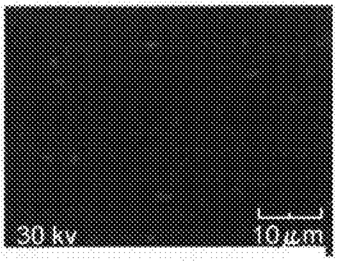

Fe FIGURE 18D

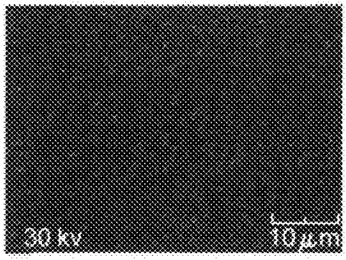

Cu FIGURE 18E

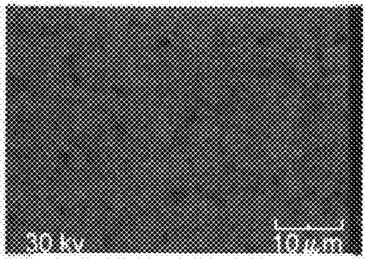

Zn FIGURE 18F

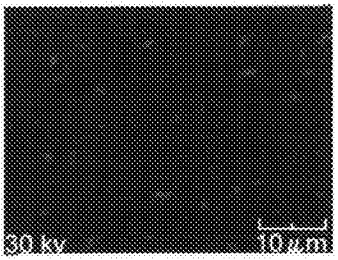

Sn FIGURE 18G

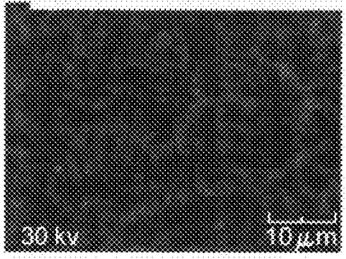

Pb FIGURE 18H

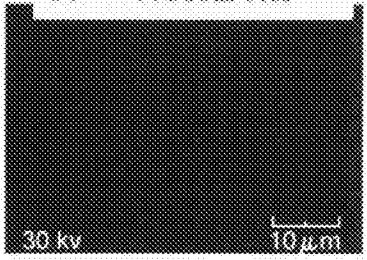

Ni FIGURE 18I

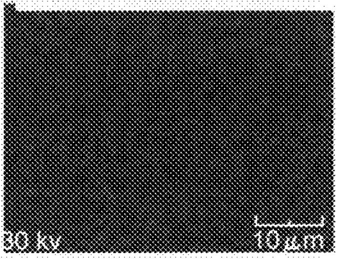

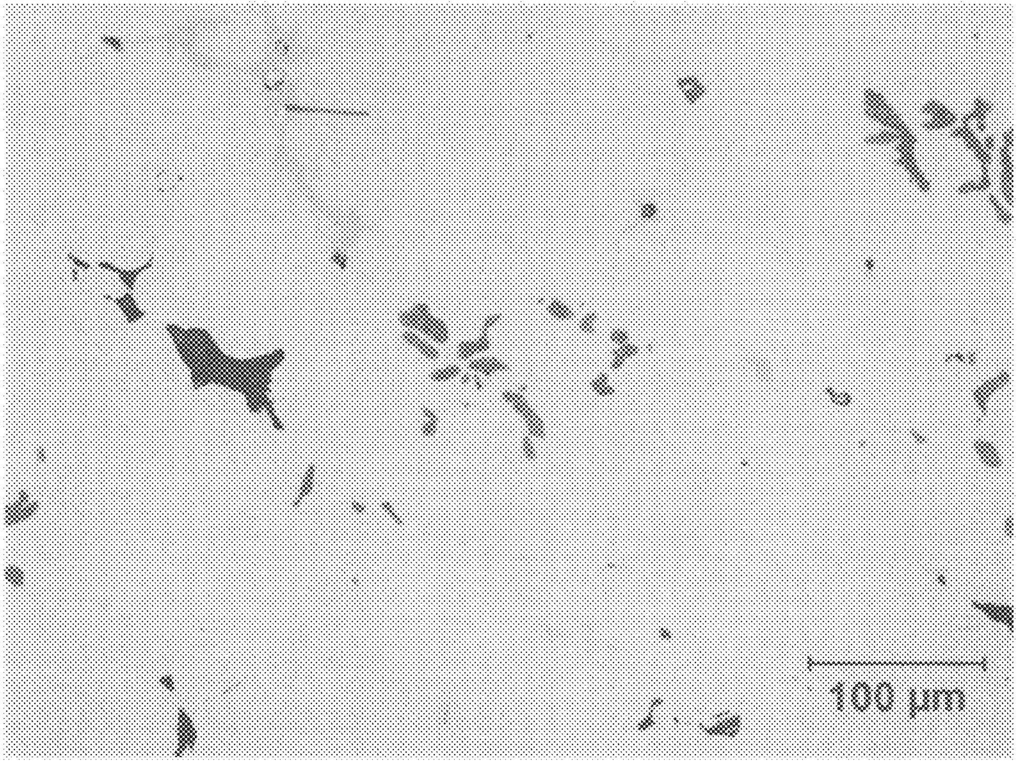

FIGURE 19A

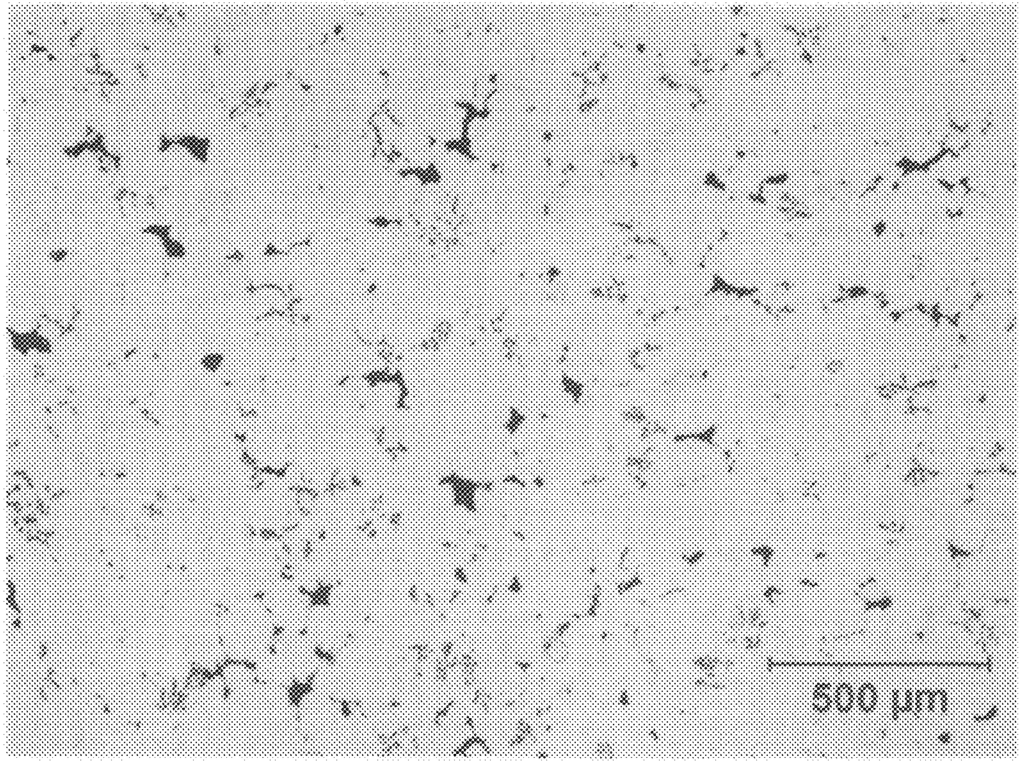

FIGURE 19B

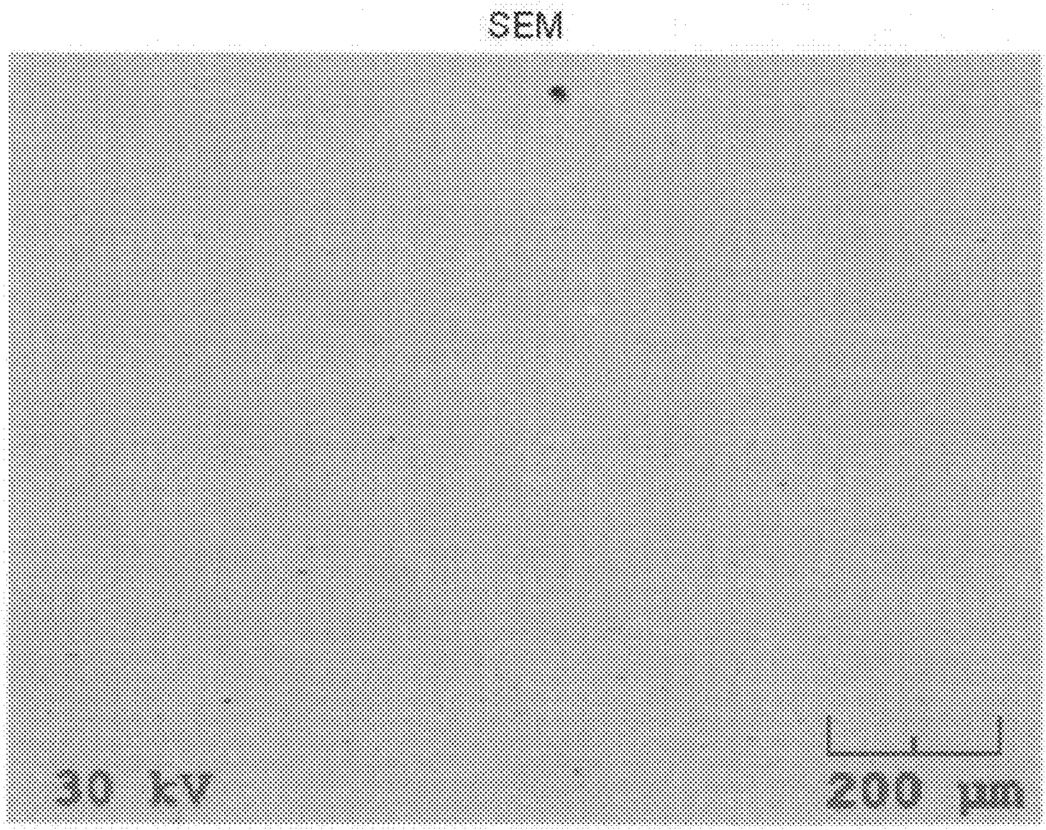

FIGURE 20A

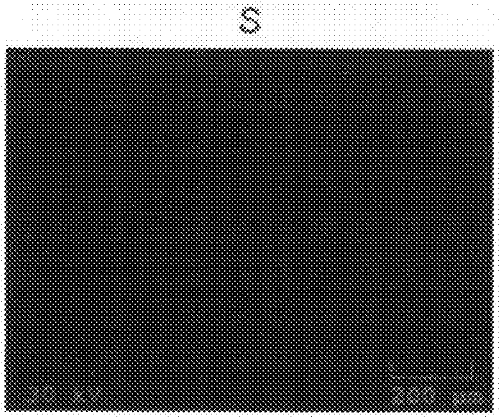

FIGURE 20B

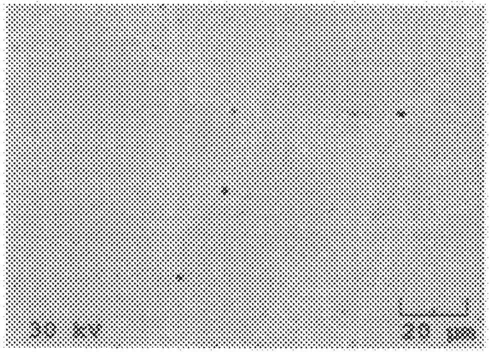

FIGURE 21A

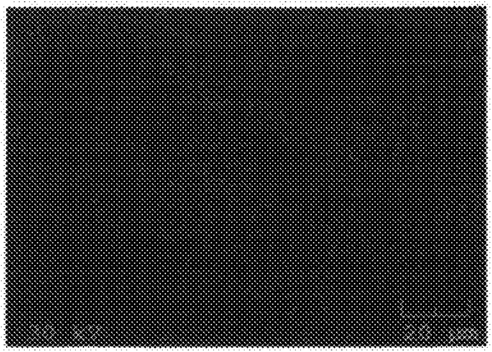

FIGURE 21B

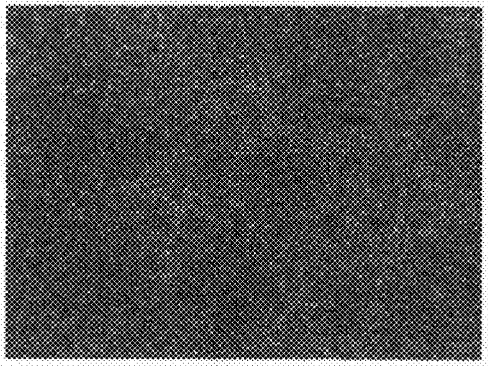

FIGURE 21C

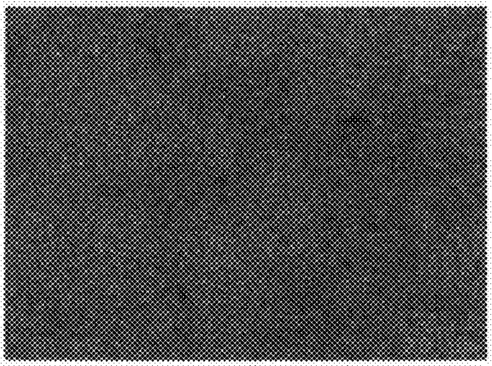

FIGURE 21D

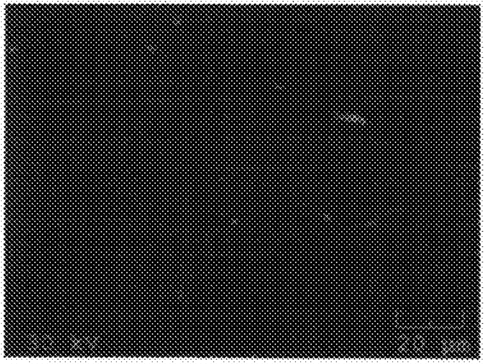

FIGURE 21E

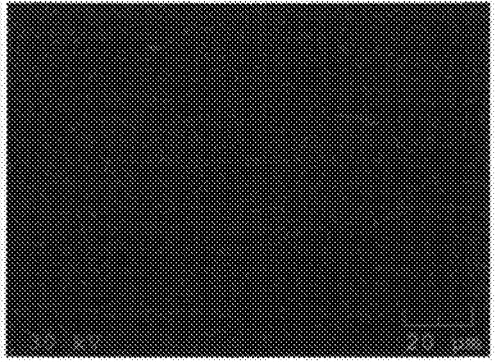

FIGURE 21F

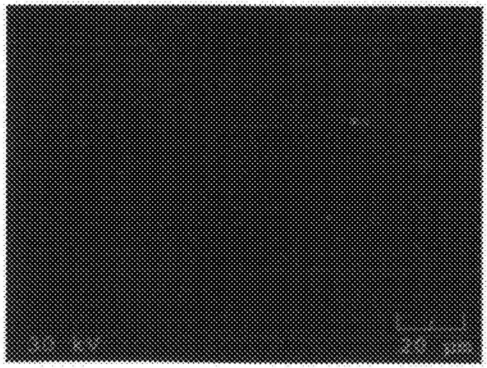

FIGURE 21G

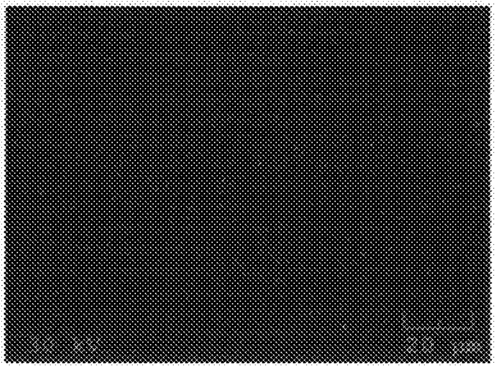

FIGURE 21H

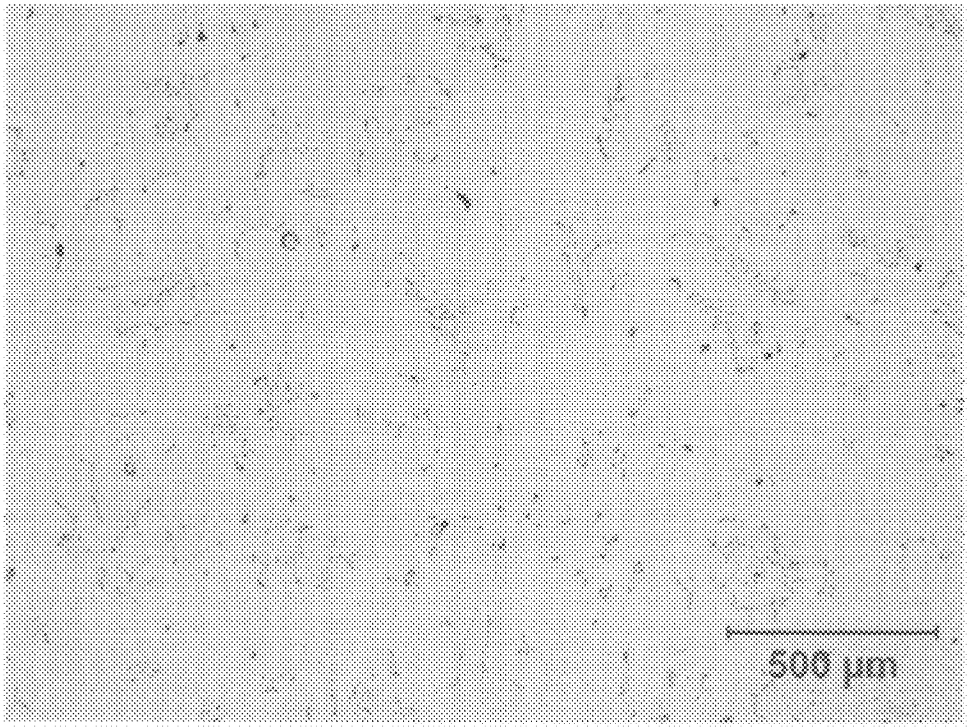

FIGURE 22A

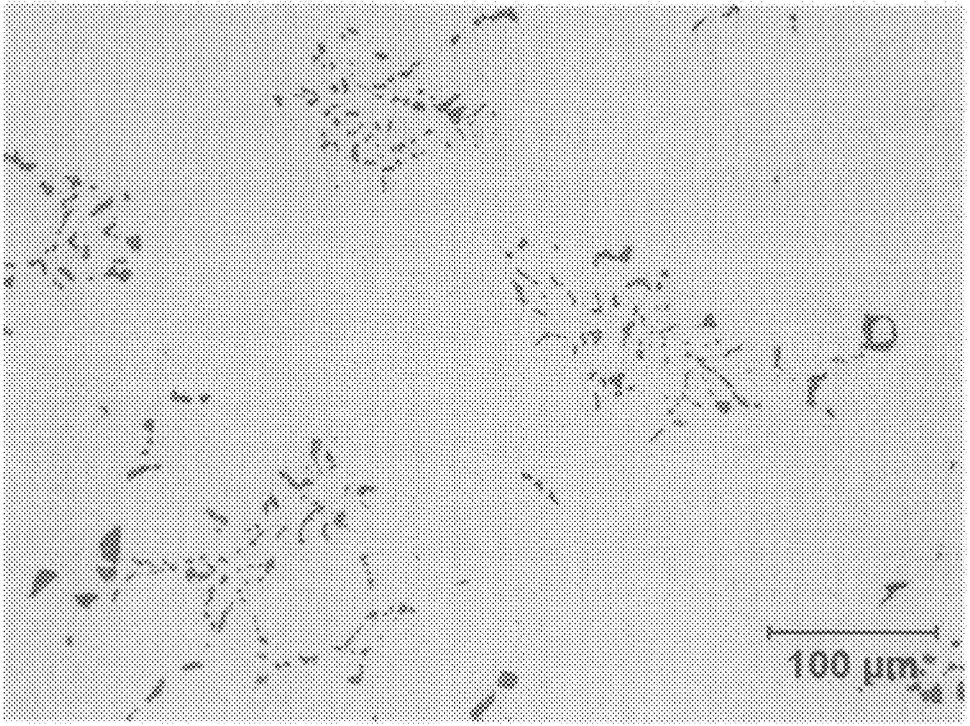

FIGURE 22B

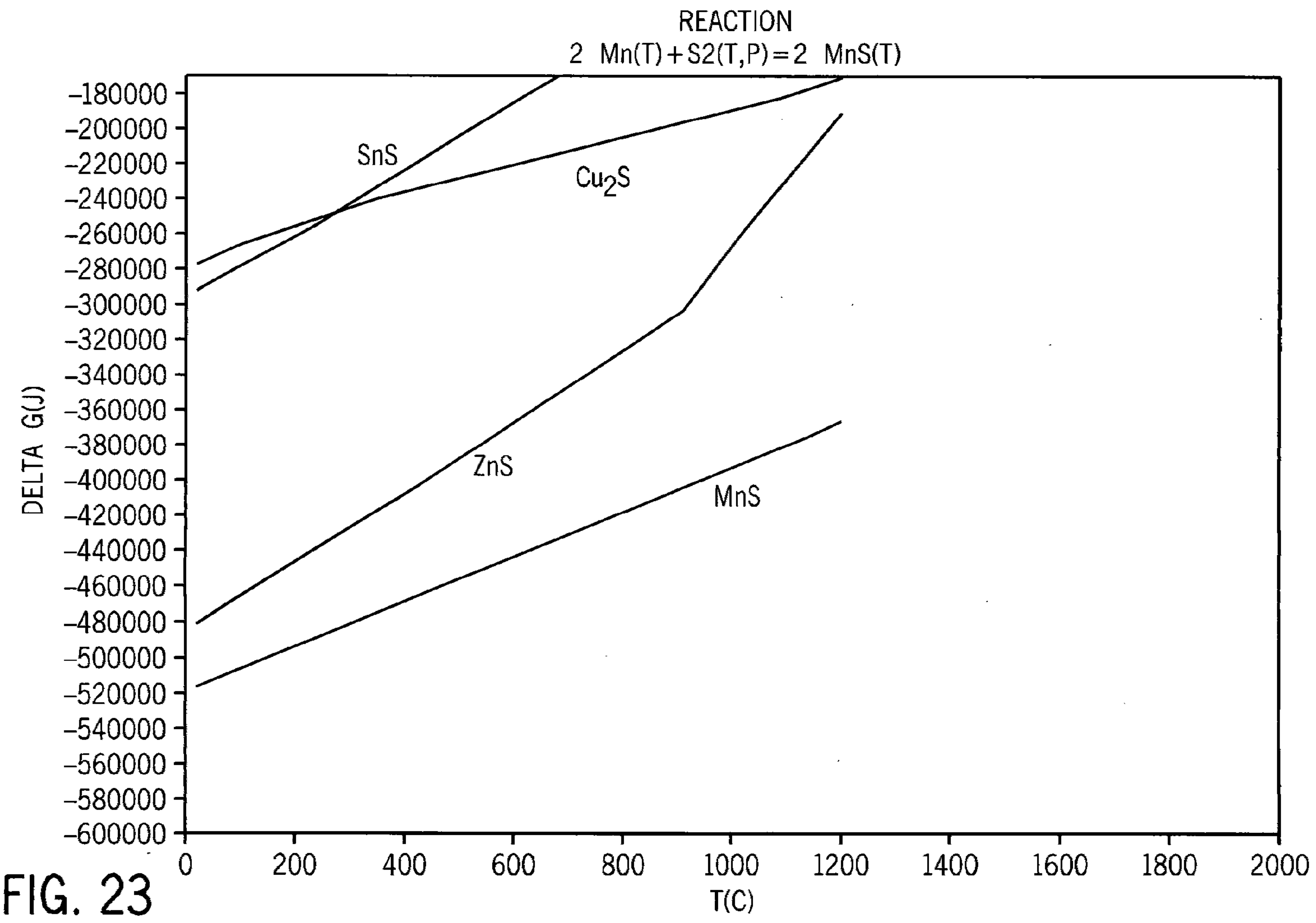
REACTION
2 Mn(T)+S2(T,P)=2 MnS(T)
DELTA G(J)
-180000
-200000
-220000
-240000
-260000
-280000
-300000
-320000
-340000
-360000
-380000
-400000
-420000
-440000
-460000
-480000
-500000
-520000
-540000
-560000
-580000
-600000
0
200
400
600
800
1000
1200
1400
1600
1800
2000
T(C)
SnS
Cu2S
ZnS
MnS

FIG. 23

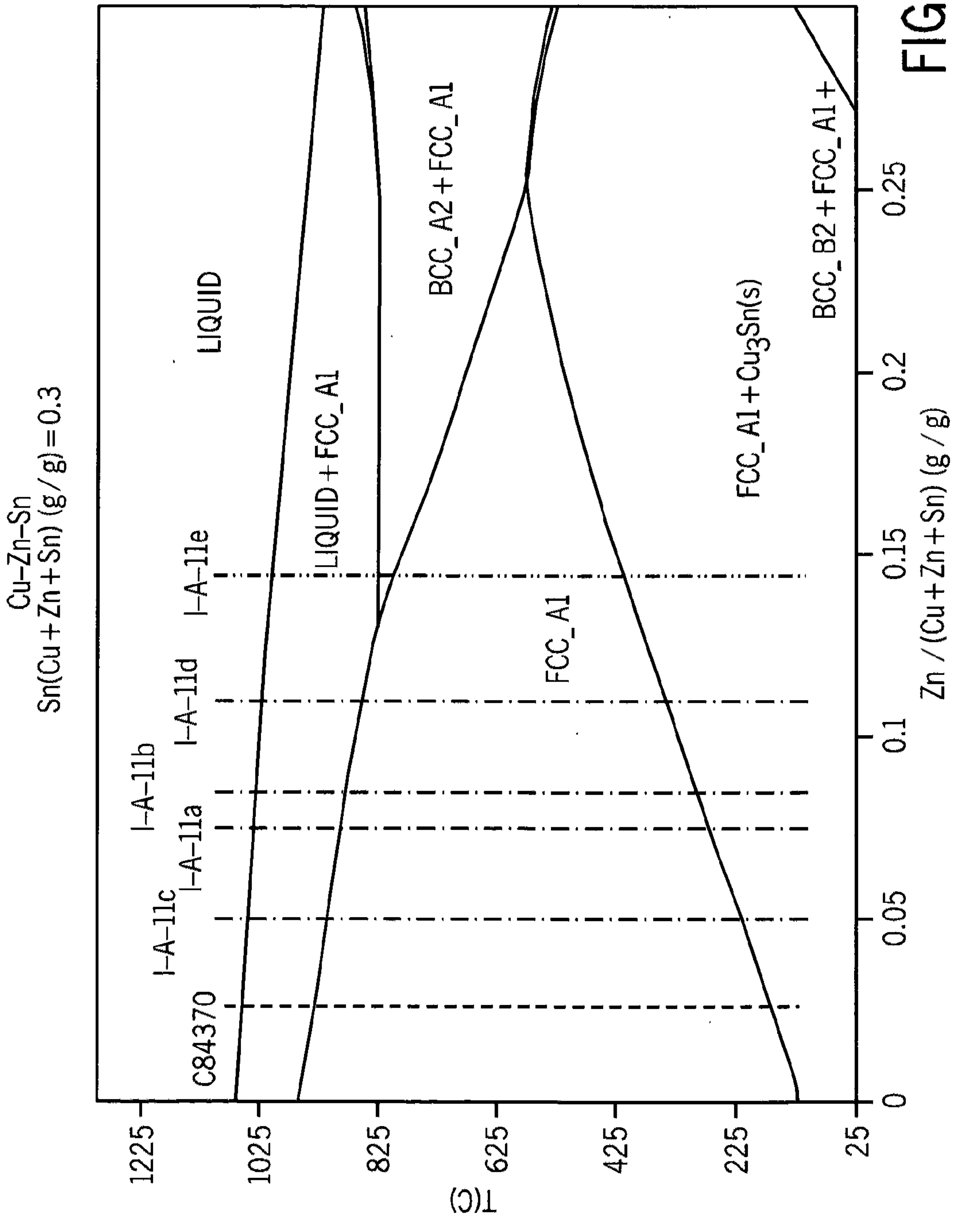
Cu–Zn–Sn
Sn(Cu+Zn+Sn) (g/g)=0.3
T(C)
1225
1025
825
625
425
225
25
0
0.05
0.1
0.15
0.2
0.25
Zn /(Cu+Zn+Sn) (g/g)
LIQUID
LIQUID+FCC_A1
BCC_A2+FCC_A1
FCC_A1
FCC_A1+$Cu_3Sn(s)$
BCC_B2+FCC_A1+
C84370
I–A–11c
I–A–11a
I–A–11b
I–A–11d
I–A–11e

FIG. 24

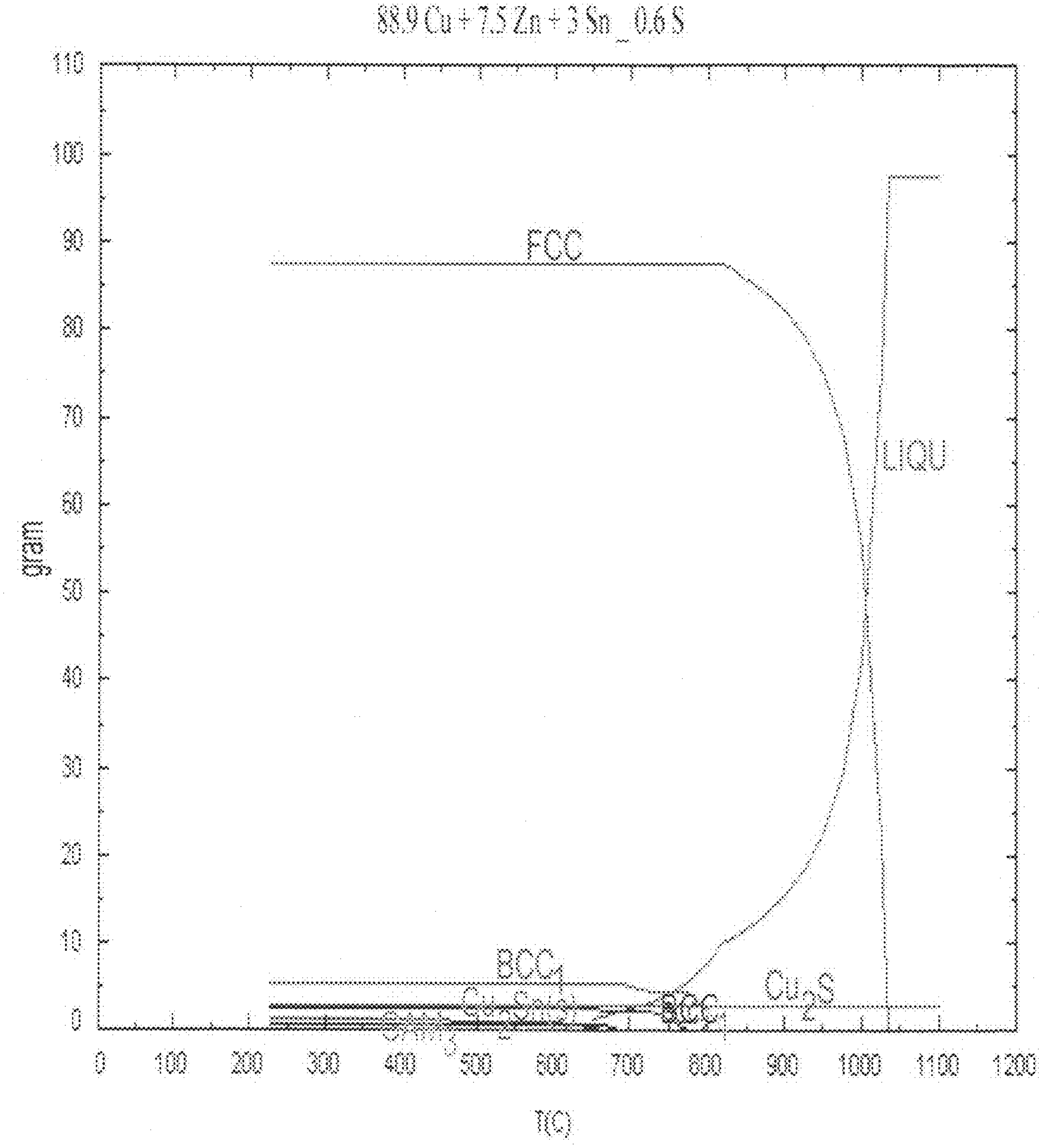
88.9 Cu + 7.5 Zn + 3 Sn _ 0.6 S
110
100
90
80
70
60
50
40
30
20
10
0
gram
FCC
LIQU
BCC1
Cu2Sn
BCC
Cu2S
0
100
200
300
400
500
600
700
800
900
1000
1100
1200
T(C)

FIG. 25A

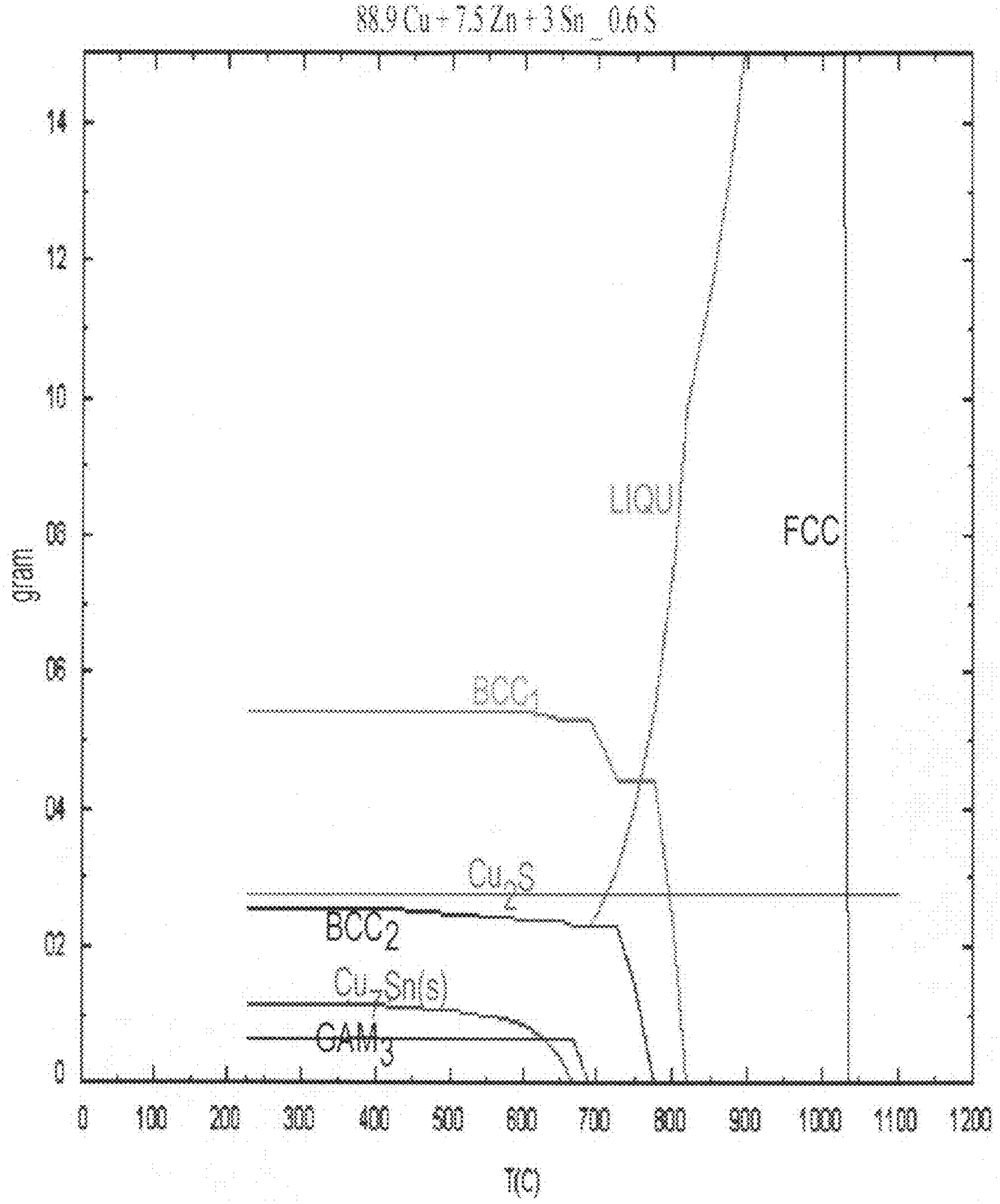
88.9 Cu + 7.5 Zn + 3 Sn _ 0.6 S
gram
T(C)
LIQU
FCC
BCC1
Cu2S
BCC2
Cu7Sn(s)
GAM3
0
02
04
06
08
10
12
14
0
100
200
300
400
500
600
700
800
900
1000
1100
1200

FIG. 25B

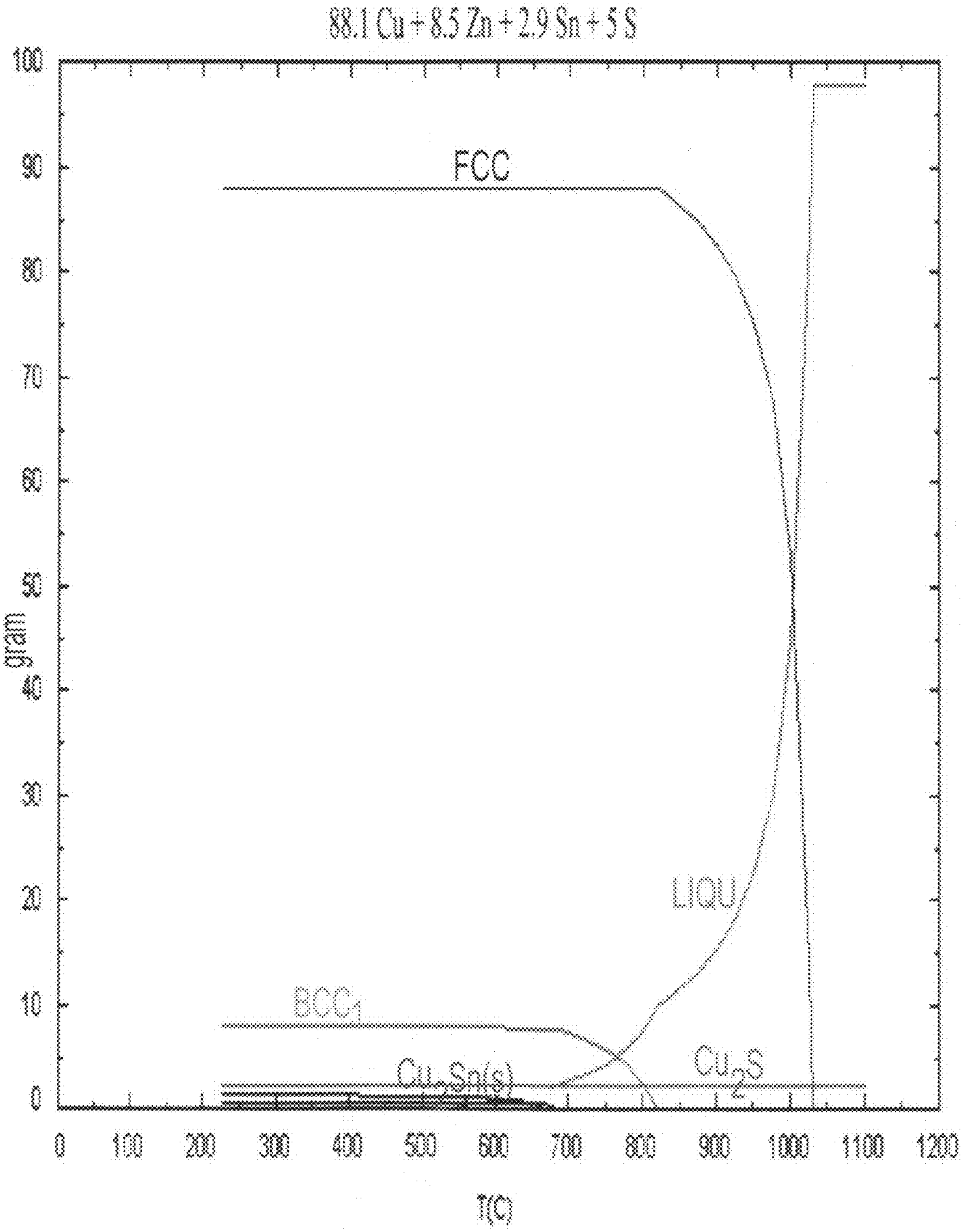
88.1 Cu + 8.5 Zn + 2.9 Sn + 5 S
gram
100
90
80
70
60
50
40
30
20
10
0
FCC
LIQU
$BCC_1$
$Cu_3Sn(s)$
$Cu_2S$
0
100
200
300
400
500
600
700
800
900
1000
1100
1200
T(C)

FIG. 26A

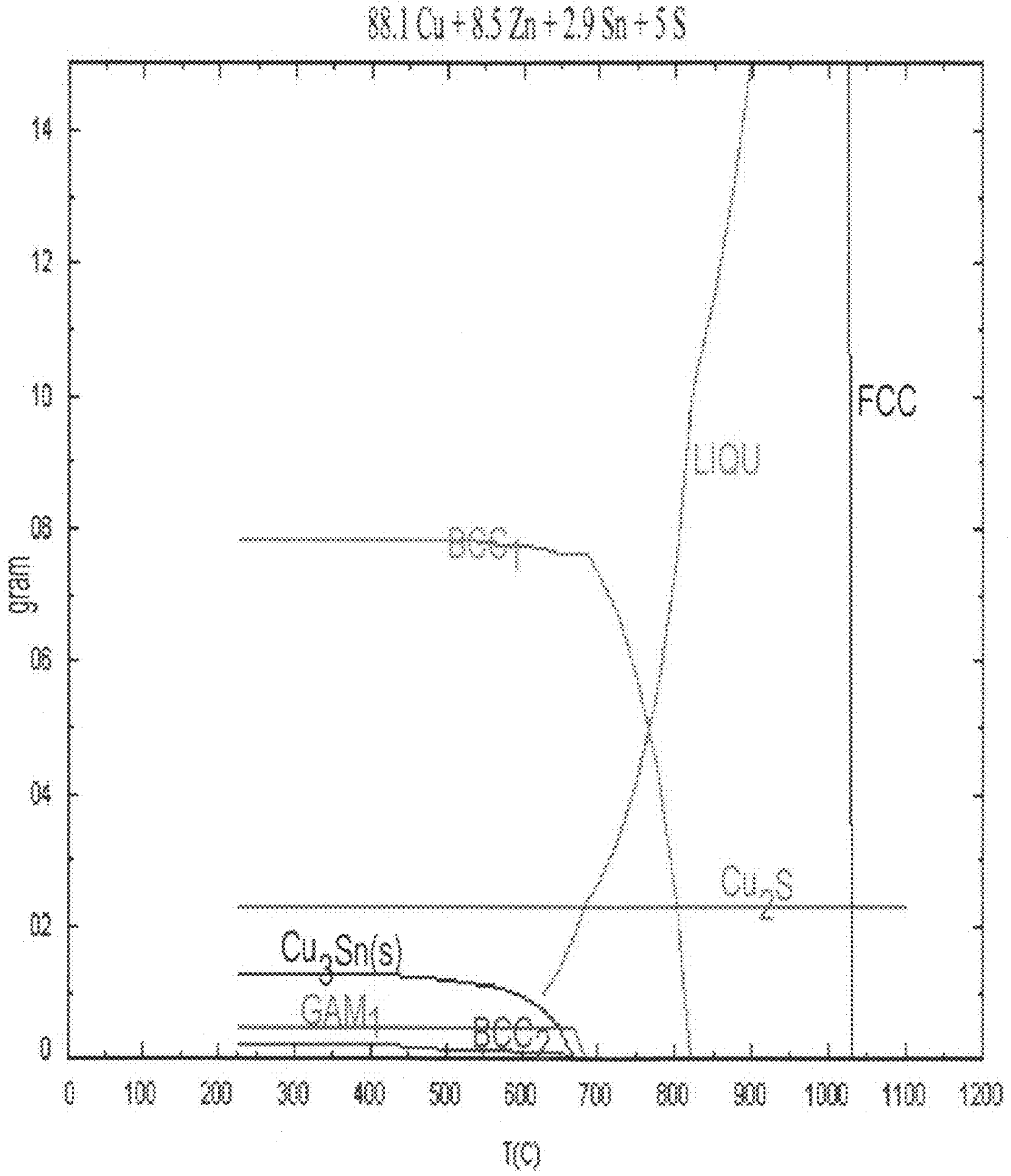
88.1 Cu + 8.5 Zn + 2.9 Sn + 5 S
gram
T(C)
0
100
200
300
400
500
600
700
800
900
1000
1100
1200
0
.02
.04
.06
.08
.10
.12
.14
FCC
LIQU
BCC1
Cu2S
Cu3Sn(s)
GAM1
BCC2

FIG. 26B

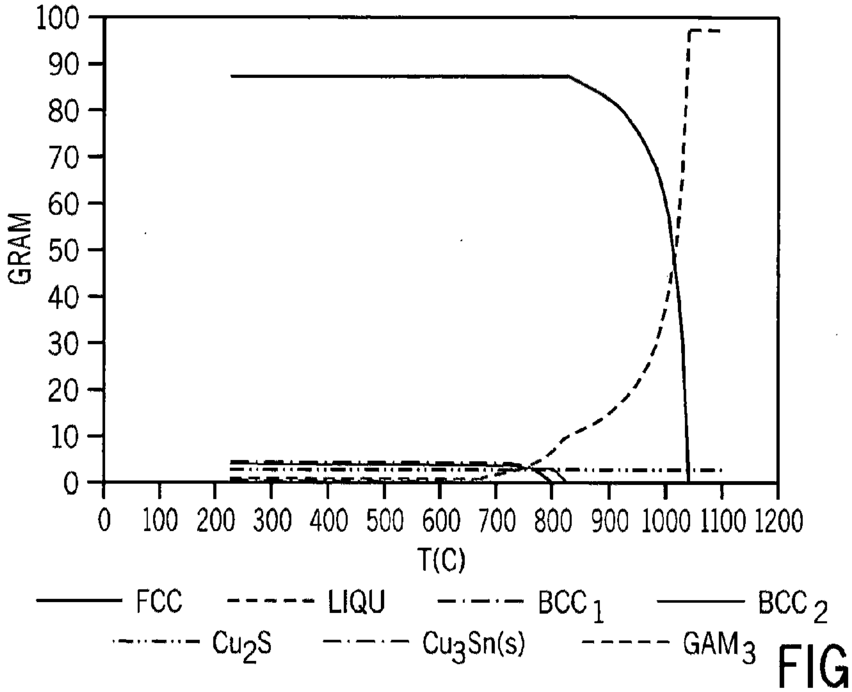

FIG. 27A

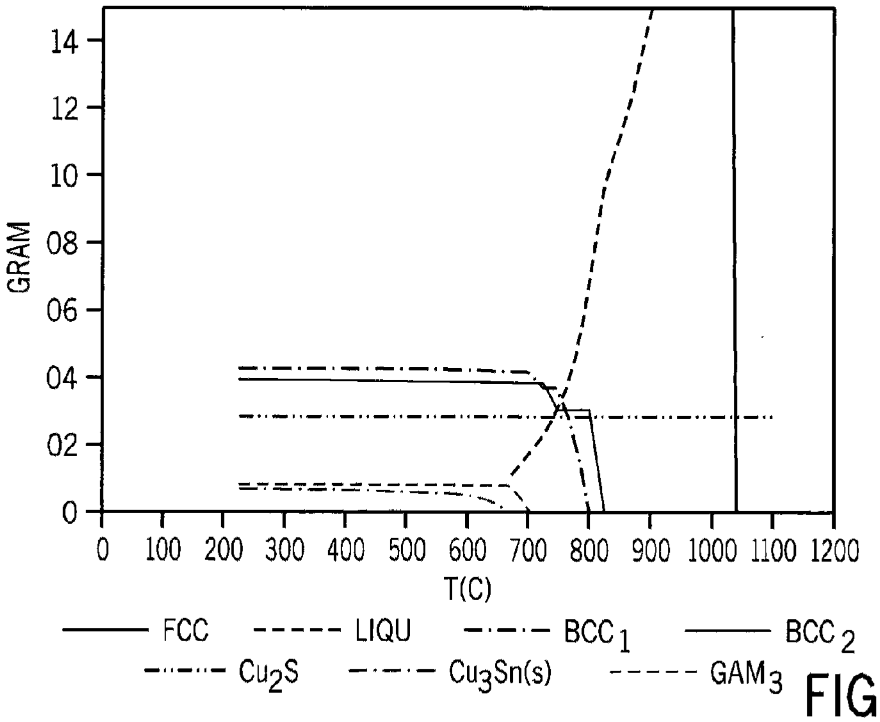

FIG. 27B

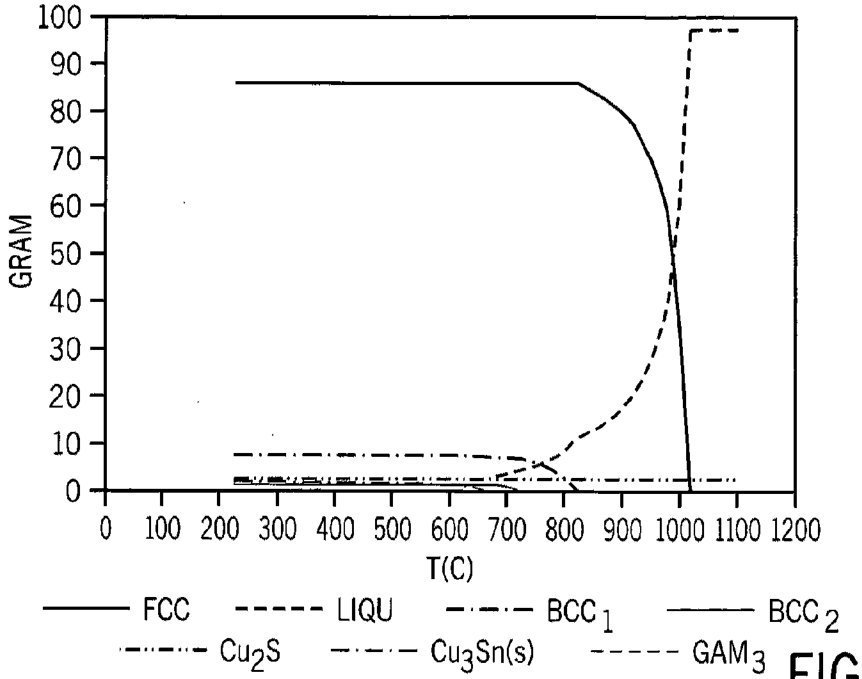

FIG. 28A

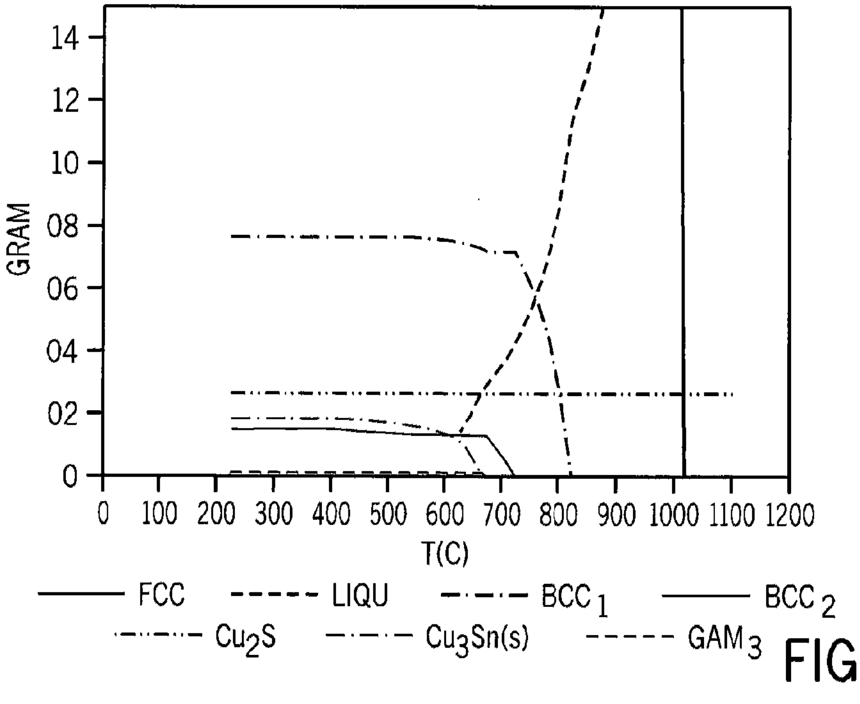

FIG. 28B

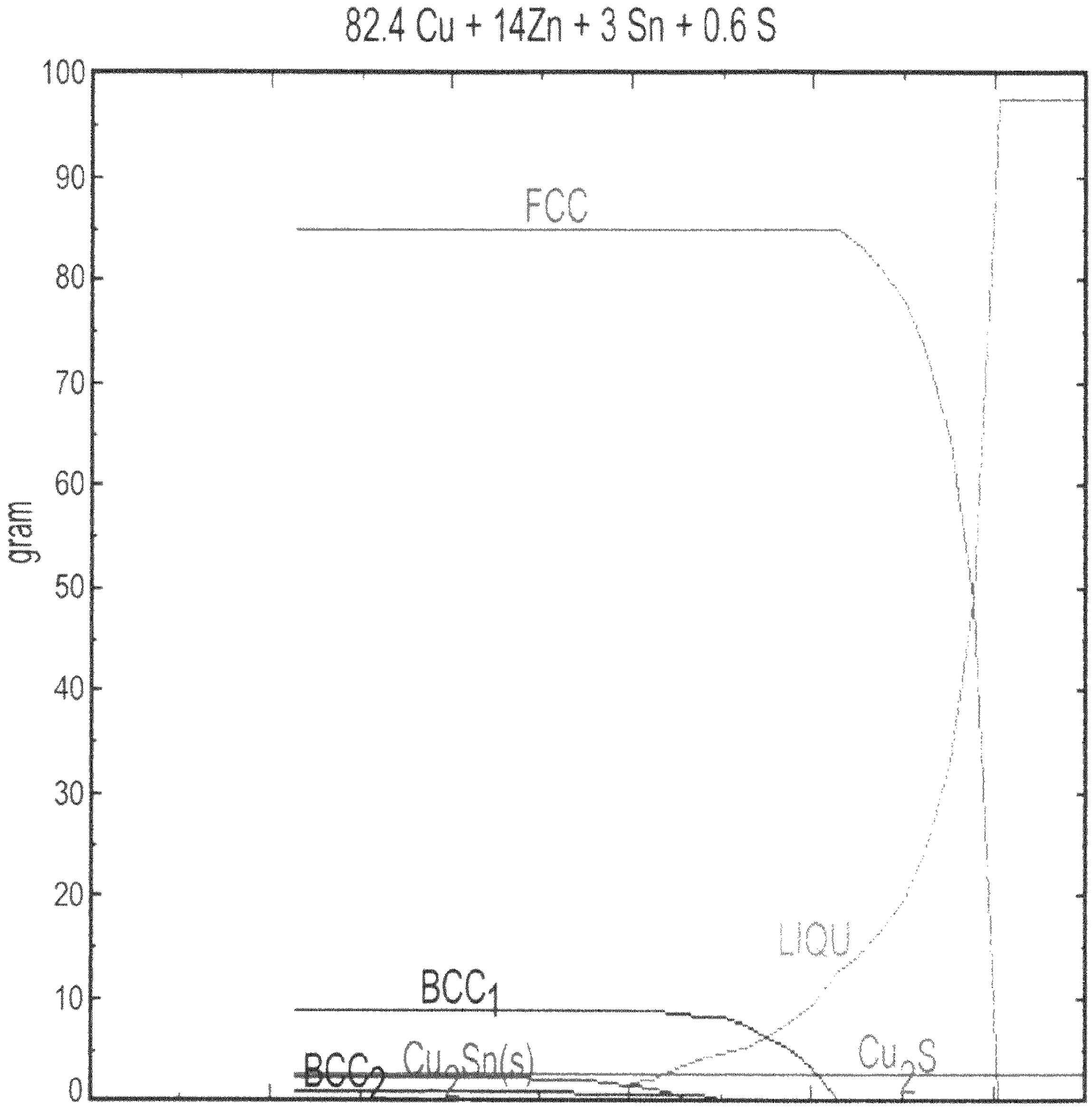
82.4 Cu + 14Zn + 3 Sn + 0.6 S
gram
T(C)
0
10
20
30
40
50
60
70
80
90
100
0
0200
0400
0600
0800
1000
FCC
LIQU
$BCC_1$
$BCC_2$
$Cu_2Sn(s)$
$Cu_2S$

FIG. 29A

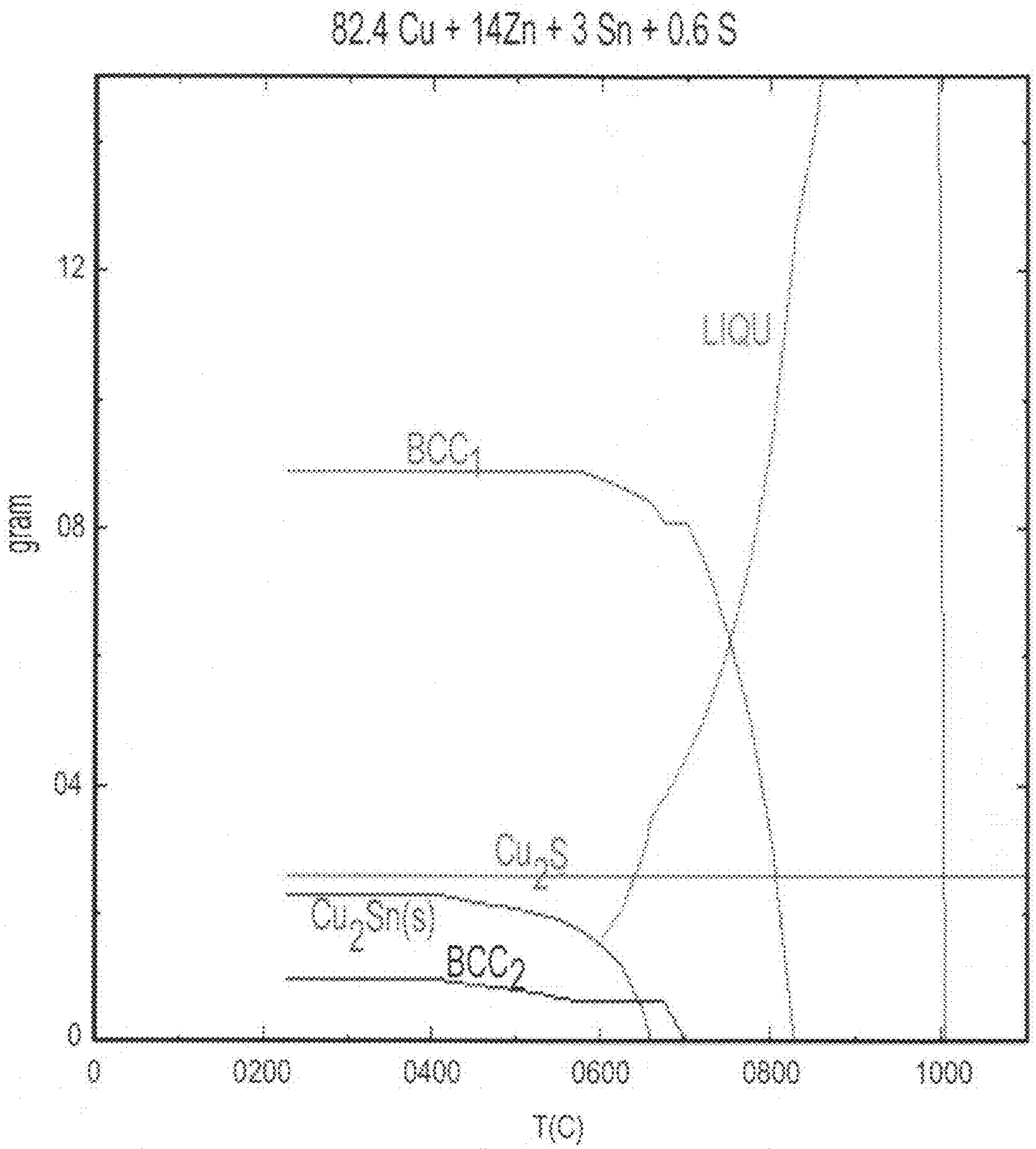
82.4 Cu + 14Zn + 3 Sn + 0.6 S
gram
12
08
04
0
0
0200
0400
0600
0800
1000
T(C)
LIQU
BCC1
Cu2S
Cu2Sn(s)
BCC2

FIG. 29B

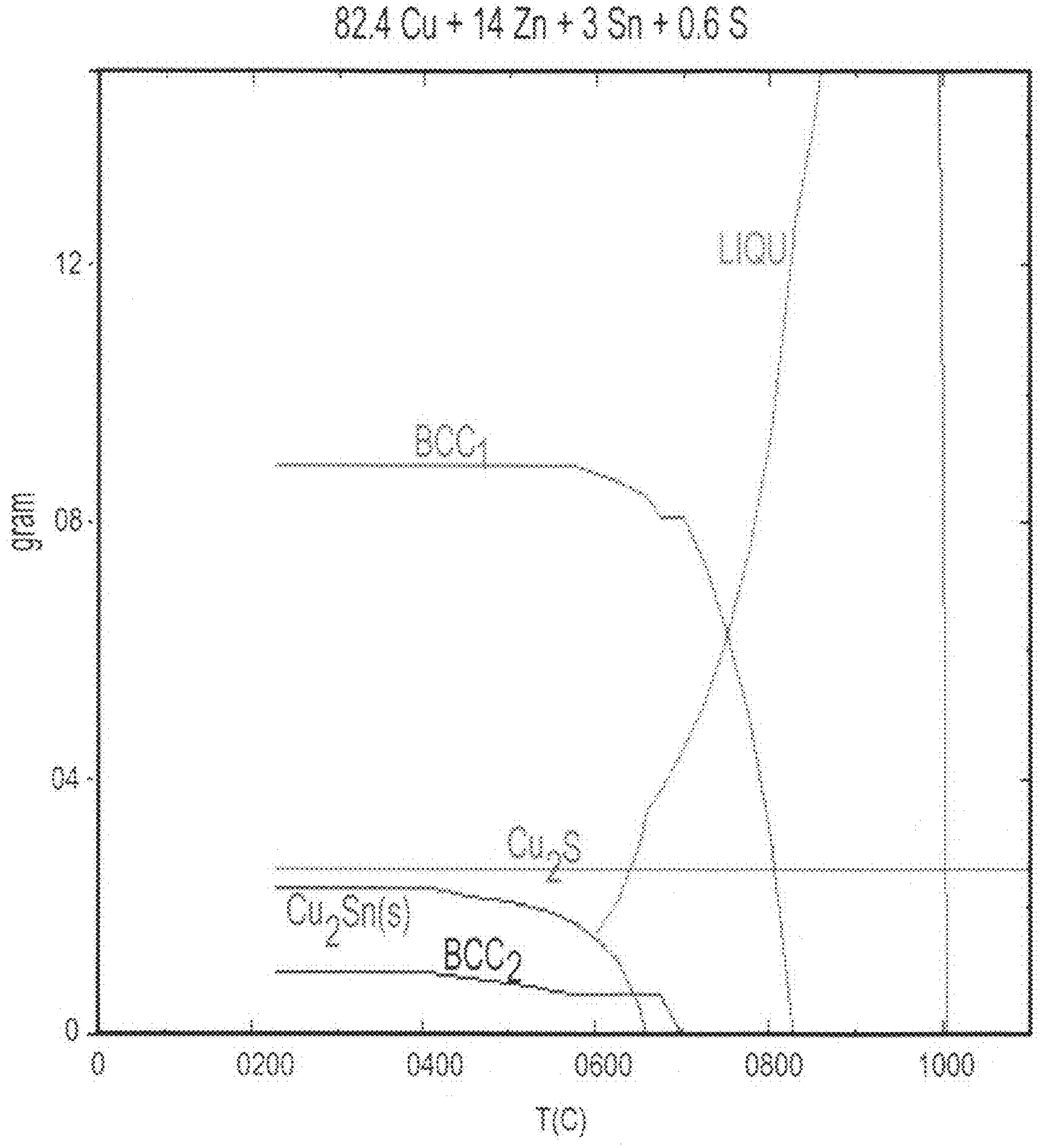
82.4 Cu + 14 Zn + 3 Sn + 0.6 S
gram
0
04
08
12
0
0200
0400
0600
0800
1000
T(C)
LIQU
$BCC_1$
$Cu_2S$
$Cu_2Sn(s)$
$BCC_2$

FIG. 30A

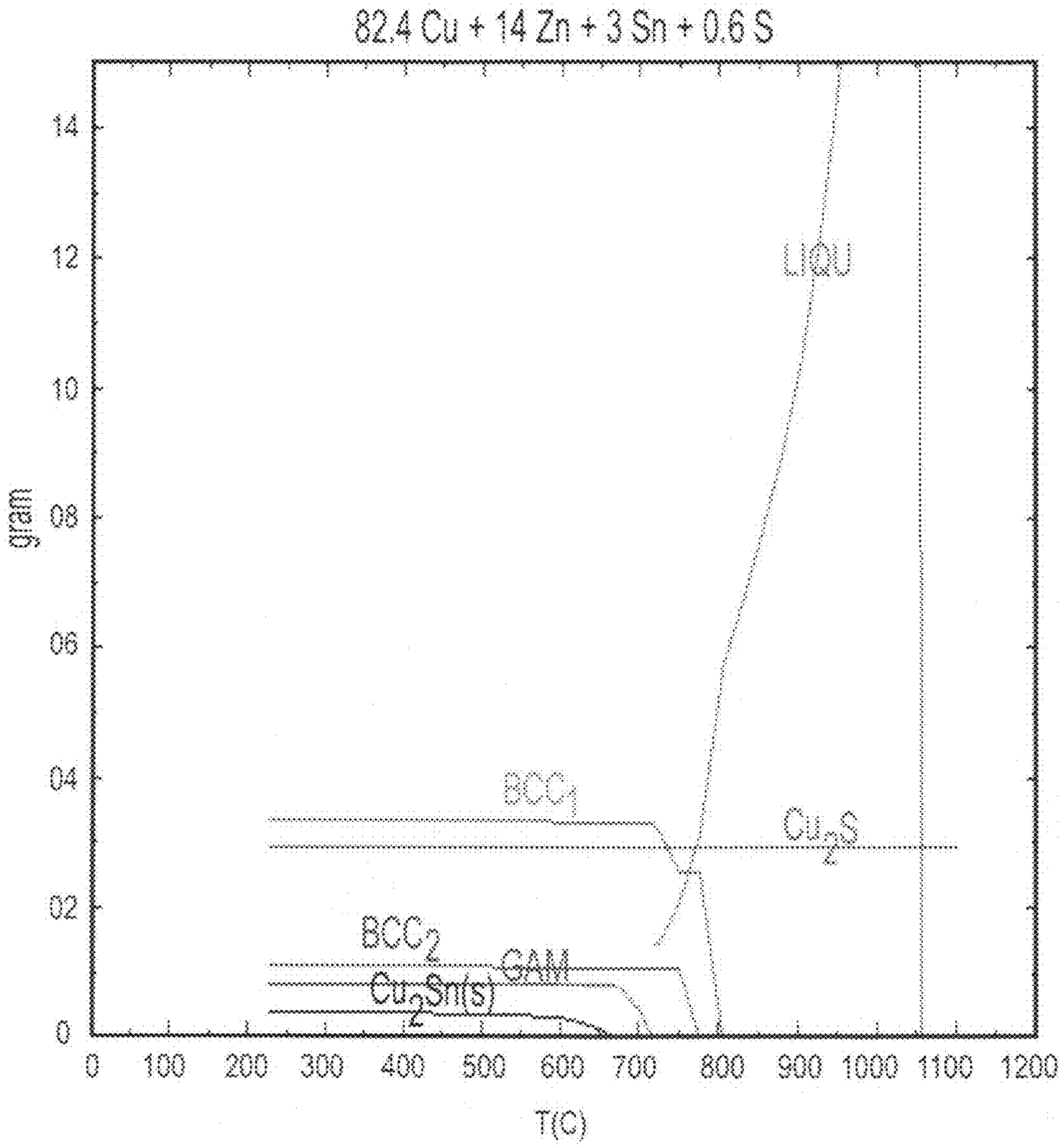
82.4 Cu + 14 Zn + 3 Sn + 0.6 S
gram
0
02
04
06
08
10
12
14
T(C)
0
100
200
300
400
500
600
700
800
900
1000
1100
1200
LIQU
BCC1
Cu2S
BCC2
GAM
Cu2Sn(s)

FIG. 30B

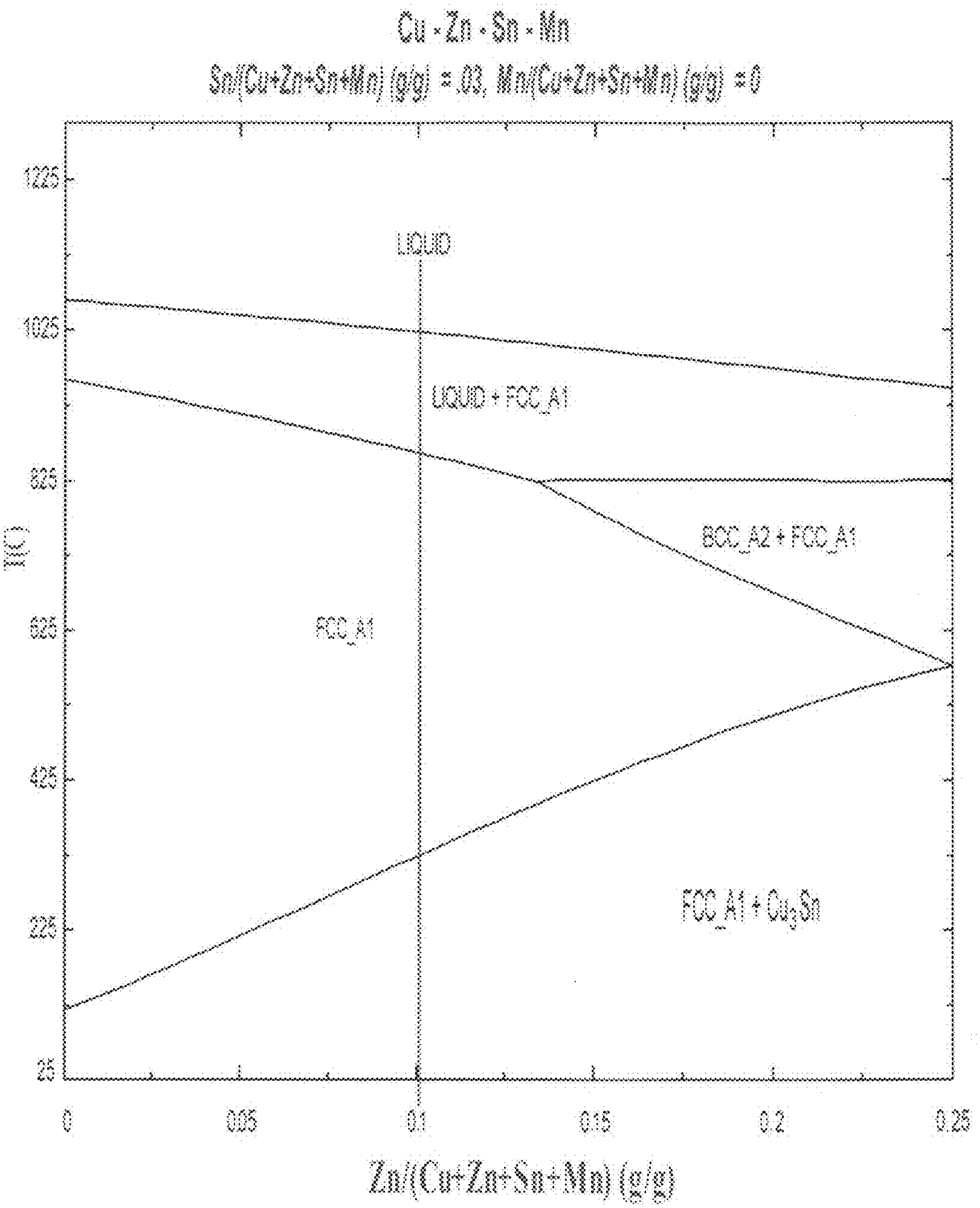
Cu - Zn - Sn - Mn
Sn/(Cu+Zn+Sn+Mn) (g/g) = .03, Mn/(Cu+Zn+Sn+Mn) (g/g) = 0
1225
1025
825
625
425
225
25
T(C)
LIQUID
LIQUID + FCC_A1
BCC_A2 + FCC_A1
FCC_A1
FCC_A1 + $Cu_3Sn$
0
0.05
0.1
0.15
0.2
0.25
Zn/(Cu+Zn+Sn+Mn) (g/g)

FIG. 31

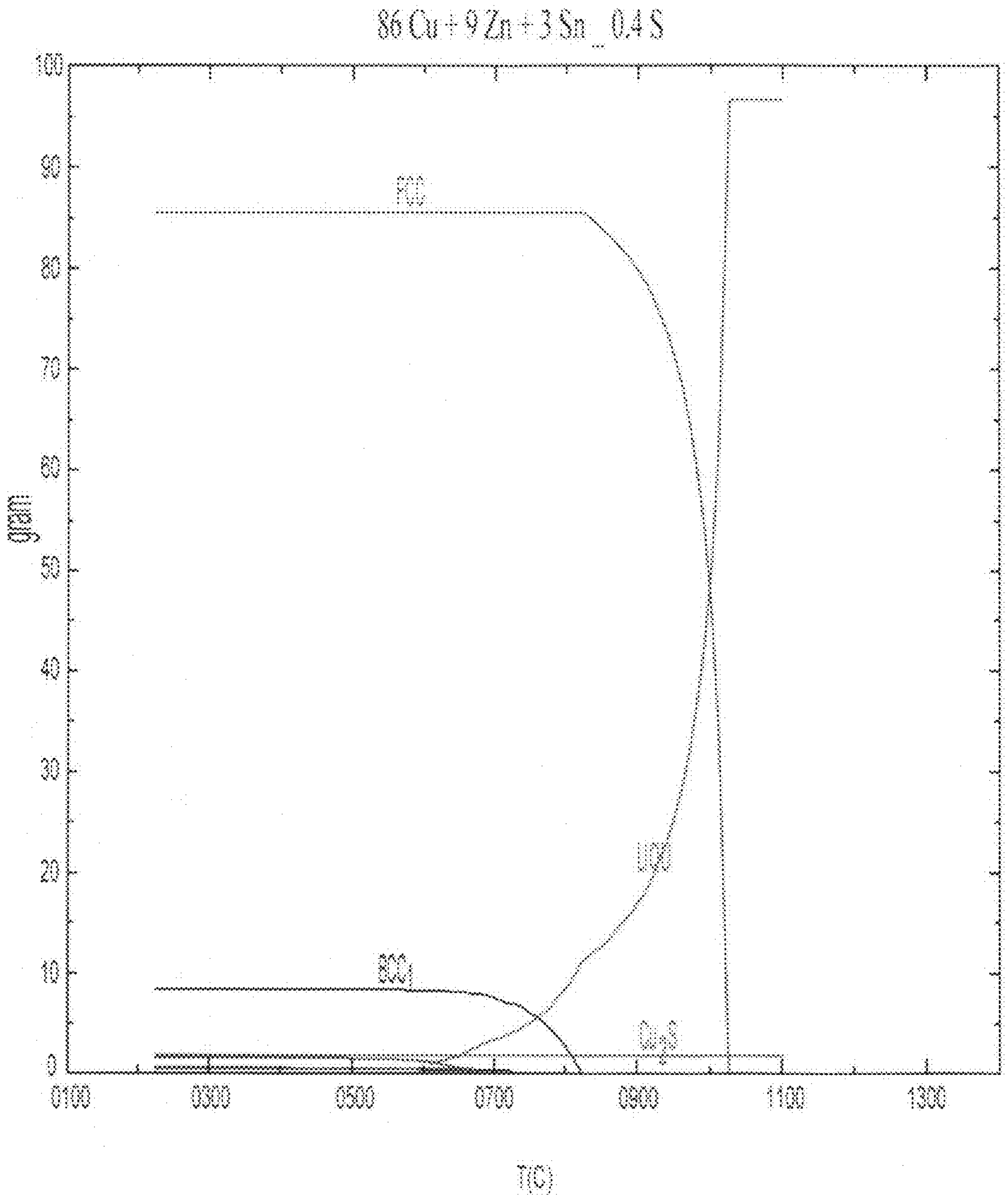
86 Cu + 9 Zn + 3 Sn _ 0.4 S
100
90
80
70
60
50
40
30
20
10
0
gram
FCC
LIQUID
BCC
$Cu_2S$
0100
0300
0500
0700
0900
1100
1300
T(C)

FIG. 32A

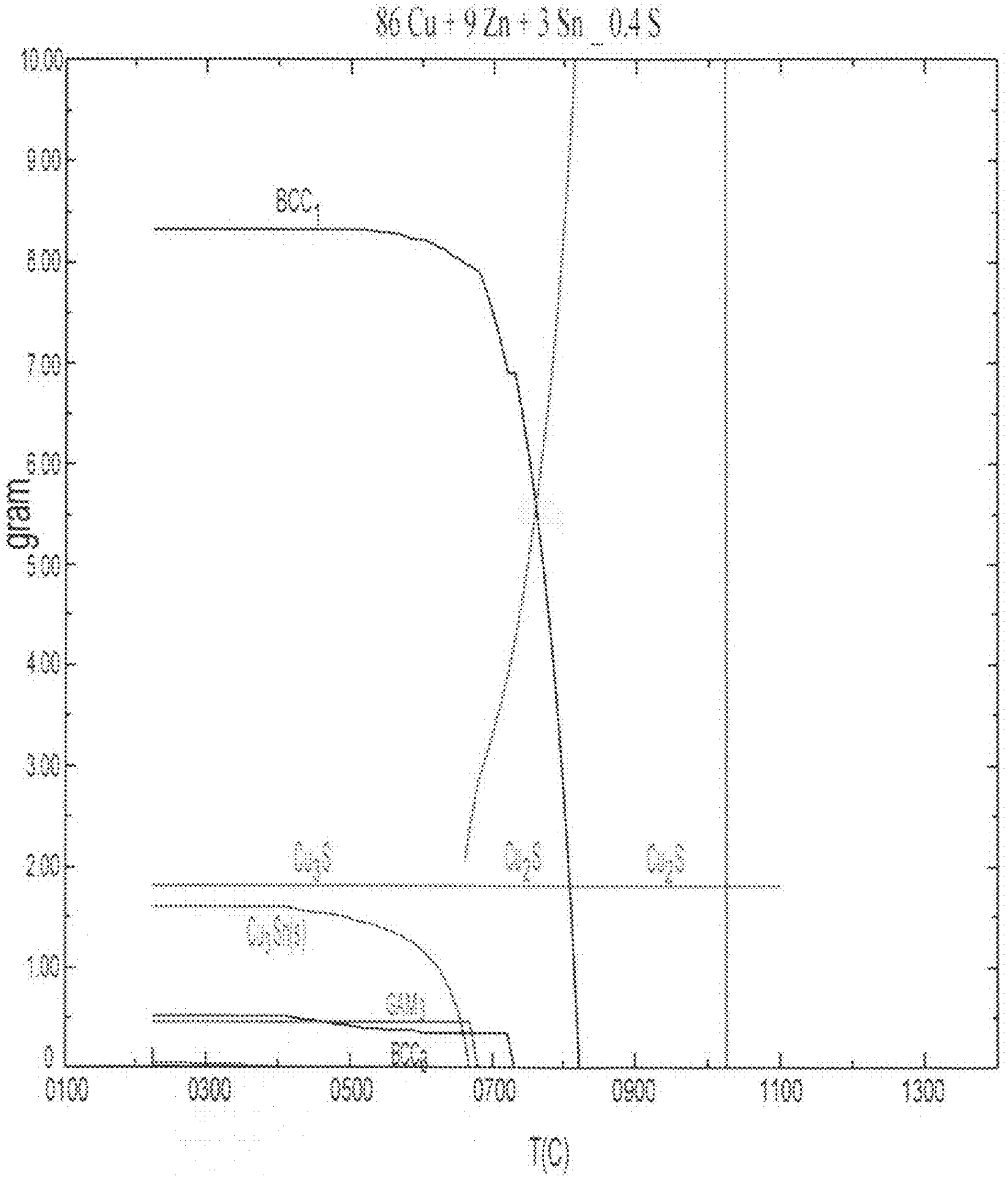
86 Cu + 9 Zn + 3 Sn _0.4 S
gram
T(C)
10.00
9.00
8.00
7.00
6.00
5.00
4.00
3.00
2.00
1.00
0
0100
0300
0500
0700
0900
1100
1300
$BCC_1$
$Cu_2S$
$Cu_2S$
$Cu_2S$
$Cu_3Sn(s)$
GAM1
$BCC_3$

FIG. 32B

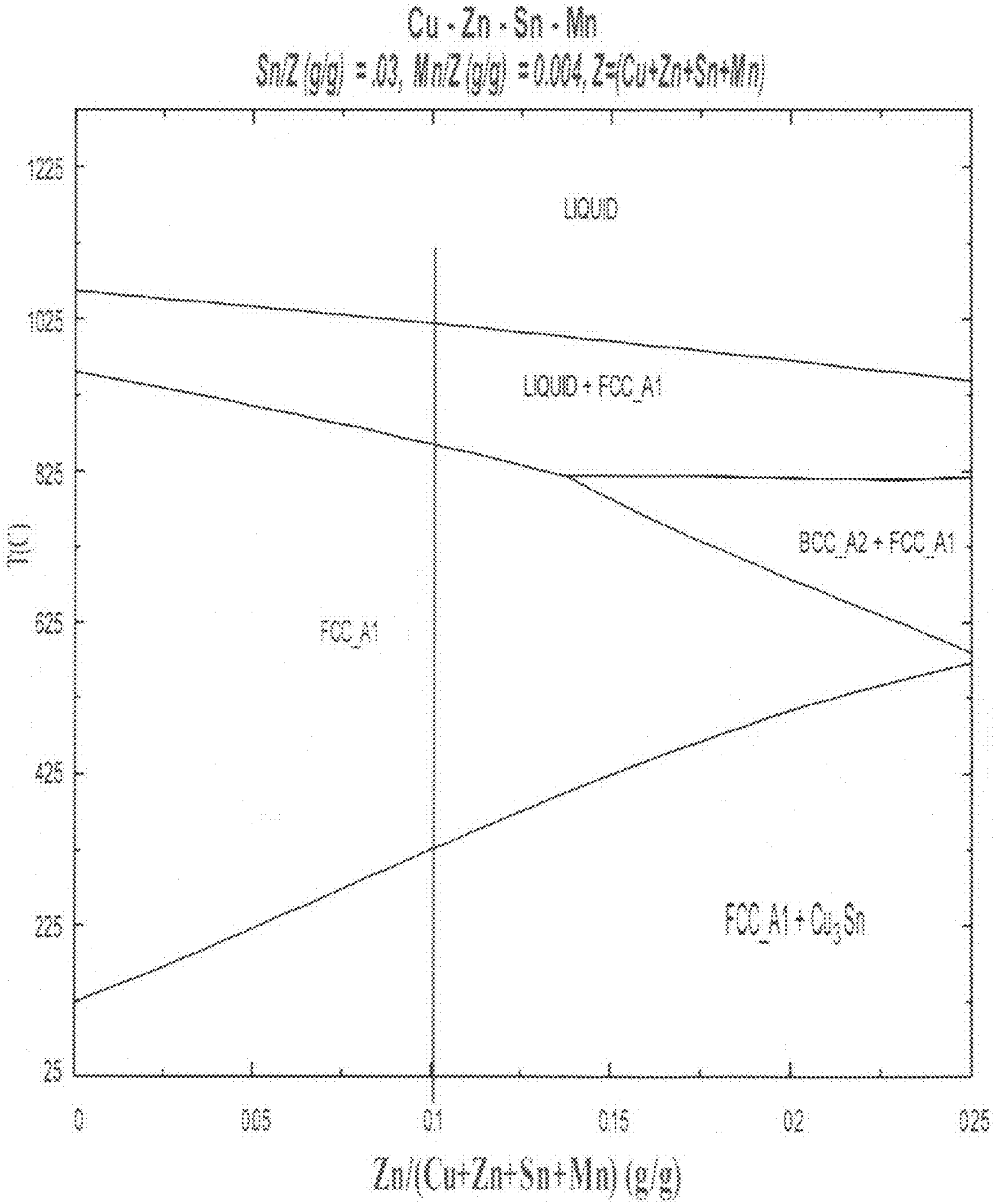
Cu - Zn - Sn - Mn
Sn/Z (g/g) = .03, Mn/Z (g/g) = 0.004, Z=(Cu+Zn+Sn+Mn)
LIQUID
LIQUID + FCC_A1
BCC_A2 + FCC_A1
FCC_A1
FCC_A1 + $Cu_3Sn$
T(C)
1225
1025
825
625
425
225
25
0
0.05
0.1
0.15
0.2
0.25
Zn/(Cu+Zn+Sn+Mn) (g/g)

FIG. 33

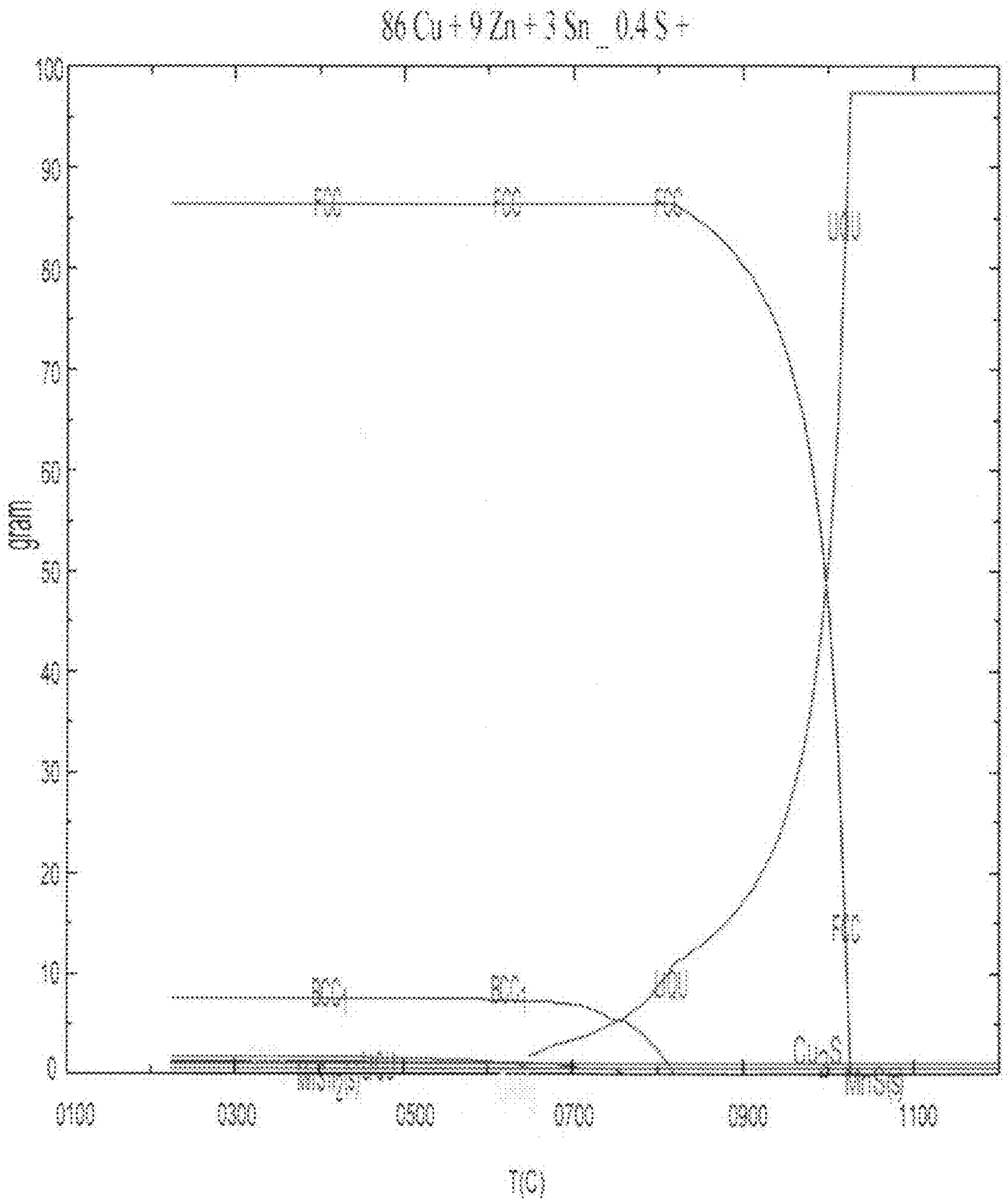
86 Cu + 9 Zn + 3 Sn _ 0.4 S +
gram
100
90
80
70
60
50
40
30
20
10
0
FCC
FCC
FCC
LIQU
FCC
BCC
BCC
LIQU
Cu2S
MnS(s)
MnS(s)
0100
0300
0500
0700
0900
1100
T(C)

FIG. 34A

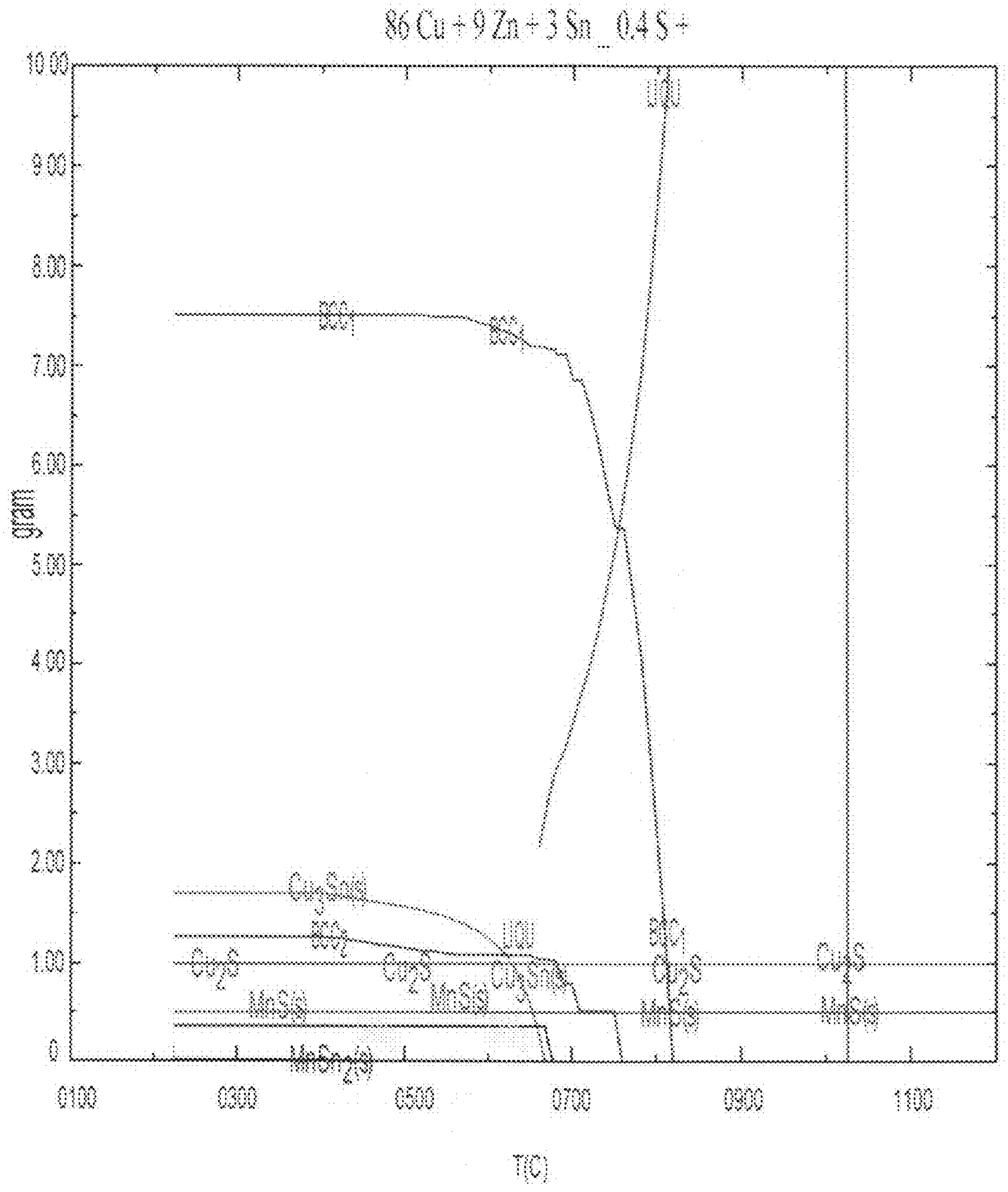
86 Cu + 9 Zn + 3 Sn _ 0.4 S +
10.00
9.00
8.00
7.00
6.00
5.00
4.00
3.00
2.00
1.00
0
gram
LIQU
$BCC_1$
$BCC_1$
$Cu_3Sn(s)$
$BCC_2$
LIQU
$BCC_1$
$Cu_2S$
$Cu_2S$
$Cu_3Sn(s)$
$Cu_2S$
$Cu_2S$
MnS(s)
MnS(s)
MnS(s)
MnS(s)
$MnSn_2(s)$
0100
0300
0500
0700
0900
1100
T(C)

FIG. 34B

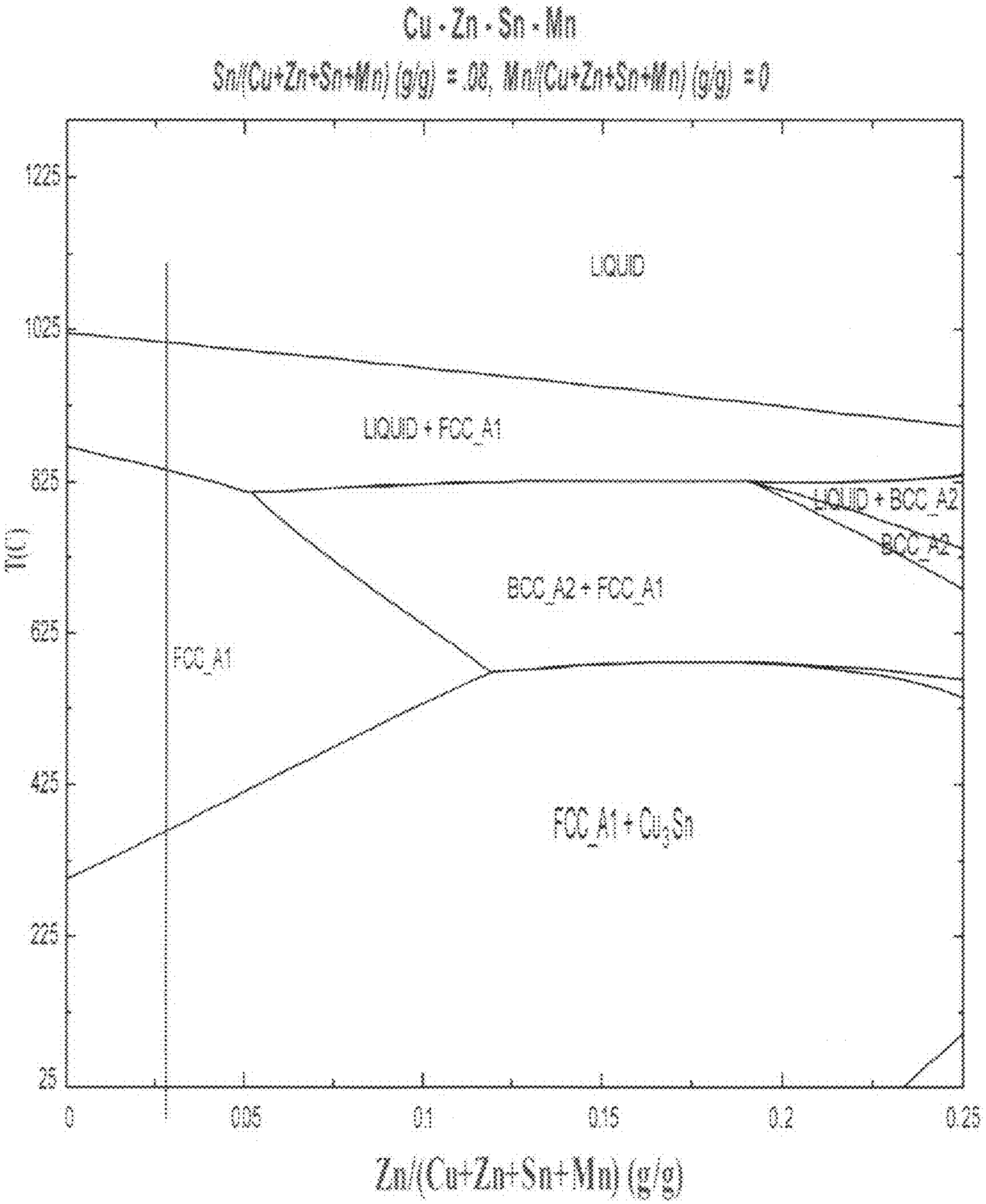
Cu - Zn - Sn - Mn
Sn/(Cu+Zn+Sn+Mn) (g/g) = .08, Mn/(Cu+Zn+Sn+Mn) (g/g) = 0
1225
1025
825
625
425
225
25
T(C)
LIQUID
LIQUID + FCC_A1
LIQUID + BCC_A2
BCC_A2
BCC_A2 + FCC_A1
FCC_A1
FCC_A1 + Cu3Sn
0
0.05
0.1
0.15
0.2
0.25
Zn/(Cu+Zn+Sn+Mn) (g/g)

FIG. 35

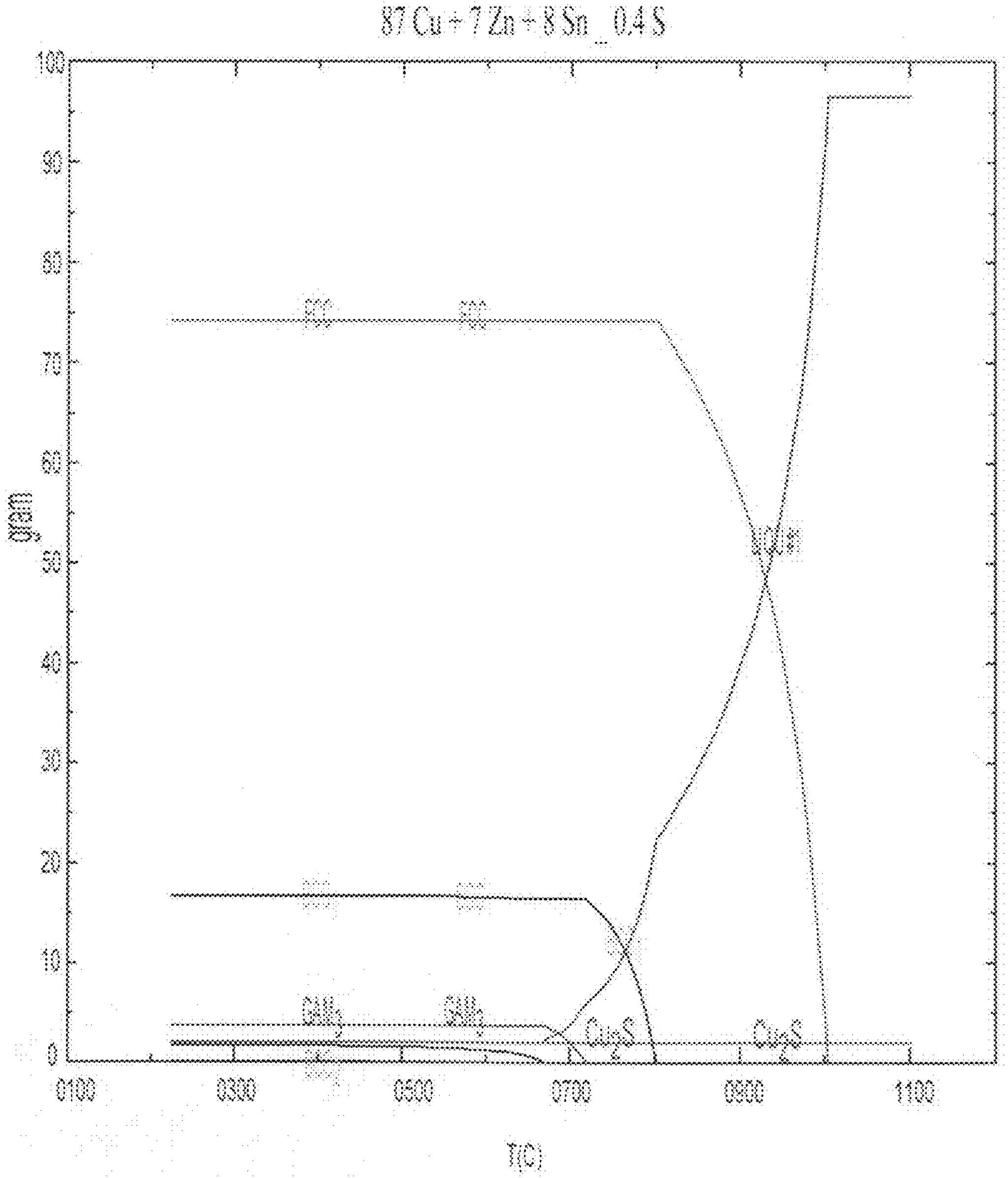
87 Cu + 7 Zn + 8 Sn _ 0.4 S
gram
100
90
80
70
60
50
40
30
20
10
0
0100
0300
0500
0700
0900
1100
T(C)
FCC
FCC
LIQUID
$CAM_2$
$CAM_2$
$Cu_2S$
$Cu_2S$

FIG. 36A

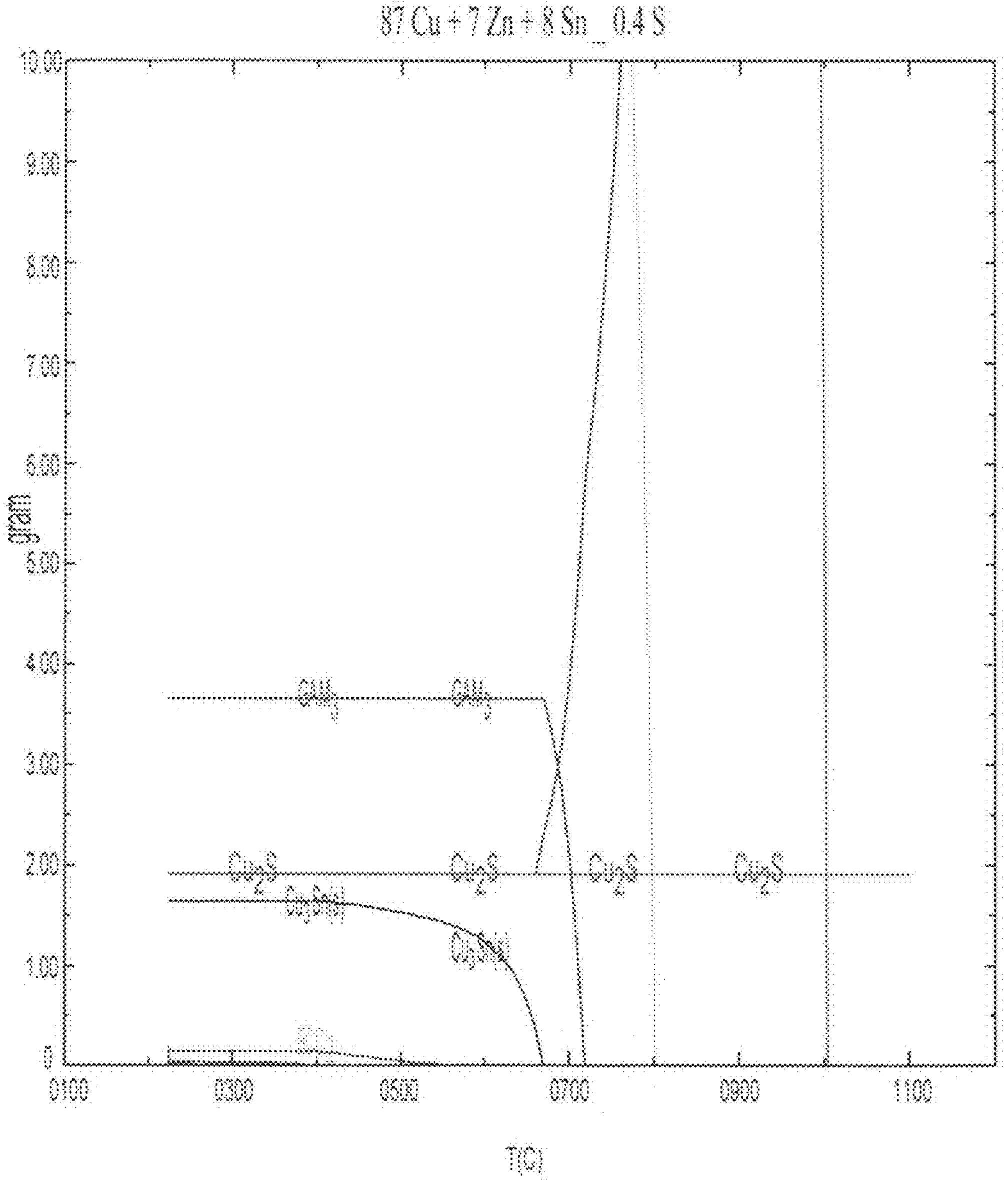
87 Cu + 7 Zn + 8 Sn _ 0.4 S
gram
10.00
9.00
8.00
7.00
6.00
5.00
4.00
3.00
2.00
1.00
0
$Cu_2S$
$Cu_2S$
$Cu_2S$
$Cu_2S$
$Cu_3Sn(s)$
$Cu_3Sn(s)$
0100
0300
0500
0700
0900
1100
T(C)

FIG. 36B

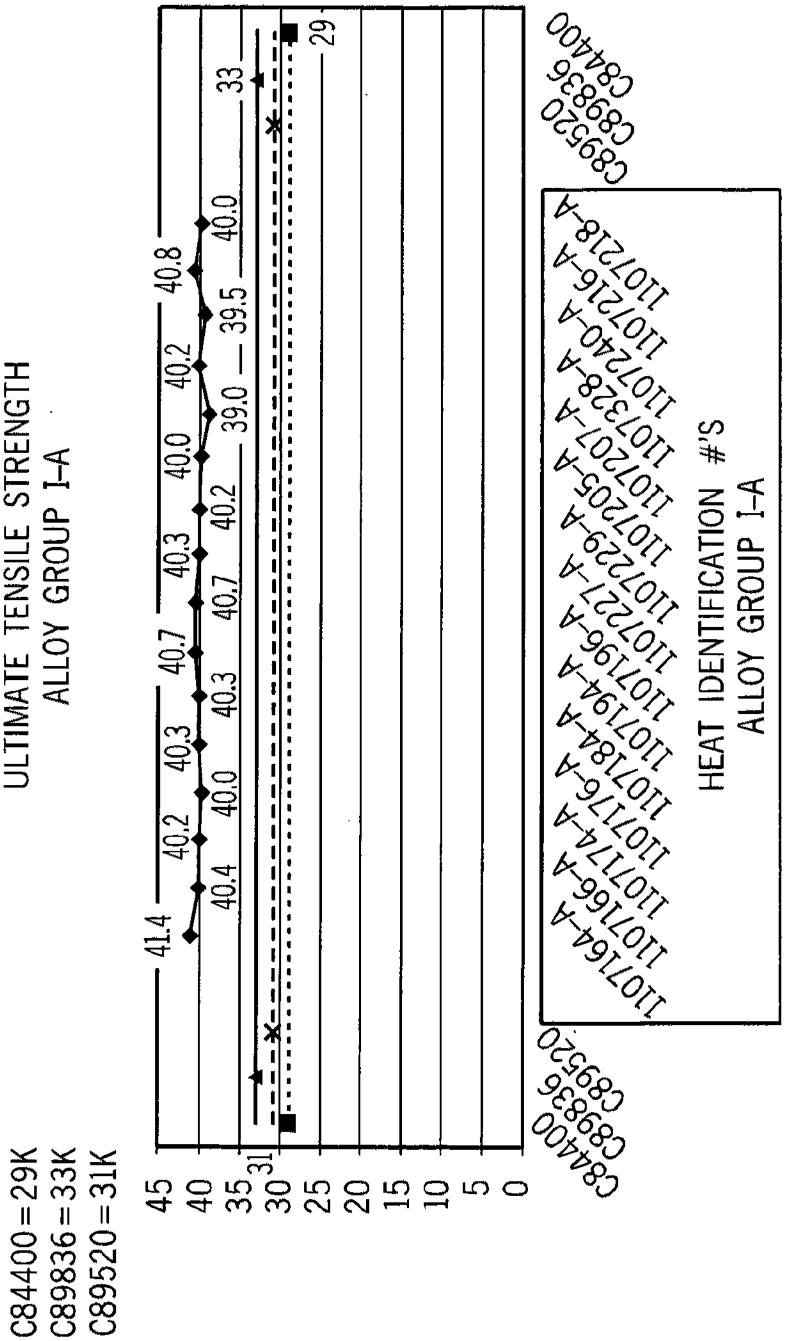
ULTIMATE TENSILE STRENGTH
ALLOY GROUP I-A
C84400=29K
C89836=33K
C89520=31K
45
40
35
31
30
25
20
15
10
5
0
41.4
40.4
40.2
40.0
40.3
40.3
40.7
40.7
40.3
40.2
40.0
39.0
40.2
39.5
40.8
40.0
33
29
C84400
C89836
C89520
110716A-A
110716 6-A
110717 4-A
110717 6-A
110718 4-A
110719 4-A
110719 6-A
110722 1-A
110722 9-A
110720 5-A
110720 7-A
110732 8-A
110724 0-A
110721 6-A
110721 8-A
C89520
C89836
C84400
HEAT IDENTIFICATION #'S
ALLOY GROUP I-A

FIG. 37

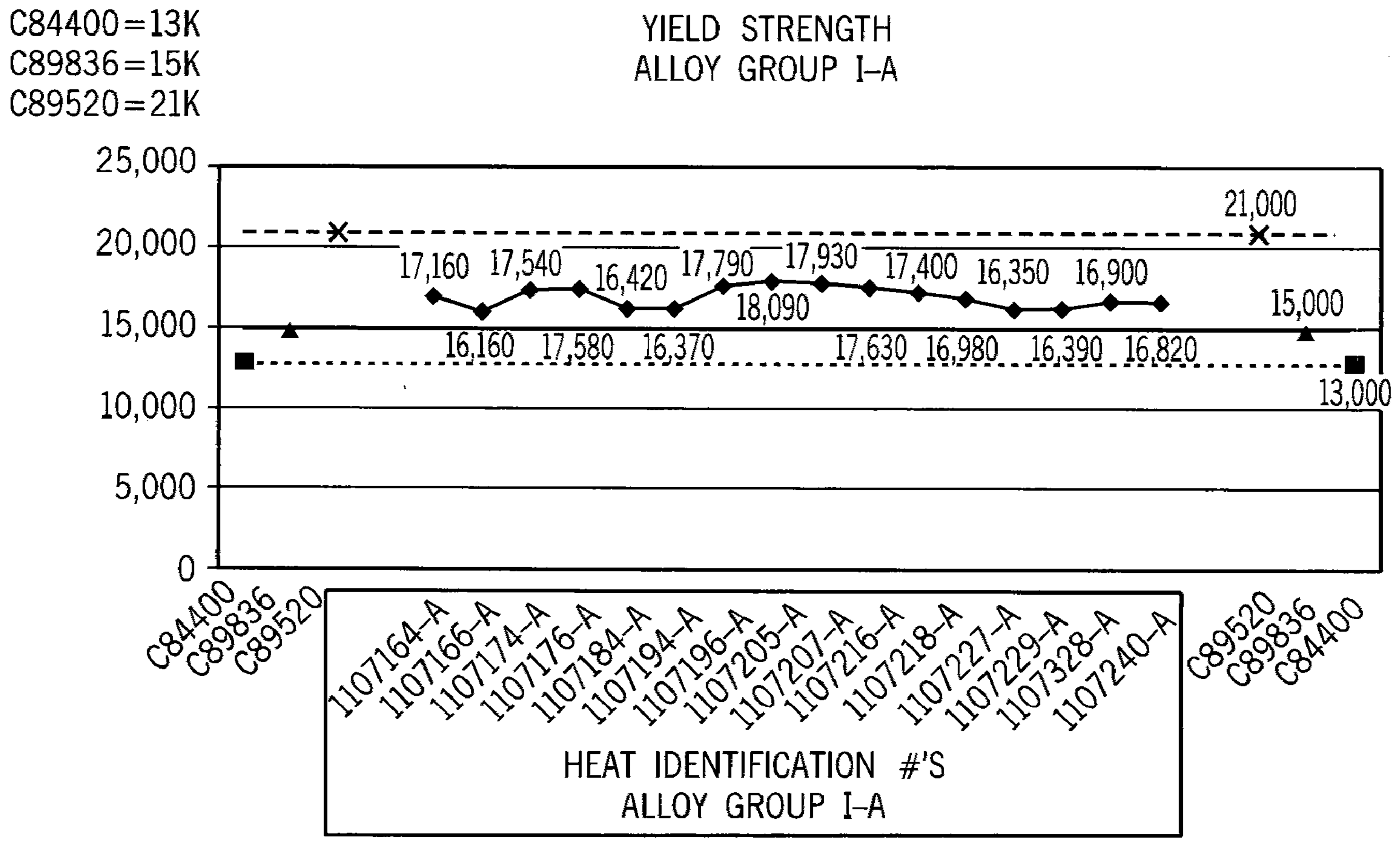
C84400=13K
C89836=15K
C89520=21K
YIELD STRENGTH
ALLOY GROUP I-A
25,000
20,000
15,000
10,000
5,000
0
21,000
17,160
17,540
16,420
17,790
17,930
17,400
16,350
16,900
18,090
15,000
16,160
17,580
16,370
17,630
16,980
16,390
16,820
13,000
C84400
C89836
C89520
1107164-A
1107166-A
1107174-A
1107176-A
1107184-A
1107194-A
1107196-A
1107205-A
1107207-A
1107216-A
1107218-A
1107227-A
1107229-A
1107328-A
1107240-A
C89520
C89836
C84400
HEAT IDENTIFICATION #'S
ALLOY GROUP I-A

FIG. 38

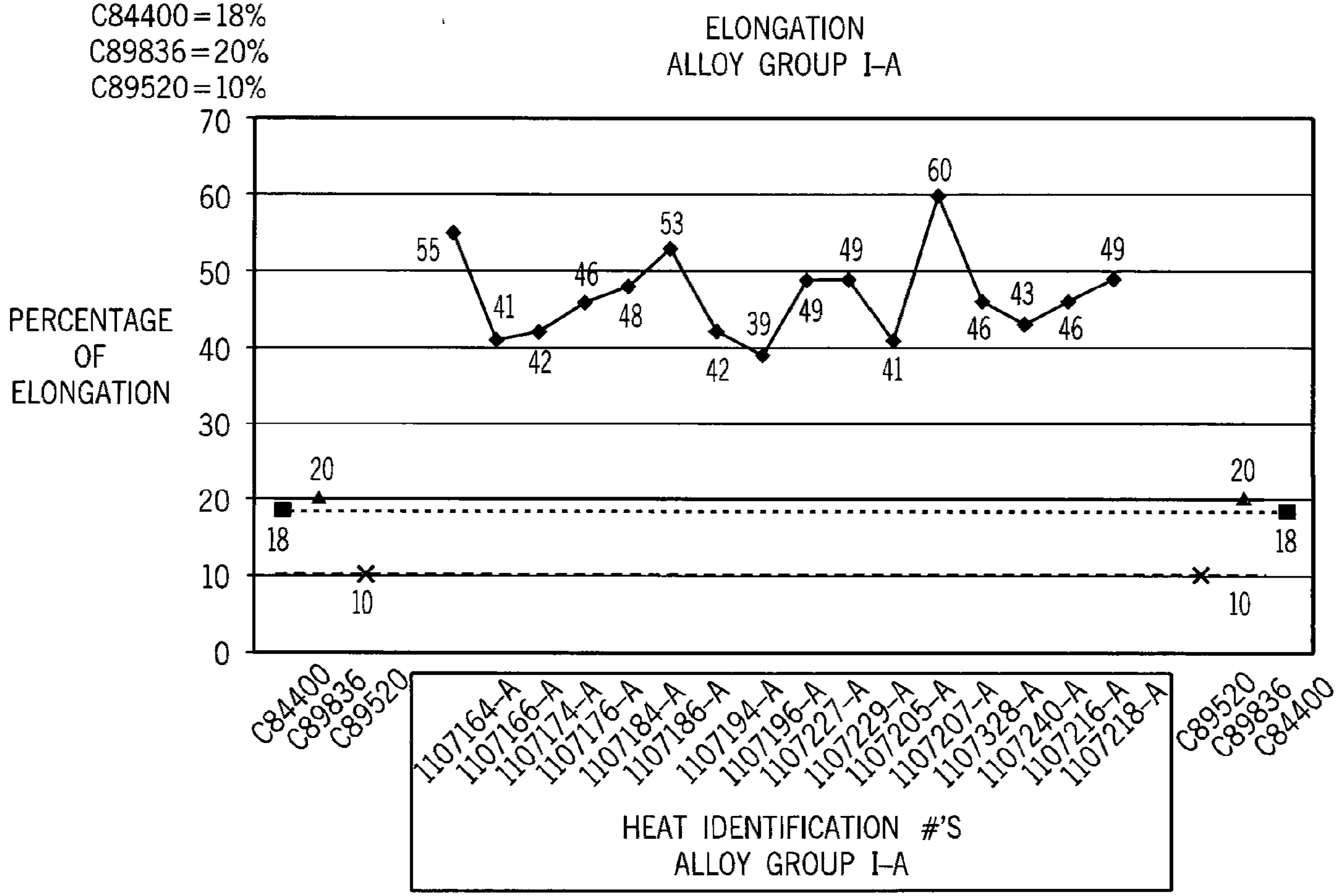
C84400=18%
C89836=20%
C89520=10%
ELONGATION
ALLOY GROUP I-A
PERCENTAGE OF ELONGATION
70
60
50
40
30
20
10
0
18
20
10
55
41
42
46
48
53
42
39
49
49
41
60
46
43
46
49
20
18
10
C84400
C89836
C89520
1107164-A
1107166-A
1107174-A
1107176-A
1107184-A
1107186-A
1107194-A
1107196-A
1107227-A
1107229-A
1107205-A
1107207-A
1107328-A
1107240-A
1107216-A
1107218-A
C89520
C89836
C84400
HEAT IDENTIFICATION #'S
ALLOY GROUP I-A

FIG. 39

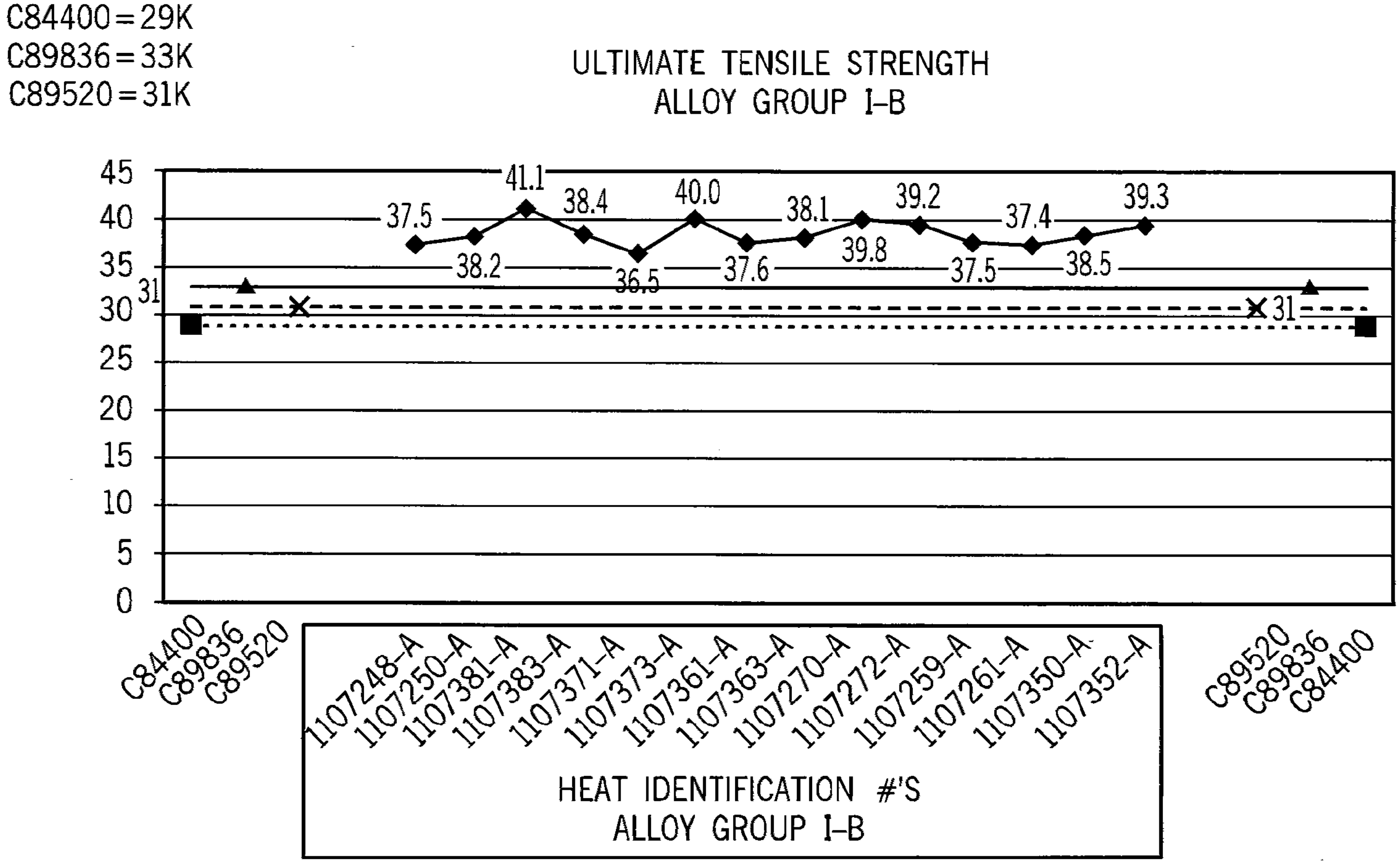
C84400=29K
C89836=33K
C89520=31K
ULTIMATE TENSILE STRENGTH
ALLOY GROUP I-B
45
40
35
31
30
25
20
15
10
5
0
37.5
38.2
41.1
38.4
36.5
40.0
37.6
38.1
39.8
39.2
37.5
37.4
38.5
39.3
31
C84400
C89836
C89520
1107248-A
1107250-A
1107381-A
1107383-A
1107371-A
1107373-A
1107361-A
1107363-A
1107270-A
1107272-A
1107259-A
1107261-A
1107350-A
1107352-A
C89520
C89836
C84400
HEAT IDENTIFICATION #'S
ALLOY GROUP I-B

FIG. 40

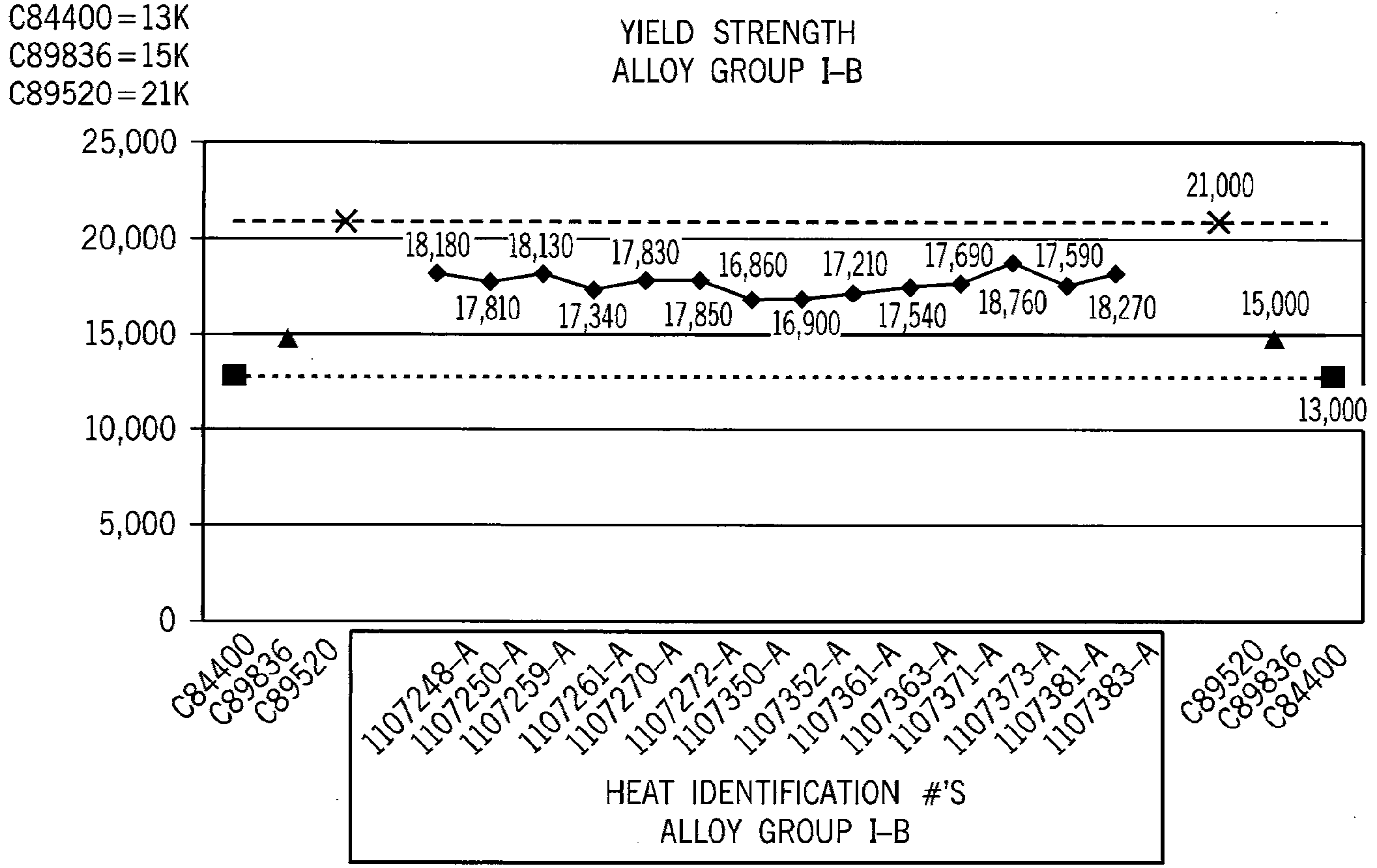
C84400=13K
C89836=15K
C89520=21K
YIELD STRENGTH
ALLOY GROUP I-B
25,000
20,000
15,000
10,000
5,000
0
21,000
18,180
18,130
17,830
16,860
17,210
17,690
17,590
17,810
17,340
17,850
16,900
17,540
18,760
18,270
15,000
13,000
C84400
C89836
C89520
1107248-A
1107250-A
1107259-A
1107261-A
1107270-A
1107272-A
1107350-A
1107352-A
1107361-A
1107363-A
1107371-A
1107373-A
1107381-A
1107383-A
C89520
C89836
C84400
HEAT IDENTIFICATION #'S
ALLOY GROUP I-B

FIG. 41

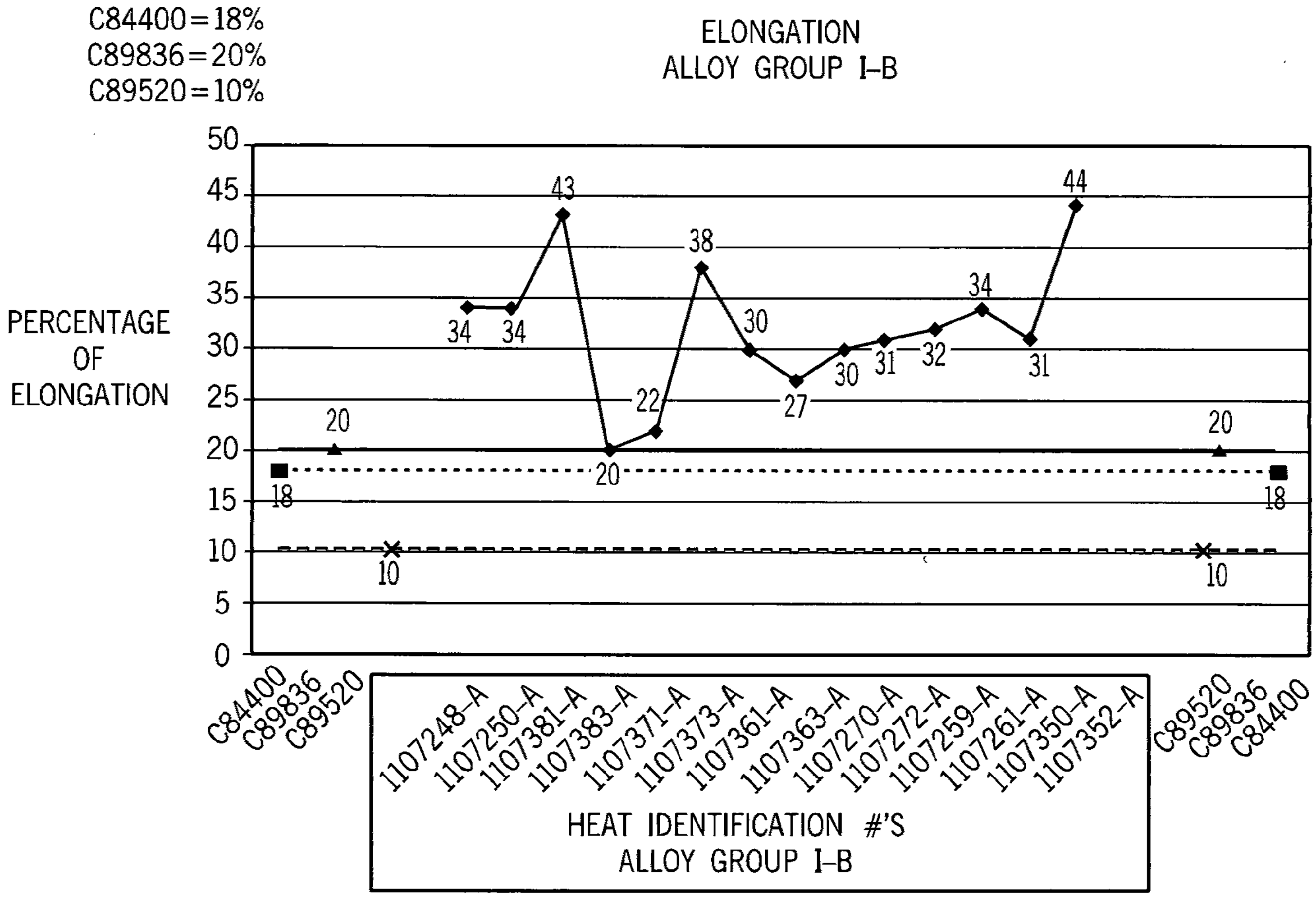
C84400=18%
C89836=20%
C89520=10%
ELONGATION
ALLOY GROUP I-B
PERCENTAGE OF ELONGATION
50
45
40
35
30
25
20
15
10
5
0
18
20
10
34
34
43
20
22
38
30
27
30
31
32
34
31
44
20
10
18
C84400
C89836
C89520
1107248-A
1107250-A
1107381-A
1107383-A
1107371-A
1107373-A
1107361-A
1107363-A
1107270-A
1107272-A
1107259-A
1107261-A
1107350-A
1107352-A
C89520
C89836
C84400
HEAT IDENTIFICATION #'S
ALLOY GROUP I-B

FIG. 42

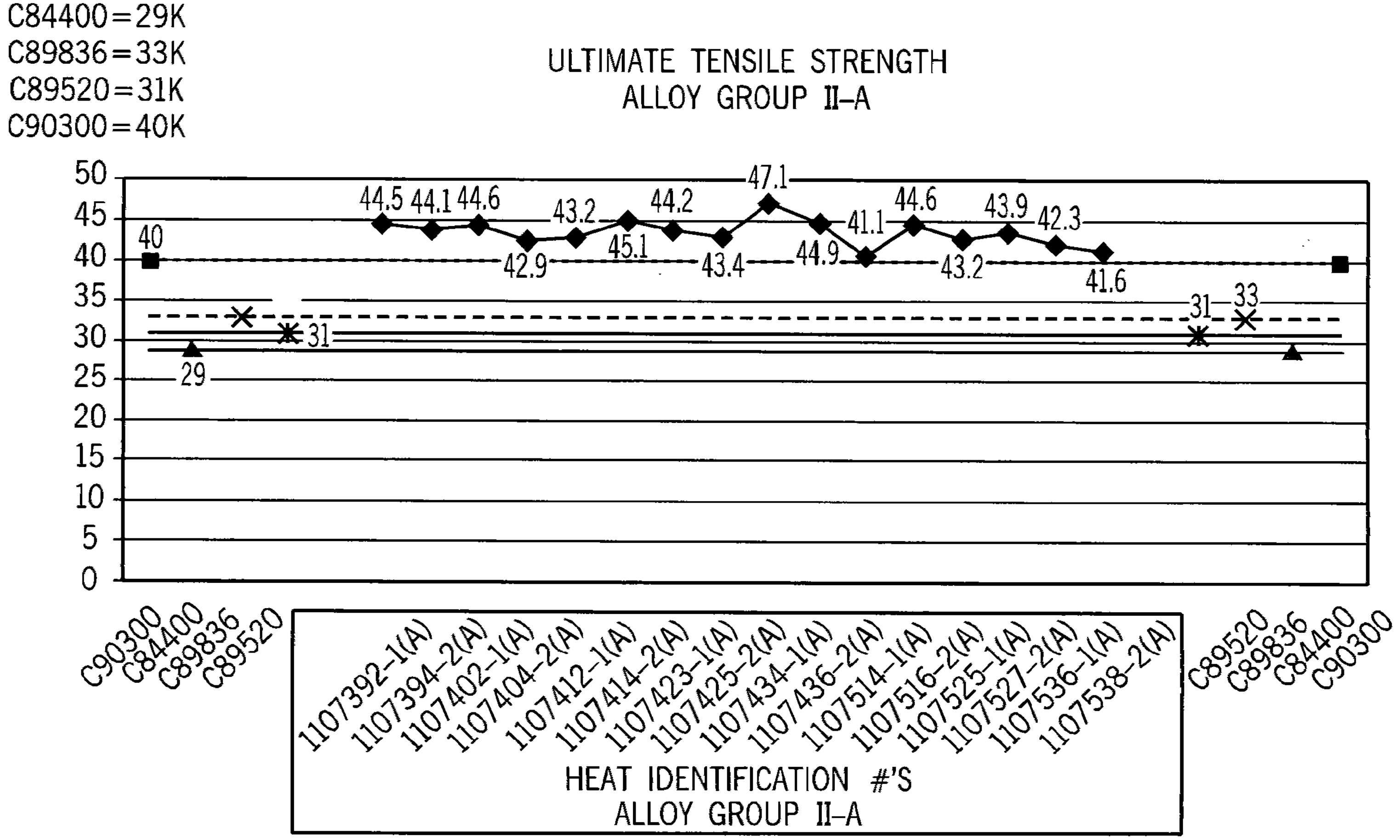
C84400=29K
C89836=33K
C89520=31K
C90300=40K
ULTIMATE TENSILE STRENGTH
ALLOY GROUP II-A
50
45
40
35
30
25
20
15
10
5
0
40
29
31
44.5
44.1
44.6
42.9
43.2
45.1
44.2
43.4
47.1
44.9
41.1
44.6
43.2
43.9
42.3
41.6
31
33
C90300
C84400
C89836
C89520
1107392-1(A)
1107394-2(A)
1107402-1(A)
1107404-2(A)
1107412-1(A)
1107414-2(A)
1107423-1(A)
1107425-2(A)
1107434-1(A)
1107436-2(A)
1107514-1(A)
1107516-2(A)
1107525-1(A)
1107527-2(A)
1107536-1(A)
1107538-2(A)
C89520
C89836
C84400
C90300
HEAT IDENTIFICATION #'S
ALLOY GROUP II-A

FIG. 43

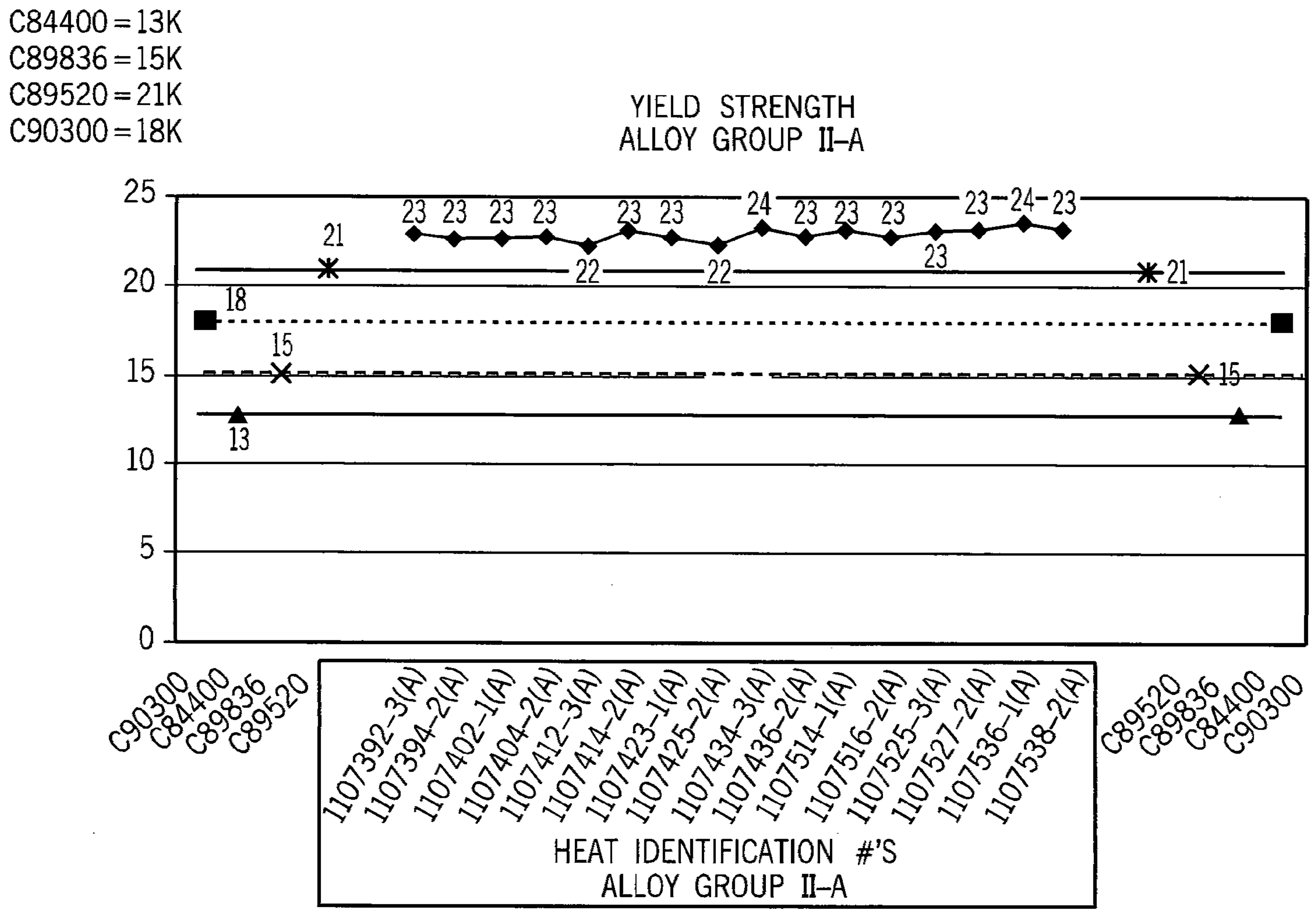
C84400=13K
C89836=15K
C89520=21K
C90300=18K
YIELD STRENGTH
ALLOY GROUP II-A
25
20
15
10
5
0
18
15
21
13
23
23
23
23
22
23
23
22
24
23
23
23
23
23
24
23
21
15
C90300
C84400
C89836
C89520
I107392-3(A)
I107394-2(A)
I107402-1(A)
I107404-2(A)
I107412-3(A)
I107414-2(A)
I107423-1(A)
I107425-2(A)
I107434-3(A)
I107436-2(A)
I107514-1(A)
I107516-2(A)
I107525-3(A)
I107527-2(A)
I107536-1(A)
I107538-2(A)
HEAT IDENTIFICATION #'S
ALLOY GROUP II-A
C89520
C89836
C84400
C90300

FIG. 44

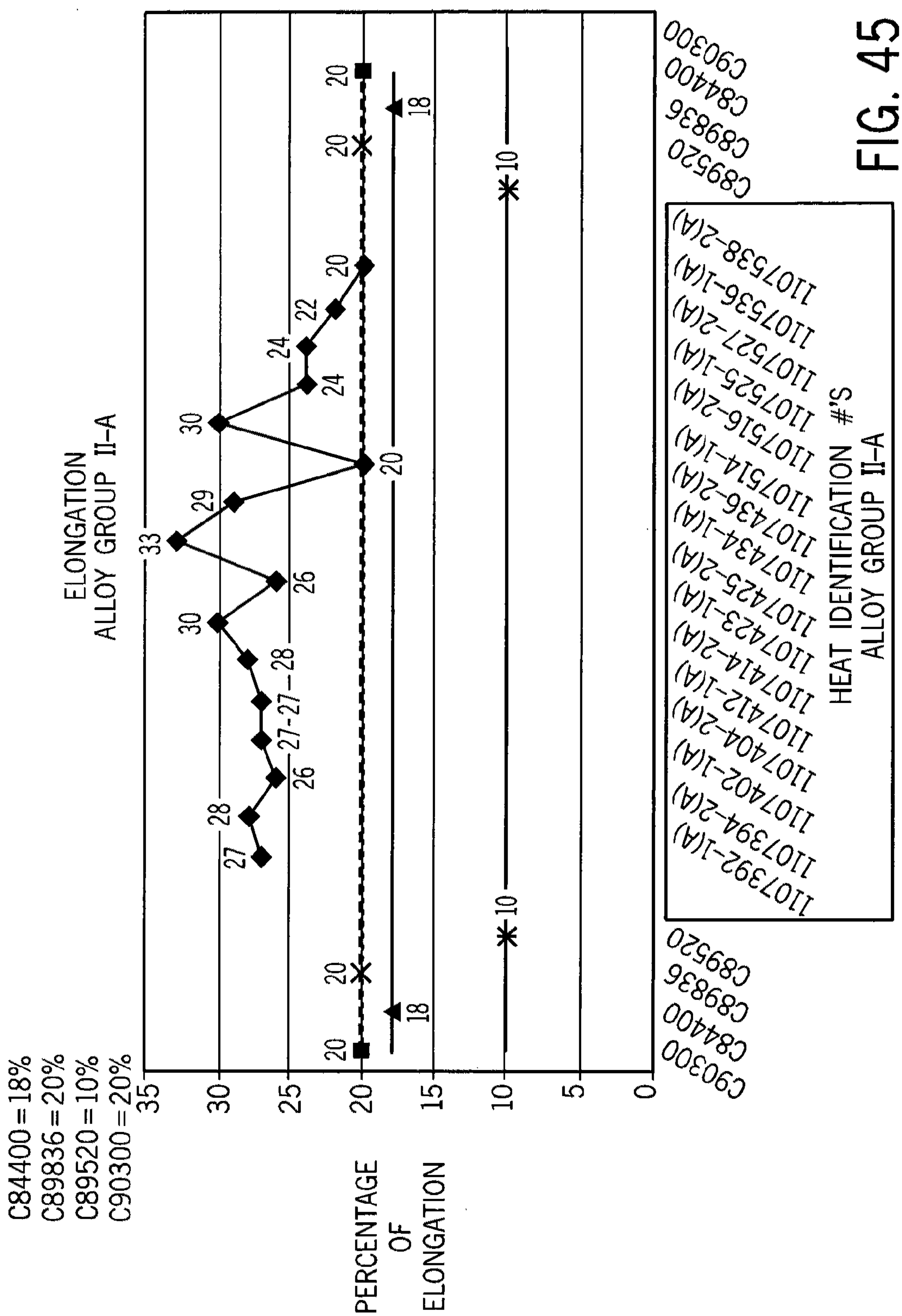
ELONGATION
ALLOY GROUP II-A
C84400=18%
C89836=20%
C89520=10%
C90300=20%
PERCENTAGE
OF
ELONGATION
35
30
25
20
15
10
5
0
C90300
C84400
C89836
C89520
20
18
20
10
27
28
26
27-27-28
30
26
33
29
20
30
24
24
22
20
10
20
18
20
II07392-1(A)
II07394-2(A)
II07402-1(A)
II07404-2(A)
II07412-1(A)
II07414-2(A)
II07423-1(A)
II07425-2(A)
II07434-1(A)
II07436-2(A)
II07514-1(A)
II07516-2(A)
II07525-1(A)
II07527-2(A)
II07536-1(A)
II07538-2(A)
HEAT IDENTIFICATION #'S
ALLOY GROUP II-A
C89520
C89836
C84400
C90300

FIG. 45

***BiWalite***

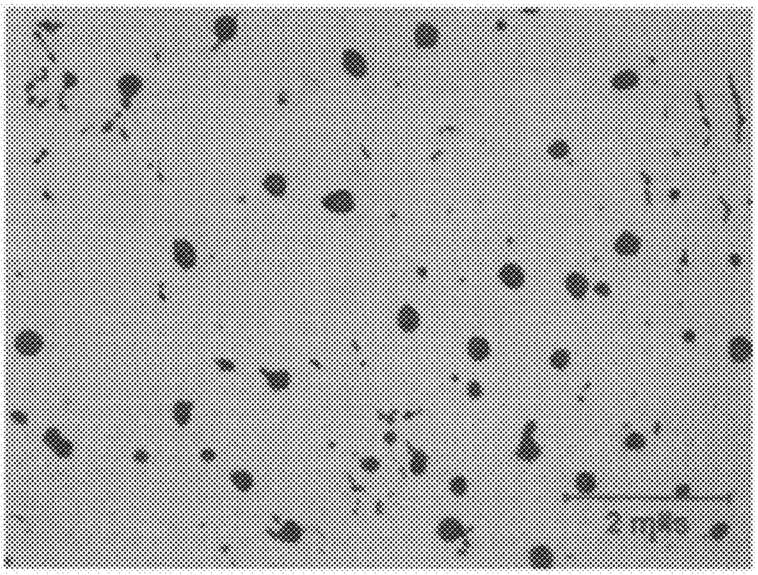

FIGURE 46A

**Alloy Group I-A**

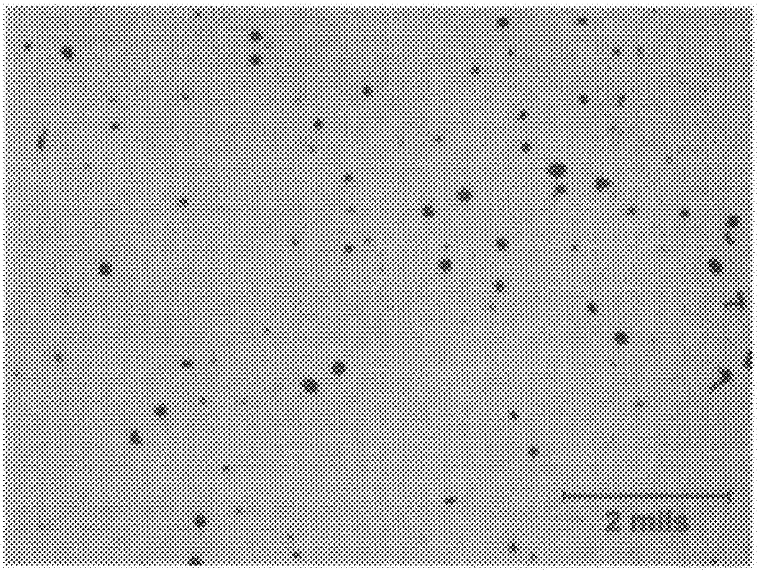

FIGURE 46B

# LOW LEAD INGOT

## CROSS-REFERENCE TO RELATED PATENT APPLICATIONS

**[0001]** This application claims priority to U.S. Provisional Patent Application No. 61/408,518, filed Oct. 29, 2010 and to U.S. Provisional Patent Application No. 61/410,752, filed Nov. 5, 2010. These applications are herein incorporated by reference in their entirety.

## BACKGROUND OF THE INVENTION

**[0002]** Current plumbing materials are typically made from lead containing copper alloys. One standard brass alloy formulation is referred to in the art as C84400 or the "81,3,7,9" alloy (consisting of 81% copper, 3% tin, 7% lead, and 9% zinc) (herein in after the "81 alloy"). While there has been a need, due to health and environmental issues (as dictated, in part, by the U.S. Environmental Protection Agency on maximum lead content in copper alloys for drinking water applications) and also for cost reasons, to reduce lead contained in plumbing fitting, the presence of lead has continued to be necessary to achieve the desired properties of the alloy. For example, the presence of lead in a brass alloy provides for desirable mechanical characteristics and to assist in machining and finishing the casting. Simple removal of lead or reduction below certain levels substantially degrades the machinability as well as the structural integrity of the casting and is not practicable.

**[0003]** Removal or reduction of lead from brass alloys has been attempted previously. Such previous attempts in the art of substituting other elements in place of lead has resulted in major machining and finishing issues in the manufacturing process, which includes primary casting, primary machining, secondary machining, polishing, plating, and mechanical assembly.

**[0004]** Several low or no lead formulations have previously been described. See, for example, products sold under the trade names SeBiLOY® or EnviroBrass®, Federalloy®, and EcoBrass® as well as U.S. Pat. Nos. 7,056,396 and 6,413,330. FIG. **1** is a table that includes the formulation of several known alloys based upon their registration with the Copper Development Association. The existing art for low lead or no lead copper based castings consists of two major categories: silicon based materials and bismuth/selenium materials.

**[0005]** However, there is a need for a low-lead casting solution providing a low-cost alloy with similar properties to current copper/lead alloys without degradation of mechanical properties or chemical properties, as well as significant disruption to the manufacturing process because of lead substitution in the material causing cutting tool and finishing problems.

## SUMMARY OF THE INVENTION

**[0006]** One embodiment of the invention relates to a semi-red brass having a composition of about 83% to about 91% copper, about 0.1% to about 0.8% sulfur, about 2.0% to about 4.0% tin, less than about 0.09% lead, about 4.0% to about 14.0% zinc, and about 1.0% to about 2.0% nickel.

**[0007]** One embodiment of the invention relates to a tin bronze having a composition of about 86% to about 89% copper, about 0.1% to about 0.8% sulfur, about 7.5% to about 8.5% tin, less than 0.09%, lead, about 1.0% to about 5.0%, zinc, and about 1.0% nickel.

**[0008]** Additional features, advantages, and embodiments of the present disclosure may be set forth from consideration of the following detailed description, drawings, and claims. Moreover, it is to be understood that both the foregoing summary of the present disclosure and the following detailed description are exemplary and intended to provide further explanation without further limiting the scope of the present disclosure claimed.

## BRIEF DESCRIPTION OF THE DRAWINGS

**[0009]** The foregoing and other objects, aspects, features, and advantages of the disclosure will become more apparent and better understood by referring to the following description taken in conjunction with the accompanying drawings, in which:

**[0010]** FIG. **1** provides Table 1 listing formulations for several known commercial copper alloys.

**[0011]** FIG. **2** provides Table 2 listing formulations for Alloy Groups in accordance with embodiments of the present invention.

**[0012]** FIG. **3**A provides Table 3 listing alloy formulations for Group I-A mechanical property examples by their respective casting heat. FIG. **3**B provides Table 4 listing the results of the average mechanical property testing of Group I-A by their respective casting heat.

**[0013]** FIG. **4**A provides Table 5 listing alloy formulations for Group I-B mechanical property examples by their respective casting heat. FIG. **4**B provides Table 6 listing the results of the average mechanical property testing of Group I-B.

**[0014]** FIG. **5**A provides Table 7 listing alloy formulations for Group II-A mechanical property examples by their respective casting heat. FIG. **5**B provides Table 8 listing the results of the average mechanical property testing of Group II-A.

**[0015]** FIG. **6** provides Table 9 listing the typical and minimum properties observed for embodiments of certain Alloy Groups of the present invention and those properties reported for commercially available alloys such as those in Table 1 (FIG. **1**).

**[0016]** FIG. **7** provides Table 10 listing the alloy compositions utilized for the SEM/EDS testing.

**[0017]** FIGS. **8**A and **8**B illustrate element mapping of sulfur in Alloy I-A-10a.

**[0018]** FIG. **9**A is an SEM of Alloy I-A-10; FIGS. **9**B-H illustrate element mapping; FIG. **9**B is an EDS for Sn; FIG. **9**C is an EDS for Zn; FIG. **9**D is an EDS for Cu; FIG. **9**E is an EDS for Fe; FIG. **9**F is an EDS for Ni; FIG. **9**G is an EDS for P; FIG. **9**H is an EDS for S.

**[0019]** FIG. **10**A is a micrograph of Alloy I-A-10a, with regions 1, 2, and 3 marked; FIGS. **10**B-D show the presence of Cu2S, ZnS and Cu—Zn intermetallic phases: FIG. **10**B is an EDS spectra from region 1; FIG. **10**C is an EDS spectra from region 2; FIG. **10**D is an EDS spectra from region 3.

**[0020]** FIGS. **11**A-B are optical images of Alloy I-A-10a at low (FIG. **11**A) and high magnifications (FIG. **11**B).

**[0021]** FIG. **12**A is a SEM of alloy I-B-10a and **12**B illustrate element mapping of sulfur in Alloy I-B-10 (0.31% S).

**[0022]** FIG. **13**A is an SEM of Alloy I-B-10a; FIGS. **13**B-H illustrate element mapping at 1000× magnification; FIG. **13**B is an EDS for Sn; FIG. **13**C is an EDS for Zn; FIG. **13**D is an EDS for Cu; FIG. **13**E is an EDS for Fe; FIG. **13**F is an EDS for Ni; FIG. **13**G is an EDS for P; FIG. **13**H is an EDS for S.

**[0023]** FIG. **14**A is an SEM of Alloy I-B-10b; FIGS. **14**B-H illustrate element mapping at 5000× magnification; FIG. **14**B is an EDS for Si; FIG. **14**C is an EDS for S; FIG. **14**D is an EDS for Fe; FIG. **14**E is an EDS for Cu; FIG. **14**F is an EDS for Zn; FIG. **14**G is an EDS for Sn; FIG. **14**H is an EDS for Pb; FIG. **14**I is an EDS for Ni.

**[0024]** FIGS. **15**A-B are optical images of Alloy I-B-10 at low (FIG. **15**A) and high magnifications (FIG. **15**B).

**[0025]** FIGS. **16**A and **16**B illustrate element mapping of sulfur in Alloy II-A-10a (0.30% S).

**[0026]** FIG. **17**A is an SEM of Alloy II-A-10a; FIGS. **17**B-H illustrate element mapping; FIG. **17**B is an EDS for Sn; FIG. **17**C is an EDS for Zn; FIG. **17**D is an EDS for Cu; FIG. **17**E is an EDS for Fe; FIG. **17**F is an EDS for Ni; FIG. **17**G is an EDS for P; FIG. **17**H is an EDS for S.

**[0027]** FIG. **18**A is an SEM of Alloy II-A-10b (0.19% S); FIGS. **18**B-I illustrate element mapping at 1000× magnification; FIG. **18**B is an EDS for Si; FIG. **18**C is an EDS for S; FIG. **18**D is an EDS for Fe; FIG. **18**E is an EDS for Cu; FIG. **18**F is an EDS for Zn; FIG. **18**G is an EDS for Sn; FIG. **18**H is an EDS for Pb; FIG. **18**I is an EDS for Ni.

**[0028]** FIGS. **19**A-B are optical images of Alloy II-A at low (FIG. **19**A) and high magnifications (FIG. **19**B).

**[0029]** FIGS. **20**A and **20**B illustrate element mapping of sulfur in Alloy III-A (0.011% S).

**[0030]** FIG. **21**A is an SEM of Alloy III-A; FIGS. **21**B-H illustrate element mapping; FIG. **21**B is an EDS for Sn; FIG. **21**C is an EDS for Zn; FIG. **21**D is an EDS for Cu; FIG. **21**E is an EDS for Fe; FIG. **21**F is an EDS for Ni; FIG. **21**G is an EDS for P; FIG. **21**H is an EDS for S.

**[0031]** FIGS. **22**A-B are optical images of Alloy III-A at low (FIG. **22**A) and high magnifications (FIG. **22**B).

**[0032]** FIG. **23** is a sulfur free-energy diagram of primary sulfides formed in Group I-A alloys.

**[0033]** FIG. **24** is a vertical section of different alloys in the Cu—Sn—Zn—S alloys

**[0034]** FIG. **25**A is a phase distribution diagram of alloy I-A-11a using Scheil cooling, FIG. **25**B is a magnified part of the phase distribution diagram showing the relative amounts of secondary phases.

**[0035]** FIG. **26**A is a phase distribution diagram of alloy I-A-11b using Scheil cooling, FIG. **26**B is a magnified part of the phase distribution diagram showing the relative amounts of secondary phases.

**[0036]** FIG. **27**A is a phase distribution diagram of alloy I-A-11c using Scheil cooling, FIG. **27**B is a magnified part of the phase distribution diagram showing the relative amounts of secondary phases.

**[0037]** FIG. **28**A is a phase distribution diagram of alloy I-A-11d using Scheil cooling, FIG. **28**B is a magnified part of the phase distribution diagram showing the relative amounts of secondary phases.

**[0038]** FIG. **29**A is a phase distribution diagram of alloy I-A-11e using Scheil cooling, FIG. **29**B is a magnified part of the phase distribution diagram showing the relative amounts of secondary phases.

**[0039]** FIG. **30**A is a phase distribution diagram of C83470 commercial alloy (Table 1, FIG. **1**) using Scheil cooling, FIG. **30**B is a magnified part of the phase distribution diagram showing the relative amounts of secondary phases.

**[0040]** FIG. **31** is phase diagram of Vertical Section of Group I-A.

**[0041]** FIG. **32**A is a Scheil Phase assemblage diagram of Group I-A, FIG. **32**B is a magnified Scheil Phase assemblage diagram of Group I-A.

**[0042]** FIG. **33** is a vertical Section of Group I-B.

**[0043]** FIG. **34**A is a Scheil Phase assemblage diagram of Group I-B FIG. **34**B is a magnified Scheil Phase assemblage diagram of Group I-B.

**[0044]** FIG. **35** is a vertical Section of Group II-A.

**[0045]** FIG. **36**A is a Scheil Phase assemblage diagram of Group II-A, FIG. **36**B is a magnified Scheil Phase assemblage diagram of Group II-A.

**[0046]** FIG. **37** is a graph of ultimate tensile strength (UTS) showing various heats of Alloy Group I-A compared to several known alloys, indicated by their CDA number.

**[0047]** FIG. **38** is a graph of yield strength showing various heats of Alloy Group I-A compared to several known alloys, indicated by their CDA number.

**[0048]** FIG. **39** is a graph of elongation showing various heats of Alloy Group I-A compared to several known alloys, indicated by their CDA number.

**[0049]** FIG. **40** is a graph of ultimate tensile strength (UTS) showing various heats of Alloy Group I-B compared to several known alloys, indicated by their CDA number.

**[0050]** FIG. **41** is a graph of yield strength showing various heats of Alloy Group I-B compared to several known alloys, indicated by their CDA number.

**[0051]** FIG. **42** is a graph of elongation showing various heats of Alloy Group I-B compared to several known alloys, indicated by their CDA number.

**[0052]** FIG. **43** is a graph of ultimate tensile strength (UTS) showing various heats of Alloy Group II-A compared to several known alloys, indicated by their CDA number.

**[0053]** FIG. **44** is a graph of yield strength showing various heats of Alloy Group II-A compared to several known alloys, indicated by their CDA number.

**[0054]** FIG. **45** is a graph of elongation showing various heats of Alloy Group II-A compared to several known alloys, indicated by their CDA number.

**[0055]** FIG. **46**A illustrates the sulfide particle sizes for a commercial sulfur brass, BiWalite™ (C83470) and FIG. **46**B is photomicrograph showing particle size of Group I-A alloy (0.13 S-4.45 Zn-3.63 Sn).

**[0056]** The patent or application file contains at least one drawing executed in color. Copies of this patent or patent application publication with color drawing(s) will be provided by the Office upon request and payment of necessary fee.

## DETAILED DESCRIPTION OF THE PREFERRED EMBODIMENTS

**[0057]** In the following detailed description, reference is made to the accompanying drawings, which form a part hereof. In the drawings, similar symbols typically identify similar components, unless context dictates otherwise. The illustrative embodiments described in the detailed description, drawings, and claims are not meant to be limiting. Other embodiments may be utilized, and other changes may be made, without departing from the spirit or scope of the subject matter presented here. It will be readily understood that the aspects of the present disclosure, as generally described herein, and illustrated in the figures, can be arranged, substituted, combined, and designed in a wide variety of different configurations, all of which are explicitly contemplated and made part of this disclosure.

**[0058]** In one embodiment, the invention relates to a composition of matter and methods for making same. The composition of matter is a copper-based alloy having a “low” level of lead as would be understood by one of ordinary skill in the art of cavity devices that make contact with potable water, including, for example, plumbing fixtures. The level of lead is below that which are normally used to impart the beneficial properties to the alloy necessary for usefulness in most applications, such as tensile strength, elongation, machinability, and pressure tightness. Prior art no-lead alternatives to leaded brass typically require changes to the metal feeding for sand castings in order to produce sufficient pressure tightness (such as having no material porosity). The alloys of the present invention include particular amounts of sulfur, and in certain embodiments, the sulfur is added through a preferred method, to impart the beneficial properties lost by the reduction in lead.

**[0059]** The alloys of the present invention relate generally to formulations of suitable semi-red brass, tin-bronze, and yellow brass. Certain embodiments are formulated for use primarily in sand cast applications, permanent mold cast applications, or wrought applications.

**[0060]** Table 2 (FIG. **2**) illustrates a group of alloys in accordance with the present invention. Each of the alloys is characterized, at least in part, by the relative low level of lead (about 0.09% or less) and the presence of sulfur (about 0.1% to 0.8%). Three groups of semi-red brass, labeled Alloy Group I-A, Alloy Group I-B, and Alloy Group I-C are provided. In one embodiment, these semi-red brass alloys are suitable for sand casting. Three groups of tin bronze, labeled Alloy Group II-A, Alloy Group II-B, and Alloy Group II-C are provided. In one embodiment, these tin bronze alloys are suitable for sand casting. Six groups of yellow brass, labeled Alloy Group III-A, Alloy Group III-B, Alloy Group III-C, Alloy Group IV-A, Alloy Group IV-B, and Alloy Group IV-C are provided. In one embodiment the Alloy Group III alloys are suitable for permanent mold casting. In one embodiment, the Alloy Group IV alloys are suitable for wrought applications.

## Alloy Components

**[0061]** The alloys of the present invention comprise copper, zinc, tin, sulfur, nickel, and phosphorus. In certain embodiments, one or more of manganese, zirconium, boron, titanium and/or carbon are included. Embodiments, other than Group IV wrought yellow brass, also include one or more of antimony, tin, nickel, phosphorus, aluminum, and silicon.

**[0062]** The alloys, comprise as a principal component, copper. Copper provides basic properties to the alloy, including antimicrobial properties and corrosion resistance. Pure copper has a relatively low yield strength, and tensile strength, and is not very hard relative to its common alloy classes of bronze and brass. Therefore, it is desirable to improve the properties of copper for use in many applications through alloying. The copper will typically be added as a base ingot. The base ingot's composition purity will vary depending on the source mine and post-mining processing. Therefore, it should be appreciated that ingot chemistry can vary, so, in one embodiment, the chemistry of the base ingot is taken into account. For example, the amount of zinc in the base ingot is taken into account when determining how much additional zinc to add to arrive at the desired final composition for the alloy. The base ingot should be selected to provide the required copper for the alloy while considering the secondary elements in the base ingot and their intended presence in the final alloy since small amounts of various impurities, such as iron, are common and have no material effect on the desired properties.

**[0063]** Lead has typically been included as a component in copper alloys, particularly for applications such as plumbing where machinability is an important factor. Lead has a low melting point relative to many other elements common to copper alloys. As such, lead, in a copper alloy, tends to migrate to the interdendritic or grain boundary areas as the melt cools. The presence of lead at interdendritic or grain boundary areas can greatly improve machinability and pressure tightness. However, in recent decades the serious detrimental impacts of lead have made use of lead in many applications of copper alloys undesirable. In particular, the presence of the lead at the interdendritic or grain boundary areas, the feature that is generally accepted to improve machinability, is, in part, responsible for the unwanted ease with which lead can leach from a copper alloy.

**[0064]** Sulfur is added to the alloys of the present invention to overcome certain disadvantages of using leaded copper alloys. Sulfur present in the melt will typically react with transition metals also present in the melt to form transition metal sulfides. For example, copper sulfide and zinc sulfide may be formed, or, for embodiments where manganese is present, it can form manganese sulfide. FIG. **23** illustrates a free-energy diagram for several transition metal sulfides that may form in embodiments of the present invention. The melting point for copper sulfide is 1130 Celsius, 1185 Celsius for zinc sulfide, 1610 Celsius for manganese sulfide, and 832 Celsius for tin sulfide. Thus, without limiting the scope of the invention, in light of the free energy of formation, it is believed that a significant amount of the sulfide formation will be zinc sulfide for those embodiments having no manganese. It is believed that sulfides that solidify after the copper has become to solidify, thus forming dendrites in the melt, aggregate at the interdentric areas or grain boundaries.

**[0065]** Sulfur provides similar properties as lead would impart to a copper alloy, without the health concerns associated with lead. Sulfur forms sulfides which it is believed tend to aggregate at the interdendritic or grain boundary areas. The presence of the sulfides provides a break in the metallic structure and a point for the formation of a chip in the grain boundary region and improve machining lubricity, allowing for improved overall machinability. The sulfides predominate in the alloys of the present invention provide lubricity. Good distribution of sulphides improves pressure tightness, as well as, machinability.

**[0066]** It is believed that the presence of tin in some embodiments increases the strength and hardness but reduces ductility by solid solution strengthening and by forming Cu—Sn intermetallic phase such as $Cu_3Sn$. It also increases the solidification range. Casting fluidity increases with tin content. Tin also increases corrosion resistance. However, currently Sn is very expensive relative to other components.

**[0067]** With respect to zinc, it is believed that the presence of Zn is similar to that of Sn, but to a lesser degree, in certain embodiments approximately 2% Zn is roughly equivalent to 1 Sn with respect to the above mentioned improvements to characteristics noted above. Zn increases strength and hardness by solid solution hardening. However, Cu—Zn alloys have a short freezing range. Zn is much less expensive than Sn.

**[0068]** With respect to certain embodiments, iron can be considered an impurity picked up from stirring rods, skimmers, etc during melting and pouring operations, or as an impurity in the base ingot. Such categories of impurity have no material effect on alloy properties.

**[0069]** For red brass and tin bronzes, antimony may be considered an impurity in the described alloys. Typically, antimony is picked up from inferior brands of tin, scrap and poor quality of ingots and scrap. However, antimony is deliberately added to yellow brasses in a permanent mold to increase the dezincification resistance.

**[0070]** In some embodiments, nickel is included to increase strength and hardness. Further, nickel aids in distribution of the sulphide particles in the alloy. In one embodiment, adding nickel helps the sulfide precipitate during the cooling process of the casting. The precipitation of the sulfide is desirable as the suspended sulfides act as a substitute to the lead for chip breaking and machining lubricity during the post casting machining operations. With the lower lead content, it is believed that the sulfide precipitate will minimize the effects of lowered machinability.

**[0071]** Phosphorus may be added to provide deoxidation. The addition of phosphorus reduces the gas content in the liquid alloy. Removal of gas provides generally provides higher quality castings by reducing gas content in the melt and reducing porosity in the finished alloy. However, excess phosphorus can contribute to metal-mold reaction giving rise to low mechanical properties and porous castings.

**[0072]** Aluminum is, in some embodiments, such as semi-red brasses and tin bronzes, treated as an impurity. In such embodiments, aluminum has harmful effects on pressure tightness and mechanical properties. However, aluminum in yellow brass castings can selectively improve casting fluidity. It is believed that aluminum encourages a fine feathery dendritic structure in such embodiments.

**[0073]** Silicon is also considered an impurity. In foundries with multiple alloys, silicon based materials can lead to silicon contamination in non silicon containing alloys. A small amount of residual silicon can contaminate semi red brass alloys, making production of multiple alloys near impossible. In addition, the presence of silicon can reduce the mechanical properties of semi-red brass alloys.

**[0074]** Manganese may be added in certain embodiments. The manganese is believed to aid in the distribution of sulfides. In particular, the presence of manganese is believed to aid in the formation of and retention of zinc sulfide in the melt. In one embodiment, a small amount of manganese is added to improve pressure tightness. In one embodiment, manganese is added as MnS.

**[0075]** Either zirconium or boron may be added individually (not in combination) to produce a fine grained structure which improves surface finish of castings during polishing.

**[0076]** Carbon may be added in certain embodiments to improve pressure tightness, reduce porosity, and improve machinability.

**[0077]** Titanium may be added in combination with carbon, such as in graphite form. Without limiting the scope of the invention, it is believed that the titanium aides in bonding the carbon particles with the copper matrix, particularly for raw graphite. For embodiments utilizing copper coated with carbon, titanium may not be useful to distribute the carbon.

## Alloy Characteristics

**[0078]** In one embodiment, an alloy of the present invention solidifies in a manner such that a multitude of discrete particles of sulfur/sulfide are distributed throughout in a generally uniform manner throughout the casting. These nonmetallic sulfur particles serve to improve lubricity and break chips developed during the machining of parts cast in this new alloy, thereby improving machinability with a significant or complete reduction in the amount of lead. Without limiting the scope of the invention, the sulfides are believed to improved lubricity.

**[0079]** The preferred embodiments of the described alloy retain machinability advantages of the current alloys such as the “81” alloy or a similar leaded alloy. Further, it is believe that due to the relative scarcity of certain materials involved, the preferred embodiments of the ingot alloy will cost considerately less than that of the bismuth and/or selenium alloyed brasses that are currently advocated for replacement of leaded brass alloys such as “81”. The sulfur is present in certain embodiments described herein as a sulfide which is soluble in the melt, but is precipitated as a sulfide during solidification and subsequent cooling of the alloy in a piece part. This precipitated sulfur enables improved machinability by serving as a chip breaker similar to the function of lead in alloys such as the “81” and in bismuth and selenium alloys. In the case of bismuth and/or selenium alloys the formation of sulfides or selenides, along with some metallic bismuth, accomplishes a similar objective as this new sulfur containing alloy. The improvement in machinability may show up as increased tool life, improved machining surfaces, reduced tool forces, etc. This new idea also supplies the industry with a low lead brass/bronze which in today’s environment is seeing any number of regulatory authorities limit by law the amount of lead that can be contained in plumbing fittings.

**[0080]** Further, alloys to which lead has been added result in an increase in the temperature range over which solidification occurs, normally making it more difficult to produce a leak tight casting, critical in plumbing fittings. However, lead segregates to the last regions to solidify and thereby seals the interdendritic and grain boundary shrinkage which occurs. This sealing of interdendritic or grain boundary porosity is not accomplished in the sulfur/sulfide containing alloys. Neither is it accomplished in the bismuth and/or selenium alloys. While bismuth is similar to lead in the periodic table of the elements, and expands during solidification, the amount of bismuth used is small compared to the amount of lead in conventional alloys such as the “81”. Bi is typically present in commercial alloys in the elemental form.

**[0081]** One of ordinary skill will appreciate the additional benefits beyond the performance properties of the present alloys. Compared to bismuth and selenium the alloys of the present invention utilize abundantly found elements, whereas both bismuth and selenium are in relatively limited supply; and the conversion of brass castings to these materials will significantly increase the demand for these limited supply materials. In addition, bismuth has some health concerns associated with its use in plumbing fixtures, in part due to its proximity to lead as a heavy metal on the periodic table. Further, in certain embodiments, the alloys of the present invention utilizes a lower percent of copper than prior art bismuth and selenium compositions.

## Yield Benefits

**[0082]** It has been observed that the use of sulfur as a substitute for lead rather than silicon provides superior “yield per melt”. With sulfur, the yield per melt ranges from 70 to 80% as compared to silicon which can yield 40 to 60% per melt. Normal leaded brass alloys yield 70 to 80% depending upon process efficiency. As can be appreciated by one of ordinary skill, such an increase in yield reflects a substantial cost of goods differential. Therefore, the capacity of the metal casting facility is significantly reduced utilizing the silicon based materials. Also, certain embodiments of the present invention have a lower zinc content than the silicon based prior art alloys which normally contain upwards of 30% of zinc which can lead to leaks due to the interaction of the zinc and water resulting in corrosion. The lower, relative to those silicon based alloys, zinc of the present invention reduces the tendency for de-zincification. Further, if typically the product is to be finished with a chrome plated surface, the silicon based materials require a copper or tin strike prior to plating which increases the cost of the plating. The alloys of the present invention do not require the additional step (and its associated costs) to allow for chrome plating.

## Melt Process

**[0083]** In one embodiment, graphite is placed on the bottom of the crucible prior to heating. In one embodiment, silicon carbide or clay graphite crucibles may be used in the melts. It is believed that the use of graphite reduces the loss of zinc during the heat without substantially becoming incorporated into the final alloy. In one embodiment, approximately two cups of graphite are used for a 90 to 95 lbs capacity crucible. For the examples used herein, a B-30 crucible was used for the melts, which has a capacity of 90 to 95 lbs of alloy.

**[0084]** Based upon the desired end alloy's formulation, the required base ingot is placed in the crucible and the furnace started. The base ingot, is brought to a temperature of about 2,100 degrees Fahrenheit to form a melt. In one embodiment a conventional gas-fired furnace is used, and in another an induction furnace is used. The furnace is then turned off, i.e. the melt is no longer heated. Then the additives, except, in one embodiment, for sulfur and phosphorus, are then plunged into the melt between 15 to 20 seconds to achieve desired levels of Zn, Ni and Sn. The additives comprise the materials needed to achieve the final desired alloy composition for a given base ingot. In one embodiment, the additives comprise elemental forms of the elements to be present in the final alloy. Then a partial amount of slag is skimmed from the top of the melt.

**[0085]** The furnace is then brought to a temperature of about 2,140 Fahrenheit. The furnace is then shut off and the sulfur additive is plunged in. For certain embodiments having phosphorus added, such as for degassing of the melt, the furnace is then reheated to a temperature of about 2,150 degrees Fahrenheit and phosphorous is plunged into the melt as a Cu—P master alloy. Next, preferably all of the slag is skimmed from the top of the crucible. Tail castings for pressure testing and evaluation of machinability and plating, buttons, wedges and mini ingots for chemical analysis, and web bars for tensile testing are poured at about 2100, about 2040, and about 2000 F respectively. In one embodiment, the furnace is fired to about 2,140 Fahrenheit for Alloy Groups I-A and I-B. In another embodiment, the furnace is fired to about 2,050 Fahrenheit for Alloy Group II-A.

## Testing/Examples

**[0086]** Machinability testing described in the present application was performed using the following method. The piece parts were machined by a coolant fed, 2 axis, CNC Turning Center. The cutting tool was a carbide insert. The machinability is based on a ratio of energy that was used during the turning on the above mentioned CNC Turning Center. The calculation formula can be written as follows:

$$C_F=(E_1/E_2)\times 100$$

**[0087]** $C_F$=Cutting Force

**[0088]** $E_1$=Energy used during the turning of the New Alloy.

**[0089]** $E_2$=Energy used during the turning of a "known" alloy C 36000 (CDA).

**[0090]** Feed rate=0.005 IPR

**[0091]** Spindle Speed=1,500 RPM

**[0092]** Depth of Cut=Radial Depth of Cut=0.038 inches

**[0093]** An electrical meter was used to measure the electrical pull while the cutting tool was under load. This pull was captured via milliamp measurement.

## Mechanical Properties

**[0094]** Mechanical properties of various embodiments of the present alloys were tested. FIGS. **3**A-**6** correspond to the specific tested formulations and the corresponding results for the Ally Group I-A, Alloy Group I-B, and Alloy Group II-A.

**[0095]** FIGS. **3**A and **3**B correspond to the specific tested formulations and the corresponding results for the Ally Group I-A. Eight sample heats, prepared in accordance with the process above to achieve a Group I-A alloy, were tested for ultimate tensile strength ("UTS"), yield strength ("YS"), percent elongation ("E %"), Brinnell hardness ("BHN"), and Modulus of Elasticity ("MoE"). The average for the eight Alloy Group I-A alloys was 40.25 ksi for ultimate tensile strength, 17.1 ksi for yield strength, 47 for percent elongation, 63 for Brinnell hardness, and 13.5 for Modulus of Elasticity.

**[0096]** FIGS. **4**A and **4**B correspond to the specific tested formulations and the corresponding results for the Ally Group I-B. Nine sample heats, prepared in accordance with the process above to achieve a Group I-B alloy, were tested for ultimate tensile strength, yield strength, percent elongation, Brinnell hardness, and Modulus of Elasticity. The average for the nine Alloy Group I-B alloys was 38.1 ksi for ultimate tensile strength, 17.5 ksi for yield strength, 32 for percent elongation, 64 for Brinnell hardness, and 13.8 for Modulus of Elasticity.

**[0097]** FIGS. **5**A and **5**B correspond to the specific tested formulations and the corresponding results for the Ally Group II-A. Eight sample heats, prepared in accordance with the process above to achieve a Group II-A alloy, were tested for ultimate tensile strength, yield strength, percent elongation, Brinnell hardness, and Modulus of Elasticity. The average for the eight Alloy Group II-A alloys was 43.8 ksi for ultimate tensile strength, 23 ksi for yield strength, 27 for percent elongation, 80 for Brinnell hardness, and 15.0 for Modulus of Elasticity.

**[0098]** Table 9 (FIG. **6**) illustrates the range of mechanical properties determined experimentally for alloys of the present invention, as well as for several known commercial alloys.

**[0099]** These results indicate that the minimum and typical UTS values for alloy I-A are higher by 50%, 18%, and 34% for minimum and 30%, 9%, and 12% for typical with respect to alloys C89520, C89836, and C83470 respectively. Similarly, the E % is higher by 550%, 95%, and 129% for minimum and 370%, 57%, and 88% for typical with respect to C89520, C89836, and C83470 respectively. The YS of I-A is higher by 8% over the Biwalite™ (C83470).

**[0100]** With respect to I-B, these values are 40%, 11%, and 26% for minimum UTS, 24%, 4%, and 7% for typical UTS; 350%, 35%, and 59% for minimum E %, and 220%, 7%, and 28% for typical E % with respect to alloys C89520, C89836, and BiWalite™ (C83470) respectively.

**[0101]** FIGS. **37** to **45** illustrate the variation between various heats within each of Group I-A (FIGS. **37** to **39**), Group I-B (FIGS. **40** to **42**), and Group II-B (FIGS. **43** to **45**). Mechanical data is also provided for three commercially available alloys, C84400 (depicted as ---), C89836 (depicted as —), and C89520 (depicted as - - - ) for comparison purposes. The data for the respective Alloy Groups of the present invention are shown as points connected by a solid line.

**[0102]** Regarding Group I-A, FIG. **37** shows the observed UTS was consistently higher than the commercial alloys. FIG. **38** shows the observed YS was consistently higher than all of the commercial alloys except C89520, an alloy containing the expensive rare element bismuth. FIG. **39** shows the observed elongation was consistently much higher than all of the commercial alloys. Elongation did exhibit variability from heat to heat for Group I-A.

**[0103]** Regarding Group I-B, FIG. **40** shows the observed UTS was consistently higher than the commercial alloys. FIG. **41** shows the observed YS was consistently higher than all of the commercial alloys, again, except C89520, an alloy containing the expensive rare element bismuth. FIG. **42** shows the observed elongation was consistently higher than all of the commercial alloys. Elongation did exhibit significant variability from heat to heat for Group I-B.

**[0104]** Group II-A alloys were also compared with leaded alloy C90300 (depicted as ---), in addition to the commercial alloys used in as previously discussed. Regarding Group II-A, FIG. **43** shows the observed UTS was consistently higher than the commercial alloys, including slightly higher than C90300. FIG. **44** shows the observed YS was consistently higher than all of the commercial alloys including C89520. FIG. **45** shows the observed elongation was consistently higher than all of the commercial alloys. Elongation did exhibit significant variability from heat to heat for Group II-A.

## Scanning Electron Microscope Analysis

**[0105]** Table 10 (FIG. **7**) lists the compositions of five alloys of the present invention, Alloy I-A-10, Alloy I-B-10, Alloy II-A-10, Alloy II-B-10, and Alloy III-A-10, that were analyzed using a scanning electron microscope equipped with energy dispersive spectroscopy (SEM/EDS). A sample of each alloy in Table 10 was mounted, metallographically prepared according to known methods and then examined both optically and using SEM/EDS. For comparison, the Biwalite™ (C83470) alloy was melted and cast under conditions similar to alloy I-A and used for evaluation and comparison of microstructure.

**[0106]** FIGS. **8**A and **8**B illustrate element mapping of sulfur in Alloy I-A-10 (0.16% S). FIG. **9**A is an SEM of Alloy I-A-10; FIGS. **9**B-H illustrate element mapping; FIG. **9**B is an EDS for Sn; FIG. **9**C is an EDS for Zn; FIG. **9**D is an EDS for Cu; FIG. **9**E is an EDS for Fe; FIG. **9**F is an EDS for Ni; FIG. **9**G is an EDS for P; FIG. **9**H is an EDS for S. FIG. **10**A is a micrograph of Alloy I-A-10a, with regions 1, 2, and 3 marked; FIGS. **10**B-D show the presence of Cu2S, ZnS and Cu—Zn intermetallic phases: FIG. **10**B is an EDS spectra from region 1; FIG. **10**C is an EDS spectra from region 2; FIG. **10**D is an EDS spectra from region 3. FIGS. **11**A-B are optical images of Alloy I-A-10 at low (FIG. **11**A) and high magnifications (FIG. **11**B). The elements are seen widely distributed except for sulfur, which appears collected at what is believe to be interdentric areas or grain boundaries.

**[0107]** FIGS. **12**A and **12**B illustrate element mapping of sulfur in Alloy I-B-10 (0.31% S). FIG. **13**A is an SEM of Alloy I-B-10; FIGS. **13**B-H illustrate element mapping; FIG. **13**B is an EDS for Sn; FIG. **13**C is an EDS for Zn; FIG. **13**D is an EDS for Cu; FIG. **13**E is an EDS for Fe; FIG. **13**F is an EDS for Ni; FIG. **12**G is an EDS for P; FIG. **13**H is an EDS for S. FIG. **14**A is an SEM of Alloy I-B-10b; FIGS. **14**B-H illustrate element mapping at 5000× magnification; FIG. **14**B is an EDS for Si; FIG. **14**C is an EDS for S; FIG. **14**D is an EDS for Fe; FIG. **14**E is an EDS for Cu; FIG. **14**F is an EDS for Zn; FIG. **14**G is an EDS for Sn; FIG. **14**H is an EDS for Pb; FIG. **14**I is an EDS for Ni. FIGS. **15**A-B are optical images of Alloy I-B-10 at low (FIG. **15**A) and high magnifications (FIG. **15**B). The elements are seen widely distributed except for sulfur, which appears collected at what is believe to be interdentric areas or grain boundaries. The higher volume fraction of the sulfides is evident due to the high sulfur content. Some of these sulfides are ZnS as evident from the EDS data. These sulfides are finer than those observed in BiWalite™ (C83470), see FIG. **46**A. Presence of the Cu—Zn intermetallic phases are evident as well.

**[0108]** FIGS. **16**A and **16**B illustrate element mapping of sulfur in Alloy II-A (0.30% S).

**[0109]** FIG. **17**A is an SEM of Alloy II-A; FIGS. **17**B-H illustrate element mapping; FIG. **15**B is an EDS for Sn; FIG. **17**C is an EDS for Zn; FIG. **17**D is an EDS for Cu; FIG. **17**E is an EDS for Fe; FIG. **17**F is an EDS for Ni; FIG. **17**G is an EDS for P; FIG. **17**H is an EDS for S. FIG. **18**A is an SEM of Alloy II-A-10b (0.19% S); FIGS. **18**B-H illustrate element mapping at 1000× magnification; FIG. **18**B is an EDS for Si; FIG. **18**C is an EDS for S; FIG. **18**D is an EDS for Fe; FIG. **18**E is an EDS for Cu; FIG. **18**F is an EDS for Zn; FIG. **18**G is an EDS for Sn; FIG. **18**H is an EDS for Pb; FIG. **18**I is an EDS for Ni. FIGS. **19**A-B are optical images of Alloy II-A at low (FIG. **19**A) and high magnifications (FIG. **19**B). The elements are seen widely distributed except for sulfur, which appears collected at what is believe to be interdentric areas or grain boundaries. These figures show the presence of Cu2S, ZnS, and intermetallic phases of Cu—Sn and Cu—Zn.

**[0110]** FIGS. **20**A and **20**B illustrate element mapping of sulfur in Alloy III-A (0.011% S). FIG. **21**A is an SEM of Alloy III-A; FIGS. **121**B-H illustrate element mapping; FIG. **21**B is an EDS for Sn; FIG. **21**C is an EDS for Zn; FIG. **21**D is an EDS for Cu; FIG. **21**E is an EDS for Fe; FIG. **21**F is an EDS for Ni; FIG. **21**G is an EDS for P; FIG. **21**H is an EDS for S. FIGS. **22**A-B are optical images of Alloy III-A at low (FIG. **22**A) and high magnifications (FIG. **22**B). The elements are seen widely distributed except for sulfur, which appears collected at what is believe to be interdentric areas or grain boundaries.

## Phase Analysis

**[0111]** Phase information was gathered for the alloys in Table 11. Alloys I-A-1 through 1-A-5 and Alloys I-B-1 and II-A-1 were formulated and made in accordance with the present invention. Alloy C83470 is a known alloy whose full composition is listed in Table 1 (FIG. **1**). Alloys 1-B-11a and II-A-11a are nominal compositions for Alloy Groups I-B and II-A respectively. For comparison, nominal composition of commercially available alloys C84000 and C83470 (Biwalite™) is also included in Table 11.

TABLE 11

| Alloy Compositions for Phase Analysis | | | | | | |
|---|---|---|---|---|---|---|
| Alloy Type | Cu | S | Sn | Zn | Ni | Mn |
| Alloy I-A-11a | 88.9 | 0.6 | 3 | 7.5 | 1 | — |
| Alloy I-A-11b | 88.1 | 0.6 | 2.9 | 8.5 | 1 | — |
| Alloy I-A-11c | 91.2 | 0.6 | 3.2 | 5 | 1 | — |
| Alloy I-A-11d | 85.4 | 0.6 | 3 | 11 | 1 | — |
| Alloy I-A-11e | 81.4 | 0.6 | 3 | 14 | 1 | — |
| Alloy I-A Nominal | 86 | 0.4 | 3 | 9 | 1 | — |
| Biwalite ™ (C83470) | 93.96 | 0.6 | 2.5 | 3 | 1 | — |
| Alloy I-B-11a | 86 | 0.5 | 3 | 8 | 1 | 0.5 |
| Alloy II-A-11a | 87 | 0.4 | 8 | 3.5 | 1 | — |

**[0112]** In order to understand the strengthening mechanisms in these alloys, phase diagrams of the Cu—Zn—Sn—S systems with and without Mn were determined using both equilibrium and non-equilibrium cooling (Scheil cooling) conditions. It should be noted that sand casting generally corresponds to non-equilibrium cooling. The phases present in these alloys have been studied using the vertical sections of the multicomponent systems.

**[0113]** Analysis done using conventional techniques was performed to determine the relative amount of the phases present at room temperature in the alloys of Table 11. In a first phase study, the five specific formulations of Alloy Group I-A were tested to observe the variance in phases within an Alloy Group. A known commercial alloy, C83470, was also studied as a reference. Table 12 lists as a percentage, the phases for each alloy. The C83470 exhibits less of the Beta phase than the alloys of Group I-A or II-A.

TABLE 12

Relative amount of the phases present at room temperature: Alloy I-A

| | Equilibrium | | | Scheil Cooling | | | | | | | |
|---|---|---|---|---|---|---|---|---|---|---|---|
| | | | | | | | | β | β' | | |
| Alloy | FCC | $Cu_3Sn$ | ZnS | FCC | $Cu_3Sn$ | MnS | $Cu_2S$ | (BCC1) | (BCC2) | MnS | γ |
| Alloy I-A-12a} | 90.8 | 7.3 | 1.8 | 87.5 | 1.1 | 0 | 2.8 | 5.4 | 2.5 | 0 | 0.6 |
| Alloy I-A-12b | 91.3 | 7.1 | 1.6 | 87.8 | 1.3 | 0 | 2.3 | 7.8 | 0.2 | 0 | 0.5 |
| Alloy I-A-12c | 90.9 | 7.3 | 1.9 | 87.5 | 0.7 | 0 | 2.8 | 4.3 | 3.9 | 0 | 0.8 |
| Alloy I-A-12d | 90.6 | 7.6 | 1.9 | 86.0 | 1.9 | 0 | 2.6 | 7.7 | 1.5 | 0 | 0.15 |
| Alloy I-A-12e | 90.5 | 7.5 | 2 | 85 | 2.3 | 0 | 2.6 | 9 | 1.1 | 0 | |
| C83470 Biwalite ™ | 93.5 | 4.7 | 1.9 | 91.5 | 0.4 | 0 | 2.9 | 3.4 | 1.1 | 0 | 0.8 |
| Alloy I-A 12f | 90.6 | 6.8 | 0.9 | 85.5 | 1.6 | 0 | 1.8 | 8.4 | 0.5 | 0 | 0.50 |
| Alloy I-B-12a | 90.8 | 6.7 | 0.5 | 86.6 | 1.7 | 0.6 | 1.0 | 7.5 | 1.3 | 0.5 | 0.4 |
| Alloy II-A-12a | 79.7 | 17.4 | 1.2 | 74.2 | 1.6 | 0 | 1.9 | 16.1 | 0.1 | 0 | 3.6 |

**[0114]** FIG. **24** plots the position of the alloys in table 12 on a copper/zinc/tin phase diagram. The alloys proceed from the highest percentage of copper and zinc on the left to the lowest copper and zinc on the right. A phase distribution diagram of I-A-11a (FIGS. **25**A and **25**B), I-A-11b (FIGS. **26**A and **26**B), I-A-11c (FIGS. **27**A and **27**B), I-A-11d (FIGS. **28**A and **28**B), I-A-11e (FIGS. **29**A and **29**B), using Scheil cooling is shown in FIGS. **25**A and **25**B. FIGS. **31**, **32**A, and **32**B correspond to Alloy I-A-12f. FIGS. **33**, **34**A, and **34**B correspond to Alloy I-B-12a. FIGS. **35**, **36**A, and **36**B correspond to Alloy II-A-12a. The relative amounts of the melt having FCC, Liquid, $BCC_1$, $BCC_2$, $Cu_2S$, and $Cu_3Sn$ in relation to temperature is shown in FIGS. **22**A and **22**B (magnified to show the distribution of the secondary phases).

**[0115]** FIGS. **30**A-**30**B illustrates a similar series of phase distributions as FIGS. **25**A-**29**, but for an existing commercial alloy, C83470. FIG. **30**A is a phase distribution diagram of C83470 alloy using Scheil cooling. FIG. **30**B is a magnified part of the phase distribution diagram showing the relative amounts of secondary phases.

**[0116]** The phase distribution diagrams show the phase that can be expected and the temperature at which they start appearing. The relative amount of each phase can also be estimated from these diagrams. Table 12 is based on these diagrams which shows that for non-equilibrium cooling, it is the β (BCC1) phase (which is an intermetallic compound of Cu and Zn) that contributes to the strength of the alloys. However, strength increases at the expense of ductility. Sloan Green alloys show high strength and ductility. Their high ductility may be due to the good melt quality, low gas content and good homogeneity. The finer distribution of sulfides also contribute to high strength and high ductility in addition to contributing to pressure tightness and machinability.

TABLE 13

Liquidus Study

| Alloy Type | Liquidus Temperature ° C. (° F.) | Solidus Temperature ° C. (° F.) | Freezing Range ° C. (° F.) |
|---|---|---|---|
| Alloy I-A-11c | 1043 (1910) | 936 (1717) | 107 (193) |
| Alloy I-A-11a | 1041 (1906) | 942 (1728) | 99 (178) |
| Alloy I-A-11b | 1036 (1897) | 947 (1737) | 89 (160) |
| Alloy I-A-11d | 1029 (1884) | 948 (1738) | 81 (146) |
| Alloy I-B-11a | 1035 (1895) | 939 (1722) | 96 (173) |
| C84400, Leaded Alloy, | 1004 (1840) | 843 (1549) | 161 (291) |

TABLE 13-continued

Liquidus Study

| Alloy Type | Liquidus Temperature ° C. (° F.) | Solidus Temperature ° C. (° F.) | Freezing Range ° C. (° F.) |
|---|---|---|---|
| Biwalite ™, C83470 | 1013 (1855) | 951 (1744) | 62 (111) |
| Biwalite ™, C83470 (Reported) | 1027, (1881) | 982 (1800) | 45 (81) |
| C90400 | 987 (1810) | 852 (1566) | 135 (244) |
| C90300, Leaded Alloy, | 1000 (1832) | 854 (1570) | 146 (262) |

## Procedure

**[0117]** Thermal investigation of the systems was performed using a DSC-2400 Setaram Setsys Differential Scanning calorimetry. Temperature calibration of the DSC was done using 7 pure metals: In, Sn, Pb, Zn, Al, Ag, and Au spanning the temperature range from 156 to 1065° C. The samples were cut and mechanically polished to remove any possible contaminated surface layers. Afterwards, they were cleaned with ethanol and placed in a graphite crucible with a lid cover to limit possible evaporation and protect the apparatus. To avoid oxidation, the analysis chamber was evacuated to $10^{-2}$ mbar and then flooded with argon. The DSC measurements were carried out under flowing argon atmosphere. Three replicas of each sample were tested. The weight of the sample was 62~78 mg.

**[0118]** The sample was heated from room temperature to 1080° C. Then it was cooled to 800° C. and kept at that temperature for 10 minutes, 600 s. This is termed "first heating and cooling cycle." In the second and third cycles the sample was heated to 1080° C. and then cooled to 800° C. twice. Finally the sample was cooled down to room temperature. A constant rate of 5° C./min was used for all heating and cooling. A baseline experiment, with two empty graphite crucibles was run using the same experimental program. The baseline was subtracted for all runs. The analysis for temperatures and enthalpies was carried on these baseline adjusted thermograms.

**[0119]** The results from the second and third cycles were used to determine the relevant thermal parameters, namely the $T_{start}$ of melting, the $T_{onset}$ of solidification, and $T_{peak}$ of melting and solidification, as well as, the enthalpy, E, of melting and of solidification. Usually, $T_{start}$ (heating) and $T_{peak}$ (cooling) were taken as the $T_S$ (solidus) and $T_L$ (liquidus).

**[0120]** The results of the liquidus study indicate that the introduction of sulphides appear to reduce the liquidus temperatures and the freezing ranges in comparison with the leaded alloys. In the A-I group of alloys, as the Zn content increases, liquidus temperature and the freezing range decrease.

**[0121]** With respect to freezing ranges, Biwalite™ (C83470), has a medium freezing range. The alloys of Table 13 have a broad freezing range. In contrast, with Biwalite™ (C83470), one can expect a deep pipe in the riser which can extend to the casting to produce shrinkage porosity. With broad freezing range alloys, porosity can be distributed well in the casting. In addition, it can be minimized/eliminated by using proper risering design and/or by using metal chills. In a way, the alloys I-A, I-B, and II-A of Table 13 can be less susceptible to shrinkage porosity. This would lead to better strength and elongation values which we have observed.

## Sulfide Particle Size

**[0122]**

TABLE 14

Alloys for Particle Size Study

| Element | Alloy I-A-14a | Alloy I-A-14b | Alloy I-A-14a | BiWalite ™ C83470 | C90300 |
|---|---|---|---|---|---|
| Cu | 88.26 | 90.46 | 87.46 | 91.82 | 87.58 |
| Ag | <0.01 | <0.01 | 0.03 | <0.01 | 0.02 |
| Bi | 0.01 | 0.01 | 0.07 | 0.01 | 0.02 |
| Fe | 0.16 | 0.05 | 0.16 | 0.26 | 0.09 |
| Mn | <0.01 | 0.01 | 0.01 | <0.01 | <0.01 |
| Ni | 0.88 | 1.13 | 0.89 | 0.69 | 0.07 |
| P | 0.012 | 0.006 | 0.015 | 0.012 | 0.023 |
| Pb | 0.02 | 0.12 | 0.01 | 0.02 | 0.11 |
| S | 0.11 | 0.13 | 0.19 | .59 | 0.012 |
| Sb | <0.01 | <0.01 | <0.01 | <0.01 | 0.01 |
| Sn | 3.23 | 3.63 | 8.18 | 4.02 | 8.22 |
| Zn | 7.32 | 4.45 | 2.99 | 2.58 | 3.84 |

TABLE 15

Particle Sizes

| Alloy | Minimum (μm) | Maximum (μm) | Average (μm) |
|---|---|---|---|
| Alloy I-A-14a | 0.1 | 9 | 2 |
| Alloy I-A-14b | 0.1 | 7 | 2 |
| Alloy I-A-14a | 0.1 | 14 | 2 |
| BiWalite ™ C83470 | 0.1 | 14 | 3 |
| C90300 | 0.2 | 5 | 2 |
| Alloy I-B-10a | 0.1 | 5 | 1 |
| Alloy III-A | 0.1 | 5 | 1 |
| Alloy I-A-10a | 0.2 | 18 | 5 |
| Alloy II-A-10a | 0.1 | 53 | 6 |

**[0123]** A study was done of the sulfide particles sizes of the alloys in Table 14 as well as select alloys in Table 10. Table 15 lists the minimum, maximum and average particle sizes for the alloys. In addition, particle sizes were reviewed for two commercial alloys, C83470 and C90300. The alloys of the present invention provide, on average, a smaller particle size than C83470 and a small minimum particle size than the commercial alloy C90300. FIG. **46**A-**46**B illustrate photomicrographs of the commercial C83470 compared with a Group I-A alloy (I-A-14b).

**[0124]** The foregoing description of illustrative embodiments has been presented for purposes of illustration and of description. It is not intended to be exhaustive or limiting with respect to the precise form disclosed, and modifications and variations are possible in light of the above teachings or may be acquired from practice of the disclosed embodiments. It is intended that the scope of the invention be defined by the claims appended hereto and their equivalents.

What is claimed is:

**1**. An alloy composition comprising:

a copper content of about 83% to about 91%;

a sulfur content of about 0.1% to about 0.8%;

a tin content of about 2.0% to about 4.0%;

a lead content of less than about 0.09%;

a zinc content of about 4.0% to about 14.0%; and

a nickel content of about 1.0% to about 2.0%

**2**. The alloy composition of claim **1** further comprising less than 0.1% iron.

**3**. The alloy composition of claim **1** further comprising less than 0.02% antimony.

**4**. The alloy composition of claim **1** further comprising about 0.05% phosphorus.

**5**. The alloy composition of claim **1** further comprising about 0.005% aluminum.

**6**. The alloy composition of claim **1** further comprising less than 0.005% silicon.

**7**. The alloy composition of claim **1** further comprising about 0.01% and about 0.7% manganese.

**8**. The alloy composition of claim **1** further comprising about 0.2% zirconium.

**9**. The alloy composition of claim **1** further comprising about 0.2% boron.

**10**. The alloy composition of claim **1** further comprising about 0.1% and about 0.7% manganese.

**11**. An alloy composition comprising:
a copper content of about 86% to about 89%;
a sulfur content of about 0.1% to about 0.8%;
a tin content of about 7.5% to about 8.5%;
a lead content of less than 0.09%;
a zinc content of 1.0% to about 5.0%; and
a nickel content of about 1.0%.

**12**. The alloy composition of claim **1** further comprising less than 0.02% to about 0.2% iron.

**13**. The alloy composition of claim **1** further comprising about 0.02% antimony.

**14**. The alloy composition of claim **1** further comprising about 0.05% phosphorus.

**15**. The alloy composition of claim **1** further comprising about 0.005% aluminum.

**16**. The alloy composition of claim **1** further comprising less than 0.005% silicon.

**17**. The alloy composition of claim **1** further comprising about 0.1% and about 0.7% manganese.

**18**. The alloy composition of claim **1** further comprising about 0.2% zircon.

**19**. The alloy composition of claim **1** further comprising about 0.2% boron.

**20**. The alloy composition of claim **1** further comprising about 0.1% and about 0.7% manganese.

**21**. A method for producing a copper alloy of claim **1**, comprising:
heating a base ingot to a temperature of about 2,100 degrees Fahrenheit to form a melt;
ceasing heating of the melt and plunging additives, except for sulfur, into the melt between 15 to 20 seconds;
skimming at least a partial amount of slag from the melt;
heating the melt to a temperature of about 2,140 Fahrenheit;
ceasing heating of the melt and plunging the sulfur into the melt;
heating the melt to a temperature of about 2,150 degrees Fahrenheit; and
removing slag from the melt.

**22**. The method of claim **21**, further comprising placing graphite on the bottom of a crucible prior to heating the base ingot in the crucible.

**23**. The method of claim **22**, wherein the crucible is heated using a gas-fired furnace.

**24**. The method of claim **22**, wherein the crucible is heated using an induction furnace and wherein the melt undergoes inductive stirring.

**25**. The method of claim **21**, further comprising plunging phosphorus into the melt after the plunger of the sulfur.

* * * * *